National Transportation Safety Board
Office of Research and Engineering
Washington, DC 20594

DCA23FM036

MATERIALS LABORATORY

Factual Report 24-011

July 5, 2024

(This page intentionally left blank)

A. ACCIDENT INFORMATION

Location: Atlantic Ocean
Date: June 18, 2023
Vehicle: OceanGate Experimental Submersible Titan
Investigator: Marcel Muise, MS-10

B. COMPONENTS EXAMINED

Carbon fiber / epoxy matrix hull fragment, approximately 61 inch x 20 inch x 1 inch, retrieved from wreckage site.
Trimmed end pieces from carbon fiber / epoxy matrix hull manufacturing process.
Trimmed end piece from first full scale hull.
Trimmed end piece from one-third-scale test article.
Additional titanium wreckage pieces.

C. EXAMINATION PARTICIPANTS

Group Chair	Donald Kramer, Ph.D. National Transportation Safety Board Washington, DC
Group Member	Lieutenant Commander [redacted] United States Coast Guard Washington, DC
Group Member	Stéphane Otin, Ph.D. Bureau d'Enquêtes et d'Analyses pour la Sécurité de l'Aviation Civile Le Bourget, France

D. DETAILS OF THE EXAMINATION

This report was prepared at the request of and in collaboration with the U.S. Coast Guard Marine Board of Investigation for the mishap involving the OceanGate submersible Titan. Retrieved wreckage was first viewed at a Coast Guard facility in Newport, RI. At the viewing, a piece of carbon fiber composite hull was identified for laboratory examination. In coordination with the U.S. Coast Guard, the piece was transported to and examined at the NTSB Materials Laboratory and is shown in figures 1a – d. The piece was recovered from the ocean floor, approximately 350 feet from the main wreckage (which consisted of the aft dome, aft segment, and aft hull fragments), as shown in figure 1e. It measured approximately 61 inch x 20 inch x 1 inch. The outer surface was coated by a green film adhesive and the inner surface was coated with white paint. One end was machined and some bits of cured adhesive were still attached. The other ends/edges were fractured. The piece was examined to

characterize the structure and properties of the composite hull material, the adhesive bonding, and to determine, where possible, the modes of separation.

Later, additional hull pieces from production articles and test articles were examined at a U.S Coard Guard facility in Seattle, WA. Some samples were then brought to the NTSB Materials Laboratory for additional examination of the composite structure, characterization of adhesive bonding, and material testing. In total, this report describes the following:

1. Manufacturing and assembly processes for the in-service hull involved in the accident.

2. Notable findings from the examination of the single-layer hull piece retrieved from the ocean floor and examined at the NTSB laboratory.

3. Fracture and wear features on the aforementioned piece.

4. Findings from multiple pieces examined at the U.S. Coast Guard facility in Seattle, WA.

5. Observations from the examination of other Titan hull components at the facility in Newport, RI.

6. The results of material property testing.

See also Materials Laboratory Factual Report 24-012 for: 1) Characterization of damage to the hull following the implosion, as observed during a search and rescue mission and a follow-up salvage mission and 2) Examination of acoustic emission sensor and strain gage data collected by the vessel's real-time monitoring system on dives leading up to the accident dive.

1.0 Composite hull manufacturing and vessel assembly

The as built and in-service Titan pressure vessel consisted of a carbon fiber epoxy matrix composite cylindrical hull mated to two titanium rings, referred to in OceanGate documents as segments, as illustrated in figure 2. The segments in-turn were capped by titanium half-domes (not shown), the forward dome including an affordance for a viewport.

The hull was manufactured from a unidirectional carbon fiber tape pre-impregnated with an epoxy resin (pre-preg) that was manufactured by Toray Composite Materials America, Inc. The Toray product number for the pre-preg system was P2362W-19L. The system consisted of a T800S-series intermediate modulus carbon fiber and a 3900-series epoxy resin with a cured ply thickness of 0.0075 inch. OceanGate had the as-received rolls slit into 0.5-inch width reels (tows) and built the hull by winding the tows onto a carbon steel mandrel by automatic fiber

placement (AFP) at an Electoimpact, Inc. facility, in Mukilteo, WA. The build sequence consisted of two cylindrical plies, laid down with tension, followed by one longitudinal ply, laid down without tension, the sequence repeated until the target number of plies was applied. The tows for the cylindrical plies were wound continuously from end to end and as such formed a helical path slightly biased off the cylindrical direction. The winding direction and bias were reversed on following cylindrical plies. There were no 45° torsion plies. The sequence was repeated until 133 plies had been applied to produce a nominal 0.9975-inch thick layer, with intermediate debulking steps included during the build.

The hull was constructed as a series of five co-bonded 1-inch layers (figures 3a – 3b). According to a former OceanGate director of engineering, the co-bonding process was chosen due to the company's experience building two one-third-scale test articles from pre-preg material and the experience of its manufacturing partners.[1] The test articles developed notable wrinkles during the build process (see Section 4.3 below). The wrinkles were thought to be responsible for premature implosion of the test articles.[2] Therefore, in an effort to mitigate wrinkle formation, OceanGate limited the build layer thickness to 1 inch prior to autoclave curing. 133 layers of pre-preg (nominally a 0.9975 inch cured layer thickness) were wound on the mandrel and cured at a time with each subsequent layer co-bonded to the layer beneath it. The co-bonding sequence entailed building the 1-inch layer, capping with a peel ply, curing the layer in an autoclave, removing the peel ply, and applying film adhesive to the freshly peeled surface. The winding, curing, and surface preparation processes were then repeated until the hull was (nominally) 5-inches thick (see the process illustration in figure 3b). Autoclave curing was performed at Janicki Industries, Inc. in Hamilton, WA. Hull production took place between November 2020 and January 2021. The hull was manufactured with excess material at either end which was subsequently trimmed off. The excess trim pieces were among the items examined at the U.S. Coast Guard facility in Seattle, WA.

The trimmed hull was then bonded to the forward and aft segments. The segments (and domes) were forged and machined from commercially pure (CP) Grade 3 titanium (UNS R50550). Illustrations of the aft segment are shown in figures 4 and 5. The hull-facing side of both segments contained an annular C-shaped channel into which the hull was inserted and butt-joined using an epoxy paste adhesive (Loctite EA 9394 AERO, also known as Hysol EA9394). The segments and domes were originally used with the first full-scale iteration of the Titan hull. After that hull was retired, the remnants of the hull were removed from the segments by machining.

---

[1] For the sub-scale test hulls, the pre-preg plies were laid onto the mandrel, with intermediate debulk steps, until the target hull thickness was achieved and the assembly was autoclave cured in a single step.

[2] The first test article imploded at a pressure equivalent to an ocean depth of approximately 2,800 m. Testing of the second test article was halted at 2,500 m, as implosion appeared to be imminent.

According to a former director of engineering and a written OceanGate process specification, the segments and hull surfaces were prepared for bonding by degreasing with methyl ethyl ketone (MEK) and roughening with stearate-free sandpaper. Contact angle measurements were taken between steps to ensure active (i.e., non-contaminated) surfaces and particulates were blown away using filtered shop air (tested by contact angle to ensure it did not introduce contamination). The adhesive was mixed and applied to both the segment and hull bonding surfaces. The hull was then inserted into the C-channel. The aft joint was formed by lowering the hull down onto the segment and the forward joint was formed by lowering the segment down onto the hull, the entire assembly oriented vertically. Spacers within the joint controlled the bond line thickness. The hull was subsequently pressure tested at the Deep Ocean Test Facility in Annapolis, MD between February 25 and March 4 to a max depth of 4,200 m. According to analysis performed under contract for OceanGate, the test depth was limited by the material properties of the CP Grade 3 Ti in the vicinity of the viewport.[3] The Titan then completed 17 dives below 1300 m prior to the mishap.

The hull was equipped with a real-time monitoring (RTM) system. The system comprised eight acoustic emission (AE) sensors, eight circumferential (hoop) strain gages, and eight longitudinal (axial) strain gages. Hoop and longitudinal strain gages were co-located. Some acoustic sensors were co-located with strain gages and some were not. See Materials Laboratory Factual Report 24-012 for additional information about and analysis of the RTM system and data. The RTM system was only operational during dives. During a dive, acoustic events were continuously monitored. After amplification of the AE signal and analog-to-digital conversion, if an acoustic event exceeded approximately 15.6% full scale amplitude, the event was counted as a 'hit.' According to a former director of engineering, if the system detected 1000 hits during a dive, the system displayed a yellow warning. If 2000 hits were detected, a red warning was displayed, and the dive was to be aborted. Hit counts did not accumulate between successive dives. 'Hit' decibel levels and cumulative warning counts were established using AE data from imploded one-third-scale test articles and testing of the first (retired from service) full-scale hull done at the Deep Ocean Test Facility.

2.0 Examination of composite structure on recovered hull piece

The hull's laminate structure and the adhesive layer were examined by optical microscopy. A strip of material was removed by making two through-thickness cuts in the circumferential direction with a wet abrasive saw (figures 6 and 7). For convenience, one of the fractured sides was labelled "Right" (R) and the other side "Left" (L). The thickness of the layer ranged between 1.025 inch and 1.032 inch, as measured by point micrometer. Figure 8a shows a cross section through the laminate

[3] The strength of the CP Grade 3 titanium segments was also a depth-limiting factor, but was secondary to the viewport.

structure. The repeating layup sequence consisted of two circumferential plies followed by one axial ply. The top of the layer was terminated by a single circumferential ply which was capped by additional resin and the adhesive layer on top. In total, the layer consisted of 133 plies. The top layer of resin and adhesive, combined, was approximately 0.005-inch thick (except as noted below).

Visual examination of the adhesive surface revealed a periodic light/dark pattern progressing along the circumferential direction, as indicated in figure 7a. As indicated in figures 8a and 8b, the color variation coincided with variations in the adhesive film thickness. The lighter/greener regions coincided with thicker regions of adhesive while the darker regions coincided with thinner regions of adhesive. The variation in adhesive color and thickness was correlated with waviness of the underlying composite layer.

Additional observations regarding the peel ply, surface resin, and film adhesive structure are shown in figures 9a – 9d. Figure 9a shows a higher magnification view of the layer's outer surface. In some regions, all adhesive and surface resin had separated, exposing the underlying composite ply. In some regions, the surface resin layer was visible but there was no adhesive. These regions could be identified by the imprint left behind by the plain-weave peel ply, used during the manufacturing process, as shown in figures 9b (also see the resin profile on the cross-section view in figure 9c taken from a trimmed end piece). These regions were shown to be associated with voids in the adhesive as discussed below in Sections 3.0 and 4.1. As seen in cross-section and in the absence of voids (figure 9c), the adhesive was bonded to the surface resin layer on one side of the joint and directly bonded to the first composite ply on the other. Plan-views of semi-translucent regions of adhesive revealed non-woven scrim material within the adhesive (figure 9d).

Closer examination of the laminate structure revealed thin layers of inter-ply resin between the carbon fiber composite plies. At the base and very top of the 1-inch layer (i.e. the top three or four plies), the inter-ply resin was comparatively well consolidated with comparatively little porosity. At the middle and towards the top of the layer, porosity was observed partitioned within this inter-ply resin. Figures 10a and 10b show cross section images at the top and bottom of the layer, respectively. The stack height of twenty layers at the top and bottom of the layer was 0.156 inch and 0.144 inch, respectively.

The increase in stack height was due in large part to porosity within the inter-ply resin. Higher magnification images from porous and non-porous regions are shown in figures 11a and b, respectively. Figure 11a shows plies 122 – 126 and figure 11b shows plies 2 – 7. In figure 11a, porosity was visible within the inter-ply resin and the stack height was visibly greater. A tangential cross section through the hull piece was prepared, as shown in figure 12. The cut made a glancing pass through the inter-ply resin in the region shown in figure 13. The area fraction of the porosity was measured for several regions (see for example figures 14a and b) and

varied between 0.18 and 0.27. The total porosity within a volume of hull material was measured later at an external laboratory in accordance with ASTM 3171-22 and that testing is reported below.

The appearance of the adhesive surface varied from right to left across the strip of hull material. The surface on the right third of the layer exhibited primarily a matte/rubbed appearance, as shown in figure 15a. In the middle third, as shown in figures 15b and c, some regions of the adhesive surface began to exhibit a glossy appearance and voids began to appear. The left third, shown in figure 15d, exhibited similar features with the addition of patches where the resin had fractured and separated, exposing the underlying composite ply.

3.0 Fracture and wear features on retrieved hull piece

The longitudinal fractures through the hull piece exhibited slant fractures and kink bands, consistent with failure under compression and bending loads. A cross section through the hull piece is shown in figure 16. Close-up images of the left and right fractured sides are shown in figures 17a and b, respectively, as indicated by the red rectangles in figure 16. In figure 17a, a nearly full-thickness kink band was observed, and a slant fracture was observed starting on the inner surface, which transitioned to a circumferential delamination. In figure 17b, a kink band was observed near the inner surface and two slant fractures were observed that transitioned to delaminations, one spanning approximately the outer third of the layer and one in the middle third of the layer.

The adhesive surface exhibited features consistent with shear sliding between the first and second layers. Inclined cracks were visible in the adhesive layer on circumferential cross section images (figures 18a and b), but not on longitudinal cross sections. The measured angles of two cracks shown in figure 18b were 43.6° and 48.9°, both close to a 45° inclination angle. Patches of the adhesive had spalled (figures 19a and b). The edges of the spalled regions formed a “C”-shape with the spall progressing from right to left. A region where the top composite ply was exposed is shown in figure 20 on a piece examined using a scanning electron microscope (SEM). Hackles, consistent with shear fracture of the epoxy matrix from right to left, were observed in multiple locations. Taken together the fracture features were consistent with shear sliding between the first and second hull layers, with layer 2 shearing from “right” to “left” with respect to layer 1.

The adhesive surface showed features consistent with rubbing damage. Three SEM images, from the piece shown in the lower image of figure 12, are shown in figures 21a – c. Rub marks were observed in the longitudinal direction in multiple locations. Wear debris had filled some of the adhesive voids, such as the void shown in figure 22a. A scalpel and flux brush were used to remove the debris. The same region post-removal is shown in figure 22b. Some of the debris was collected (figure 23a) and its chemical composition was examined using a Fourier-transform

infrared spectrometer equipped with an attenuated total internal reflectance bench accessory (FTIR-ATR). FTIR-ATR spectra for the debris and for a sample of the adhesive are shown in figure 23b. The spectra exhibited similar peak positions and relative peak intensities, consistent with the debris originating from the adhesive due to rubbing damage.

There were two impact / contact marks on the "left" side of the hull piece, as shown in figures 6 and 24a. One mark was approximately 6 inch long and centered 39 inch from the machined end. The second mark was approximately 8 inch long and 49 inch from the end. A piece of metal mesh/rope was wedged in the hull piece at the edge of the 6-inch impact mark as shown in figure 24b. The material was extracted and identified as predominantly lead (Pb) using an SEM equipped with an energy dispersive X-ray spectrometer (EDS), consistent with material from a drop weight.

Most of the adhesive originally used to bond the hull to the titanium segment had disbonded from the machined end of the hull piece, but there was an approximately 3.5-inch-long patch where some adhesive bits were still attached, shown in figures 25a and b. Most of the patch was between 0.030 inch and 0.034 inch thick. In a smaller region, the adhesive measured between 0.055 inch and 0.064 inch thick, all measurements performed by caliper. As previously described, the process for bonding the hull to the segments involved applying excess epoxy adhesive to both the end of the carbon fiber hull and the flat face of the titanium segment's C-channel. The appearance and thickness of the thinner adhesive region was consistent with a separation at the interface between the adhesive applied to the hull and the adhesive applied the titanium. The appearance of the thicker patch was consistent with a separation at the interface between the adhesive and the titanium.

4.0 Examination of hull and test article trimmed end pieces

Investigators from NTSB and the U.S. Coast Guard examined trimmed end pieces from the first and second full-scale Titan hulls and a one-third-scale test article at a Coast Guard facility in Seattle, WA. Some pieces were selected for closer laboratory examination and material testing as described below.

4.1 Examination of the second full-scale-hull trimmed ends

Trimmed ends from the second Titan hull, involved in the accident, are shown in figures 26 and 27. For convenience, the ends were labelled 'A' and 'B', respectively. The words, "OUTER DIAM" were marked on the outer surface of end 'A', near the outer cutout (figure 26a). Otherwise, the ends were unmarked. Both ends were cut through the wall and around the circumference of the hull.[4] The ends

[4] There was also a 10-inch-long through-wall cut on trimmed end 'A', adjacent to and intersecting the primary cut, presumably where a cutting tool was started off of and then moved onto the trim line.

showed modifications used to facilitate trimming and handling of the rough hull. Each end had two through-holes that were drilled approximately 140° apart from one another and each end had an associated foam block that had been inserted and bonded to the inside of the rough hull at one point. The puck-shaped blocks had blade cuts on their cylindrical surfaces, indicating that they were likely inserted inside the rough hull during trimming.

Blocks of composite material had been cut from each trimmed end. Two blocks had been cut out from end 'A', each nominally 1-inch thick, one from the outer surface, and one from the inner surface. An arc of material was removed from end 'B' that was about 6 inches wide and ran the entire length of the trimmed end. As shown for end 'B' (figure 27b), the outer surface of the ends had a gradual slope in the longitudinal direction for the first three layers, after which the slope increased significantly, such that layers 4 and 5 were roughly the same length. The two ends had different tapers and lengths. End 'A' was about 8.5 inch long and end 'B' was about 11.6 inch long.

Dimensional measurements were taken on each scrap end where possible. Outer and inner diameter measurements were taken on end 'A' using a tape measure at 45° clock intervals and wall thickness measurements were taken on both ends using a caliper at 30° intervals. Clock positions were assigned to each piece with the cutouts on each piece assigned the 12:00 position. For the hull diameter measurements on end 'A', the 12:00 measurement was 66-5/16 inch and 55—7/8 inch for the outer and inner diameters, respectively. All other outer and inner diameter measurements were 66-3/8 inch and 56 inch, respectively. Wall thickness measurements on end 'A' varied between a low of 5.154 inch and a high of 5.177 inch, with an average of 5.164 inch. Similar but slightly more consistent results were achieved on end 'B'. The lowest wall thickness was 5.166 inch, the highest was 5.175 inch, and the average was 5.171 inch.

The scrap ends exhibited a notable amount of waviness and wrinkles of the composite plies, particularly for layers 2 through 5. Figures 28a and b show images of the trimmed end faces under oblique lighting conditions for ends 'A' and 'B', respectively. The oblique lighting combined with the variation in fiber ply orientation resulted in light/dark brightness variations across the surface. Waviness features were seen around the entire circumference on both ends. The end faces were examined with a handheld stereo binocular magnifier and anomalies were observed associated with some wrinkles. Voids were observed in the adhesive from fiber bridging / tenting on one or both sides of some smaller amplitude wrinkles (figure 29a). Other wrinkles showed signs of grinding to bring protruding regions flush with the outer surface (figure 29b). Using oblique lighting and the magnifier, end 'B' was examined in its entirety to count the number of fiber bridging / tenting features and grinding features associated with each layer. The results are shown in table 1 and a markup of the trimmed end is shown in figure 30a. In the photo, fiber bridging locations are

marked with two opposing diagonal tick marks (/ \) and flush-ground wrinkles are marked with a single vertical tick mark (|).

Table 1. Number of anomalies by layer on trimmed end 'B'.

Layer	Fiber bridges (with one or more voids)	Ground wrinkles
1	0	1
2	4	8
3	9	14
4	5	24
5	N/A	N/A

The anomalies were distributed randomly and were present in every quadrant. In many instances, a ground wrinkle or fiber bridge in one layer would result in another fiber bridge or wrinkle in the layer above, as seen in figure 30b.

Two samples from end 'B' were removed for laboratory examination and material testing, as indicated in figure 30b. Both pieces were adjacent to the preexisting cut, one on either side. One smaller piece contained representative wrinkle grinding features. The other larger piece contained fiber bridging features, ground wrinkles, and an area that was relatively free of anomalies, used for a part of the material testing. Laboratory images of the smaller and larger pieces are shown in figures 31 and 32, respectively.

The thickness of each co-cured layer, the number of plies per layer, the thickness of the adhesive layer, and the layup sequence for each layer were all examined with the aid of a digital optical microscope. The thickness of each layer, starting from layer 1 and ending with layer 5 was approximately 1.028 inch, 1.027 inch, 1.029 inch, 1.019 inch, and 1.033 inch (Note: Due to the inherent waviness of the layers, there was some variability in layer thickness). Each layer consisted of 133 plies. The repeating ply layup schedule maintained its two circumferential ply followed by one longitudinal ply sequence regardless of the periodic insertion of adhesive layers. Thus, for the layer 1 / layer 2 (hereafter written as layer 1/2, etc.) interface, the adhesive was sandwiched between two circumferential plies, whereas for the layer 2/3 interface, the top ply for layer 2 was circumferential while the first ply for layer 3 was longitudinal, and so on. The adhesive thickness varied between 0.006 inch and 0.010 inch due to the waviness of the composite structure, with an average of approximately 0.008 inch. The calculated hull thickness, based on a cured ply thickness of 0.0075 inch (from the Toray specification sheet), an adhesive layer thickness of 0.008 inch, and the number of plies and adhesive layers was 5.0195 inch. As previously noted, the average thickness of the trimmed ends was 5.164 inch and 5.171 inch.

The locations of two notable wrinkle grinding features on the smaller end piece are indicated in figure 31a and shown in greater detail in figures 33a and b. A fiber bridging feature with voids in the adhesive on either side of the incipient wrinkle is indicated in figure 32 and shown in greater detail in figure 34. For the piece in figure 31, a total of 6 grinding features were observed. The number of ground plies for each of the features (from most to least) was 12, 10, 6, 5, 5, and 1.

Voids were observed in the adhesive used to join the co-bonded layers. The voids were most prominent on longitudinal cross-sections at the layer 1/2 interface and the layer 3/4 interface. As shown in figures 35a – d, some voids were observed in the adhesive at every co-bonded interface. However, the voids at the layer 2/3 and layer 4/5 interfaces were fewer in number and typically discrete, nominally spherical voids. By contrast, the voids at the layer 1/2 and layer 3/4 interfaces formed elongated features along the interface with the lower layer. For example, one void along the layer 1/2 interface, in figure 35a, was approximately 0.6 inch long and one void along the layer 3/4 interface was approximately 0.4 inch long. These larger voids constituted a gap between the adhesive and the supporting layer beneath it. Figure 36 shows a higher magnification image at another spot along the layer 3/4 interface where gaps between the top of layer 3 and the adhesive were present. Figure 37 shows the results of a lab fracture of a strip of hull material at the layer 1/2 interface. The upper image shows a cross-section view, similar to those shown in figures 35 and 36. The lower image shows a plan view of the fractured strip. In areas where the adhesive joint was sound, either the adhesive fractured in a cohesive manner, or an adjoining composite ply fractured. The regions that contained voids showed the peel ply imprint pattern in resin, left over from curing layer 1, as indicated in the lower image of figure 37. The feature was identical to that seen periodically on the layer 1 piece from the accident hull, shown previously in figures 6 and 22 and discussed in Section 2.0.

4.2 Examination of a trimmed end piece from the first (retired from service) full-scale Titan hull

A block of trimmed end material from the first Titan hull is shown in figures 38a and b. The hull was manufactured in 2017 and retired from service in 2019. Measured by caliper, the thickness of the end piece was 4.974 inch. A visual comparison illustrating the difference in thickness between the first and second full-scale hull trimmed ends is shown in figure 39. The first-hull's trimmed end contained multiple delaminations and voids. Of particular note was a centerline delamination, near the mid-thickness of the piece, which is shown from two directions in figures 40a and b.

4.3 Examination of a trimmed end piece from a one-third-scale pre-preg test article

Prior to manufacturing the second full-scale hull, OceanGate manufactured two one-third-scale test articles. A trimmed end piece from the first test article is shown in figure 41. The piece had two notable wrinkles that are indicated in the figure and are shown in figures 42a and b. A mid-thickness delamination was observed around nearly the entire perimeter, only terminating on either side of the dominant wrinkle. The two ends of the delamination are just visible at the edges of figure 42a and a typical appearance for the delamination is shown in the image of the secondary wrinkle in figure 42b. The second test article (not shown) contained similar wrinkle and delamination features.

5.0 Other Titan hull components examined in Newport, RI

The titanium segments and domes were examined in Newport, RI. The forward and aft segments are shown in figures 43a and b, respectively. The segments were slightly ovalized. The top and bottom of each segment had deformed radially outward and the port and starboard sides had deformed radially inward. The inner rims on the C-channels were completely separated and the outer rims were mostly separated, remaining attached by one or two shorter ligaments on the order of 6 to 12 inches. The rim fractures were examined using a binocular magnifier. A typical section of the forward segment C-channel is shown in figure 44. The inner rim fractures all exhibited flat smeared surfaces with shear marks pointing radially inward and a shear deformation lip along the edge of the inner surface, consistent with inward shear fractures. The outer flange fractures were rough by comparison with fracture features progressing radially outward with either plastic damage or a plastic hinge along the edge of the outer surface, consistent with bending / tensile fracture. There were no features indicative of metal fatigue.

The adhesive used to bond the hull to the titanium segments had disbonded from the entire forward segment and most of the aft segment, except for an approximately 90° arc located at and centered approximately about the top (12:00) of the vessel. General lighting and oblique lighting images are shown in figures 45a and b, respectively. The adhesive contained an imprint of the machined end of the carbon fiber composite hull near the outer surface but near the inner surface, the adhesive surface had a rubbed appearance. Using the data gathered from the trimmed ends examination, the locations of some of the layer interfaces were marked on the image, as shown in the top image of figure 46. The rubbed region appeared to begin near the base of layer 4 and continue radially inward. As indicated in the top image of figure 46 and shown in greater detail in the lower image, an imprint of a filled wrinkle was observed within layer 4.

A photo of the aft dome and the viewport seat on the forward dome are shown in figures 47a and b, respectively. The domes were ovalized, similar to the segments, and the mating flanges were warped. The retaining ring used to hold the viewport in place had separated. The bolts used to secure the retaining ring all had flat fractures that originated at thread roots, consistent with tensile fractures (Note: the bolts were through-drilled).

One additional large piece of carbon fiber hull material was recovered, as shown in figures 48a and b. The piece was approximately 2 inches (2 layers) thick and comprised layers 4 and 5. The outer surface was coated with a rubber material and the inner surface was delaminated adjacent to the layer 3/4 adhesive layer interface, as evidenced by occasionally visible adhesive. Based on video footage from the search and rescue mission (see Materials Laboratory Factual Report 24-012) the forward and aft ends were identified. The piece was approximately 97 inch long and was originally located near the top (12:00 position) of the vessel. The forward end was machined. The aft end was fractured and approximately 3 inches was missing. At the forward end, the outer surface had been visibly trimmed to facilitate insertion into the segment's C-channel for adhesive bonding. Portions of the outer surface had a wavy appearance, consistent with wrinkling of the composite plies as shown in the top image of Figure 49. A screen capture from an OceanGate video taken during the manufacturing process indicated that similar features were likely present around the entire surface of the hull as shown in the lower image of figure 49.

6.0 External laboratory testing

Pieces of hull material were sent to an external laboratory for volumetric constituent content measurements, longitudinal compression tests, and V-notch inter-ply shear tests. The volumetric constituent content measurements were performed for three samples in accordance with ASTM 3171-22. The void percentages by volume were 3.6%, 1.1%, and 3.3%. The fiber volume percentages were 53%, 54%, and 52%. According to a property sheet for Toray P2362W-19L obtained by OceanGate, the expected mean void volume percentage was 0.462% with a standard deviation of 0.238% and the expected mean fiber volume percentage was 55.2% with a standard deviation of 1.06%.

The compression tests were performed in the longitudinal direction on samples that were machined from the piece of layer 1 that was recovered from the ocean floor and examined as part of this report. The test specimens were approximately 0.5 inch in width and between 0.093 inch and 0.119 inch in thickness. The long side of the specimen was aligned with the circumferential direction of the hull (figure 50a) and the short side was aligned with the through-thickness direction of the hull (figure 50b). The results are shown in table 2 below. Finite element analysis performed for OceanGate under contract assumed an allowable compressive strain

to failure of 0.0133 in the fiber direction based on the available material property data.[5]

Table 2. Results from longitudinal compression tests in accordance with ASTM 6641-23.

Sample	Max load, lbs	Compressive Strength, ksi	Modulus, Msi	Compressive strain at failure
1	4,220	70.7	7.7	Unavailable
2	3,490	60.4	5.8	0.0152
3	3,640	70.0	7.3	0.0103
4	2,580	55.5	5.7	0.0159
5	2,500	53.3	6.0	0.0107*

* Strain gage broke just before sample and strain relaxed.

Table 2 (cont.). Additional data from compression tests. BGM failure mode code: B = Brooming, G = Gage, and M = Middle.

Sample	Width, in	Thickness, in	Failure mode
1	0.501	0.119	BGM
2	0.500	0.119	BGM
3	0.499	0.104	BGM
4	0.499	0.093	BGM
5	0.501	0.094	BGM

The V-notch shear specimens were cut from a through-thickness circumferential slice of the hull (figure 50c). The samples were nominally 0.5 inch wide and between 0.095 inch and 0.097 inch thick. The long side of the gage section was aligned with the through-thickness direction of the hull and the short side of the gage section was aligned with the longitudinal direction of the hull. The shear displacement was applied in the through-thickness direction, which resulted in a 1,3-type shear to the circumferential plies (1 equates to the V-notch shear plane being perpendicular to the principal fiber axis and 3 equates to the shear direction being perpendicular to the plies). The results are shown below in table 3. A report obtained by OceanGate reported a 1,3 shear strength for a unidirectional laminate of Toray P2362W-19L of 12,400 psi with a standard deviation of 500 psi.

[5] The analysis performed for OceanGate under contract indicated that the critical failure mode of the carbon fiber hull was expected to be buckling and not compressive failure. The calculated critical buckling load occurred at an ocean depth of approximately 7,500 m and the calculated compressive strength limit occurred at a depth ranging from approximately 12,600 m to 13,800 m depending on the analysis method that was used.

Table 3. Results from V-notch shear tests in accordance with ASTM 5379-19. HGN failure mode code: H = Horizontal cracking, G = Gage section, and N = Between notches.

Sample	Max load, lbf	V-Notch shear strength, psi	Modulus, ksi	Width, in	Thickness, in	Failure mode
1	425	9,016	310	0.491	0.096	HGN
2	564	12,052	330	0.492	0.095	HGN
3	329	6,999	293	0.492	0.095	HGN
4	393	8,415	319	0.492	0.095	HGN
5	329	6,920	292	0.491	0.097	HGN

Examples of a typical post-failure compression and V-notch specimen are shown in figures 51a and b, respectively. The compression test sample exhibited brooming and slant fractures. The shear test specimen exhibited horizontal cracking along the interface between a radial ply and a circumferential ply and inclined cracks in the radial plies.

Submitted by:

Donald Kramer, Ph.D.
Senior Materials Engineer

a)

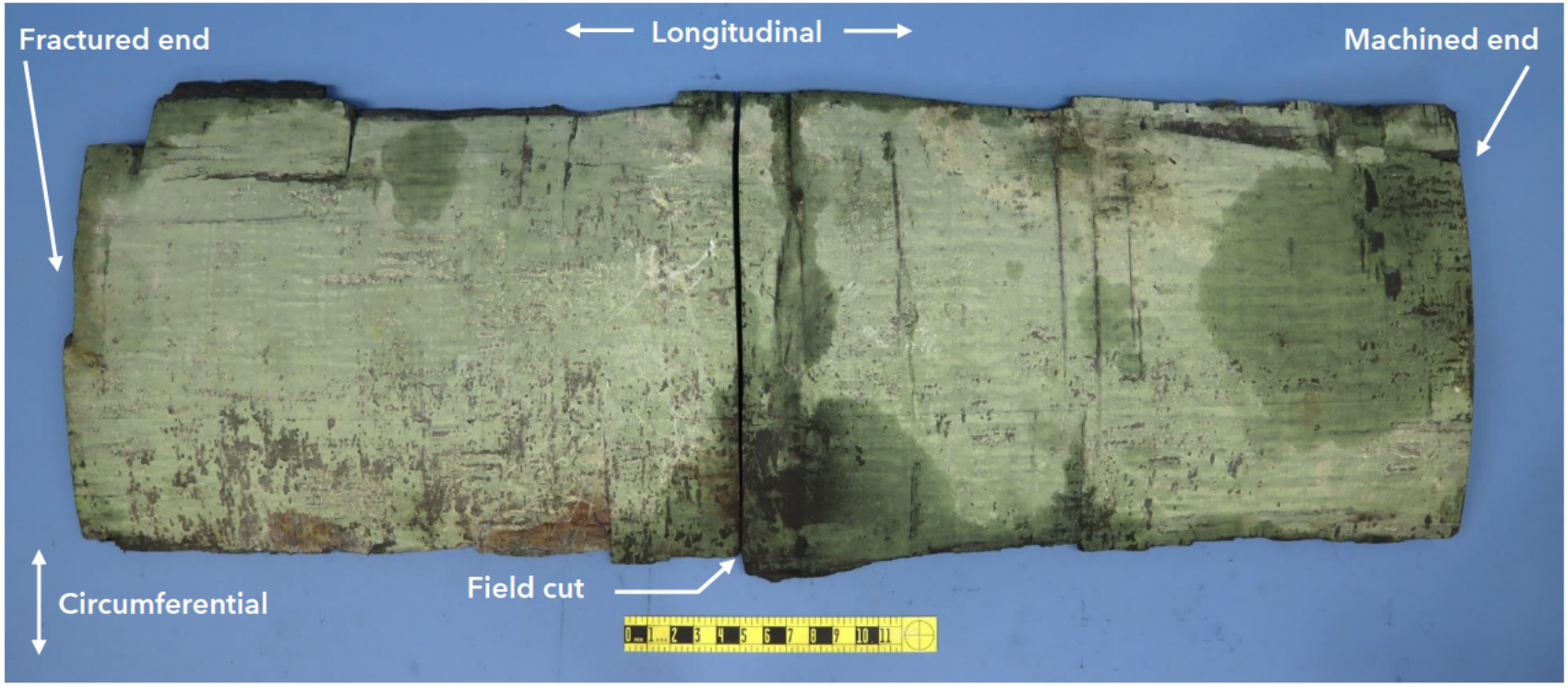

Figure 1. Images of recovered carbon fiber composite hull piece: a) Outer surface;

b) 

Figure 1 (cont.). b) inner surface;

c)

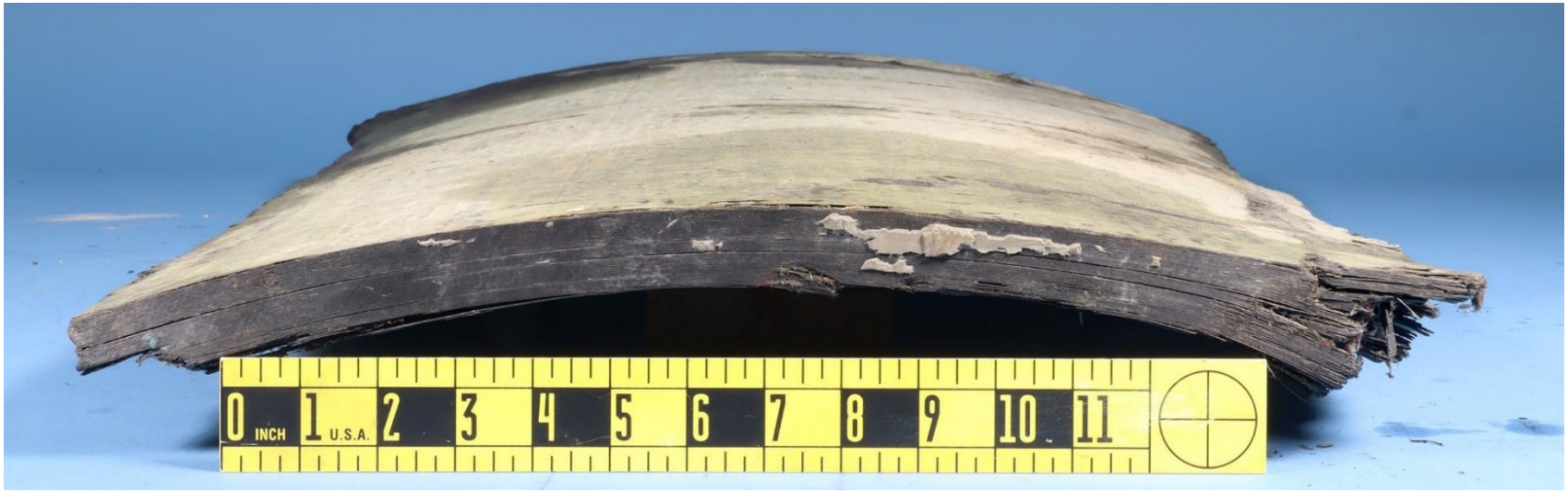

d)

Figure 1 (cont.). c) machined end face; d) mid-span fractured face; and

e) 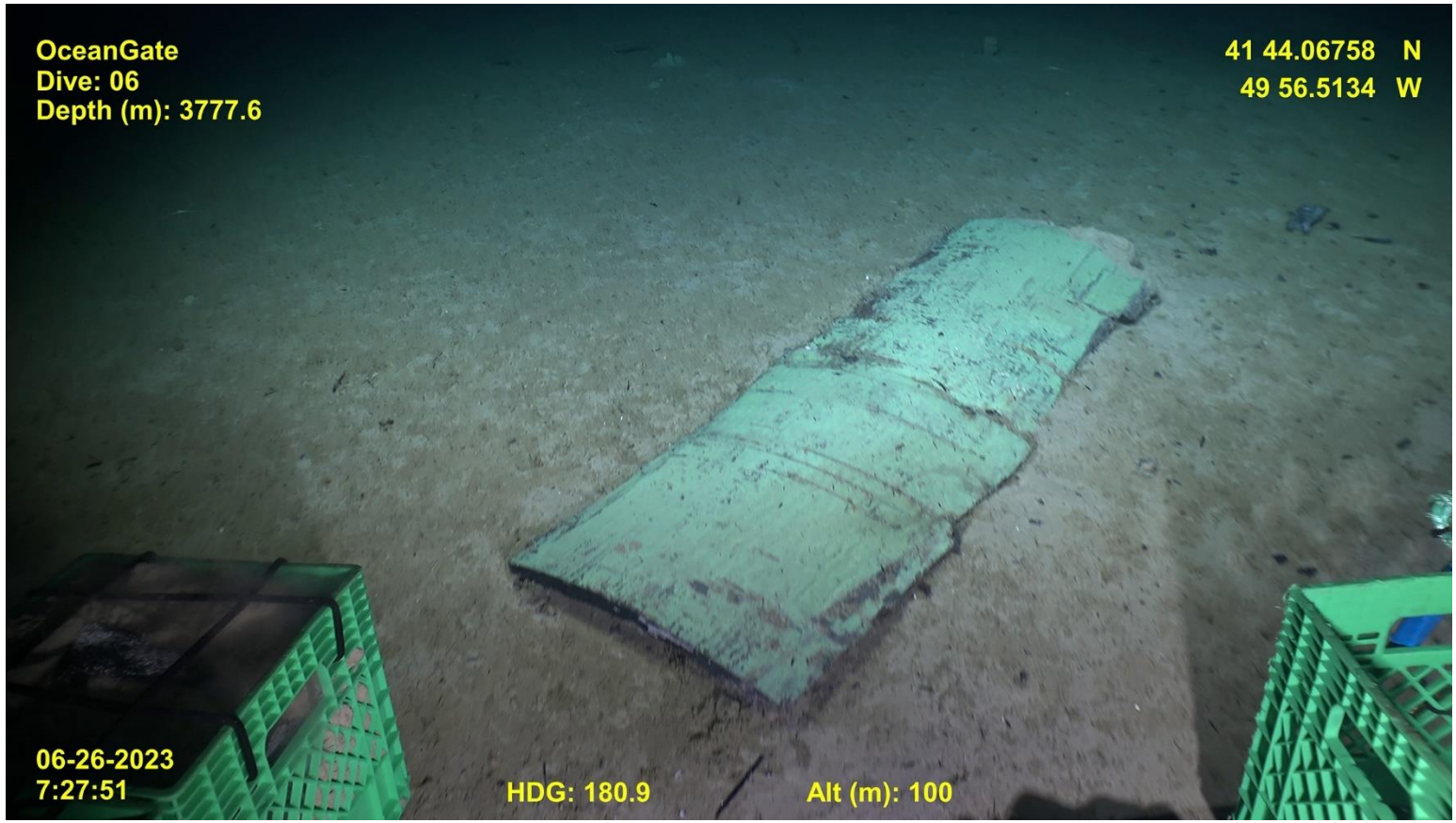

Figure 1 (cont.). e) hull piece as found on the ocean floor.

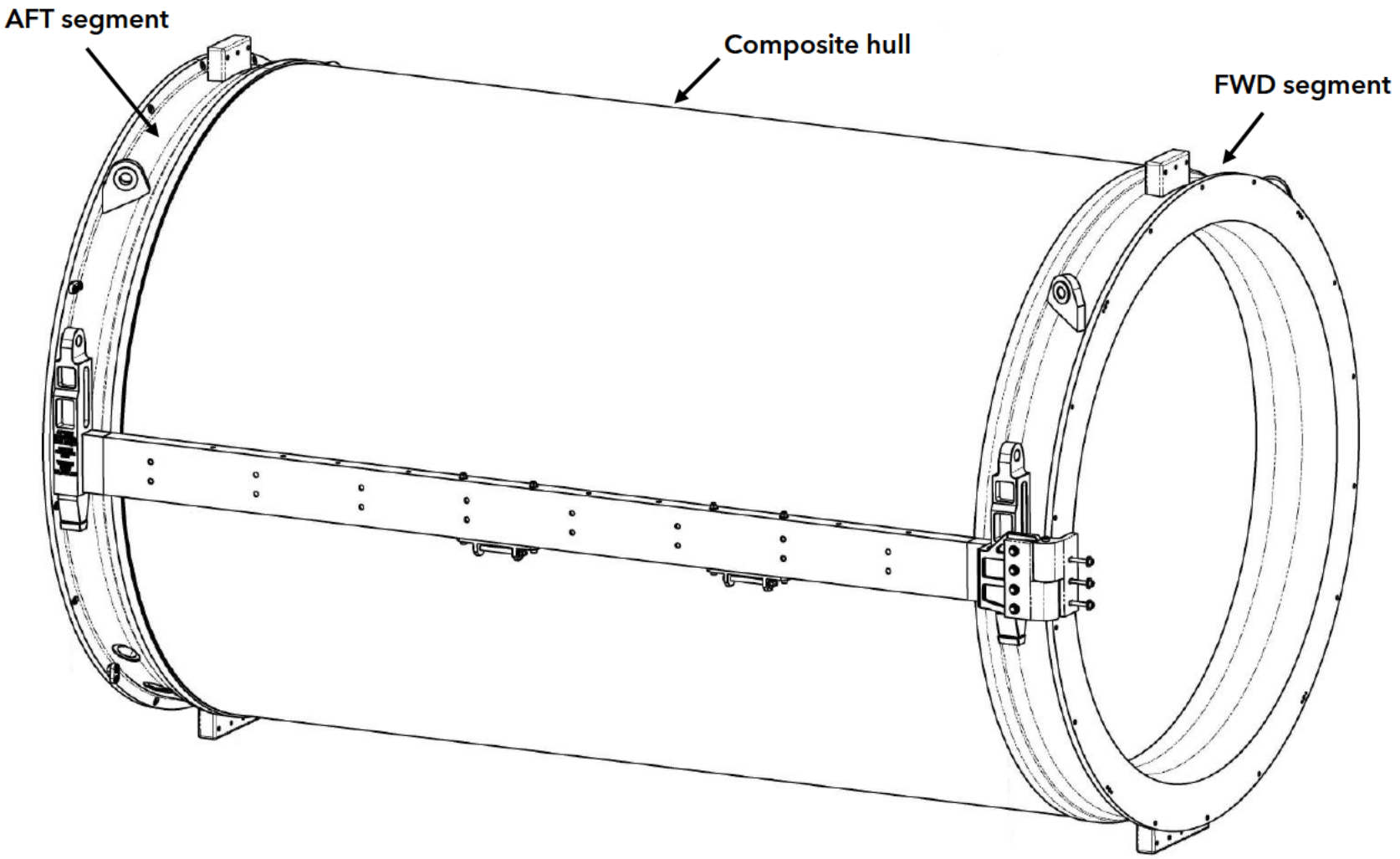

Figure 2. Illustration of the pressure vessel hull and end segments. Spherical half-domes (not shown) were bolted to the segments at either end.

a)

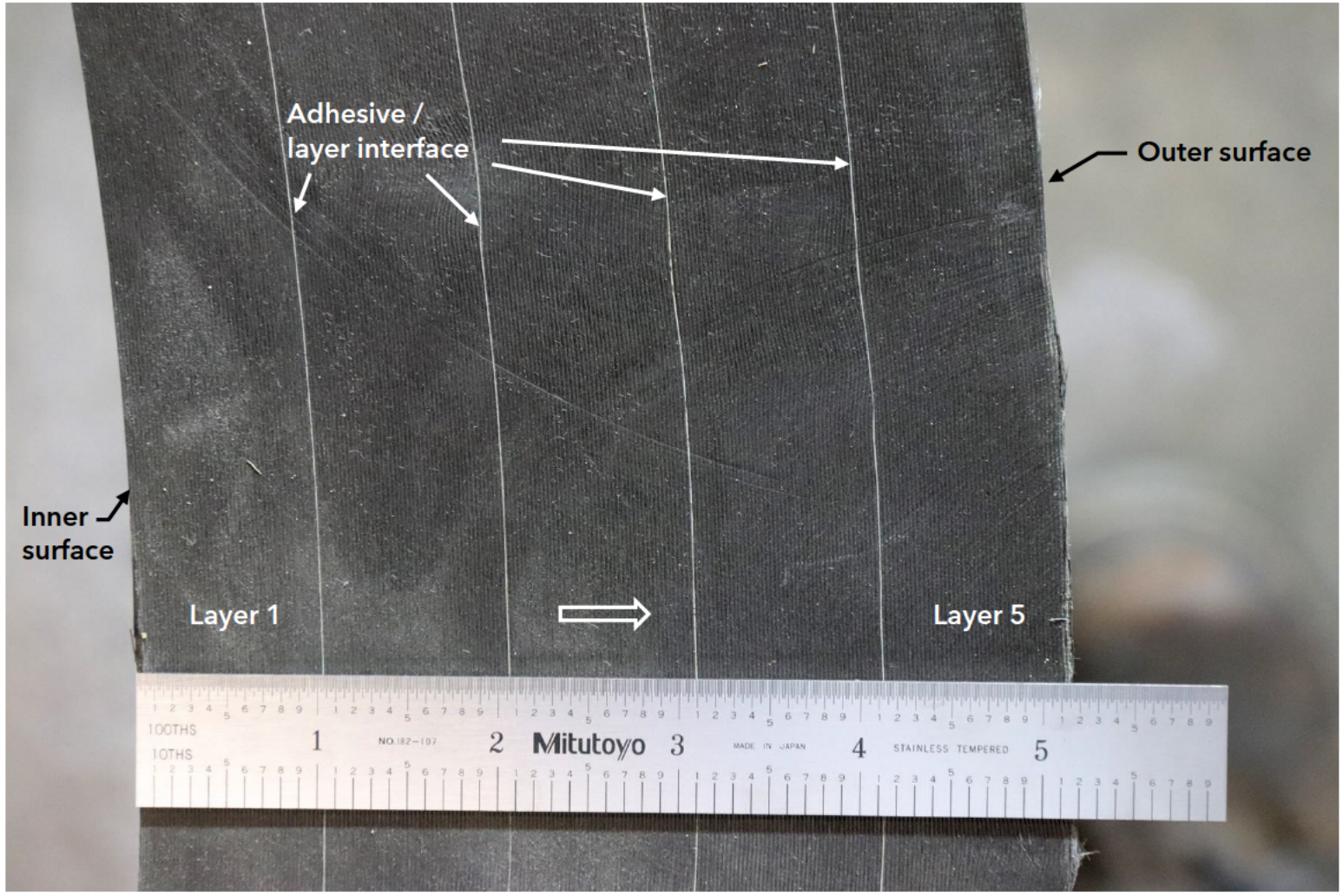

Figure 3. a) Cross section through the hull wall showing the co-bonded layered structure.

b)

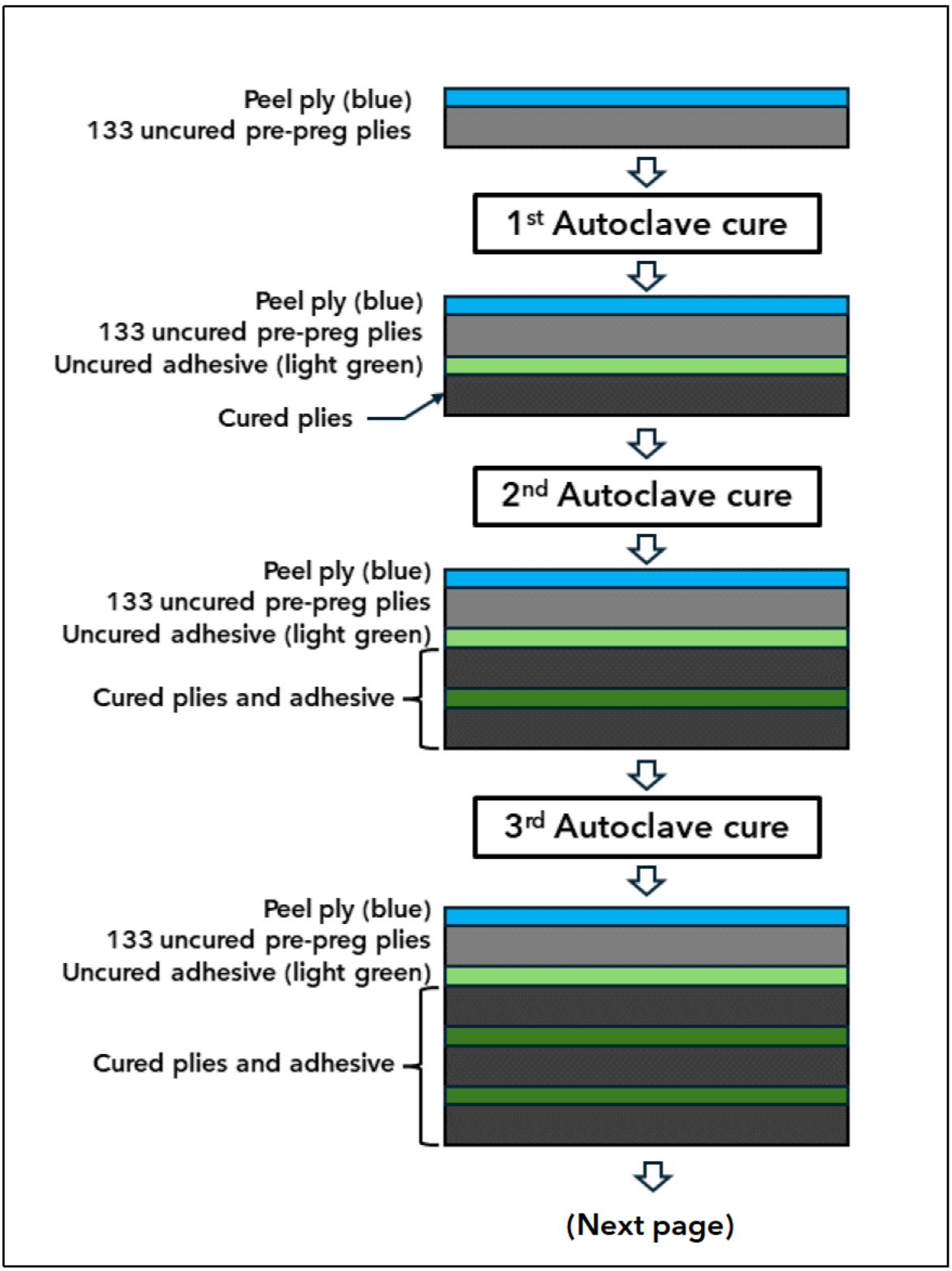

Figure 3 (cont.). b) Illustration showing the co-bonding process in cross-section by which the Titan hull was manufactured.

b)

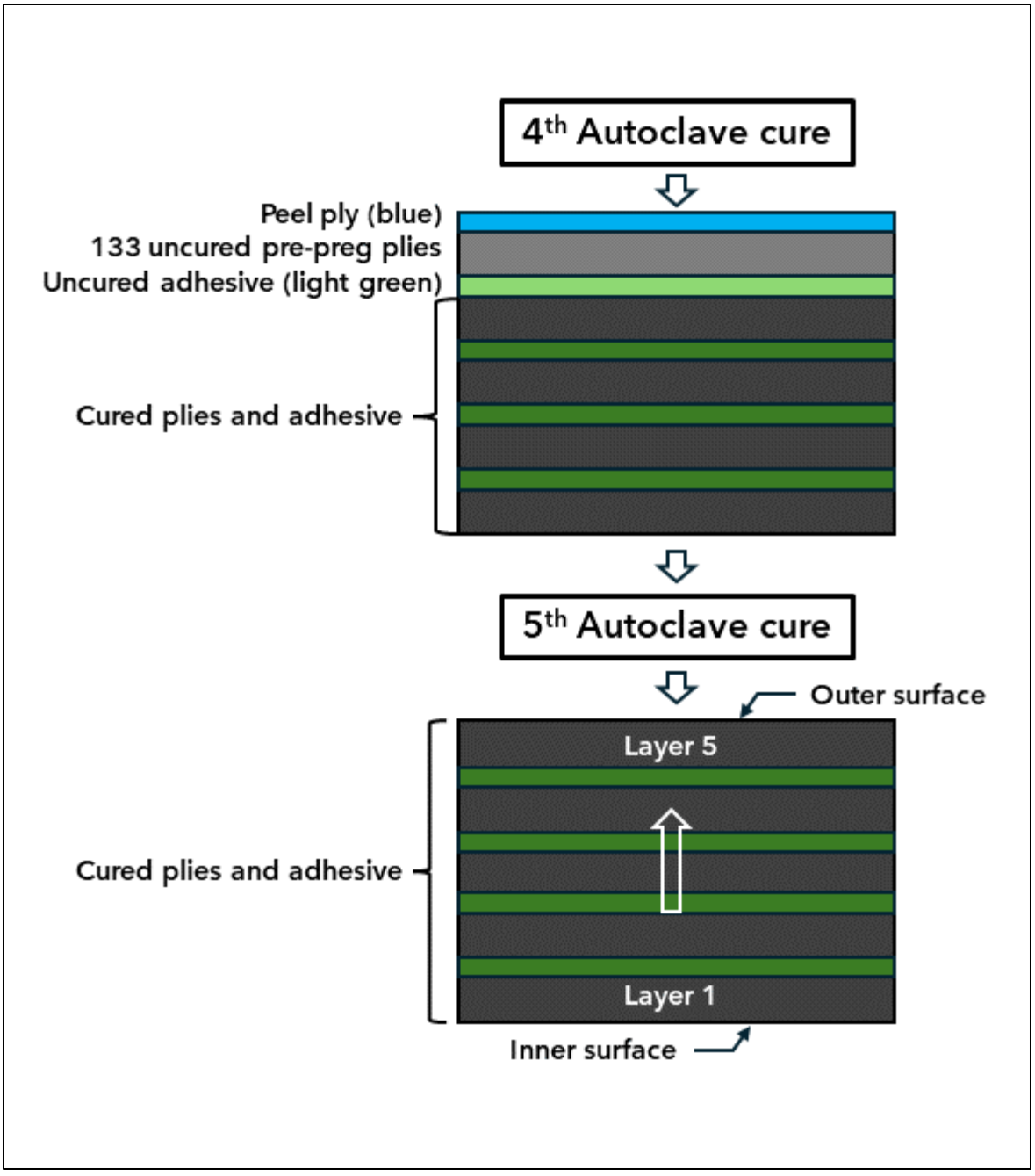

Figure 3 (cont.). b) Illustration showing the co-bonding process in cross-section by which the Titan hull was manufactured.

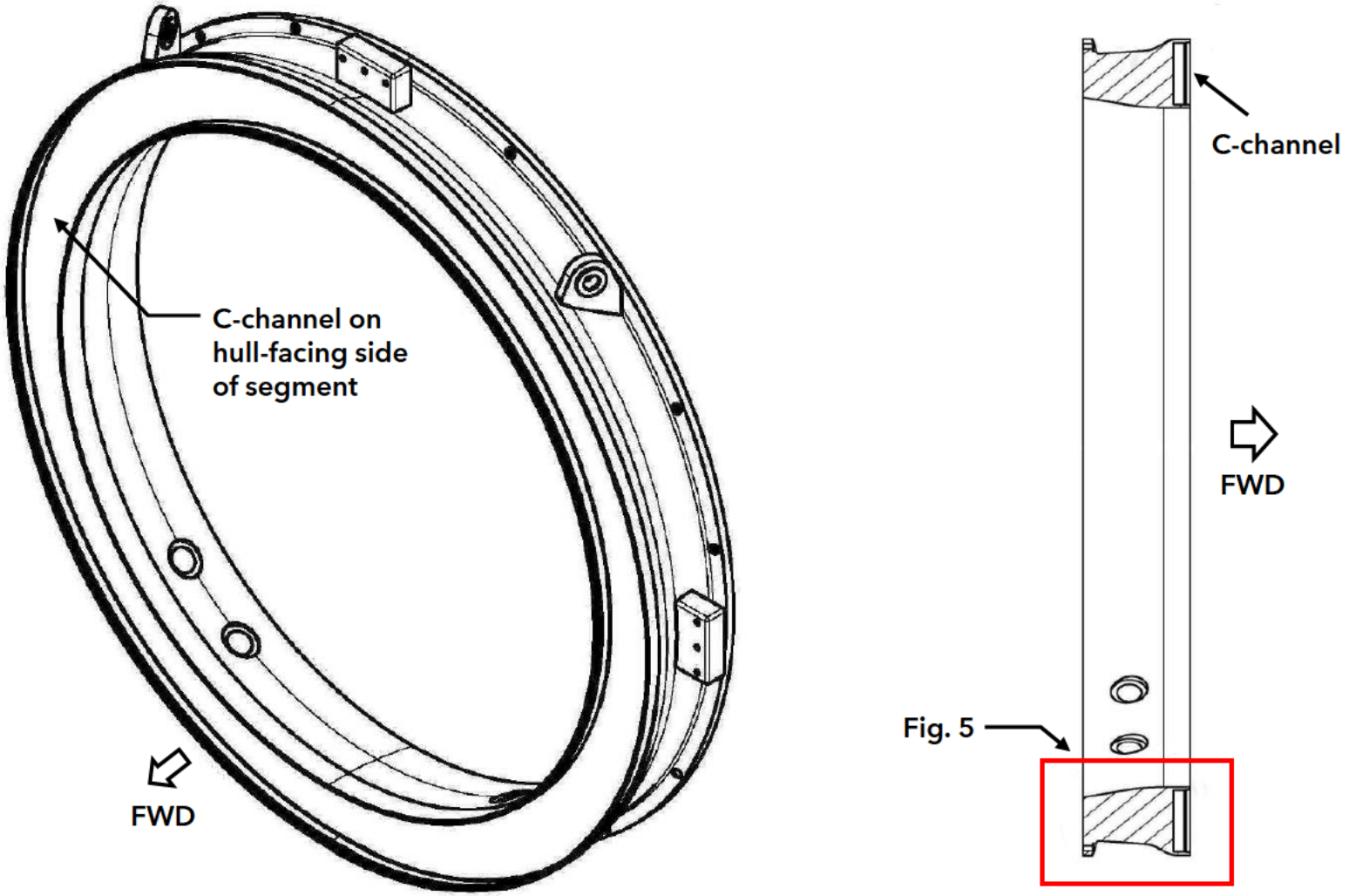

Figure 4. Illustrations of the aft hull segment.

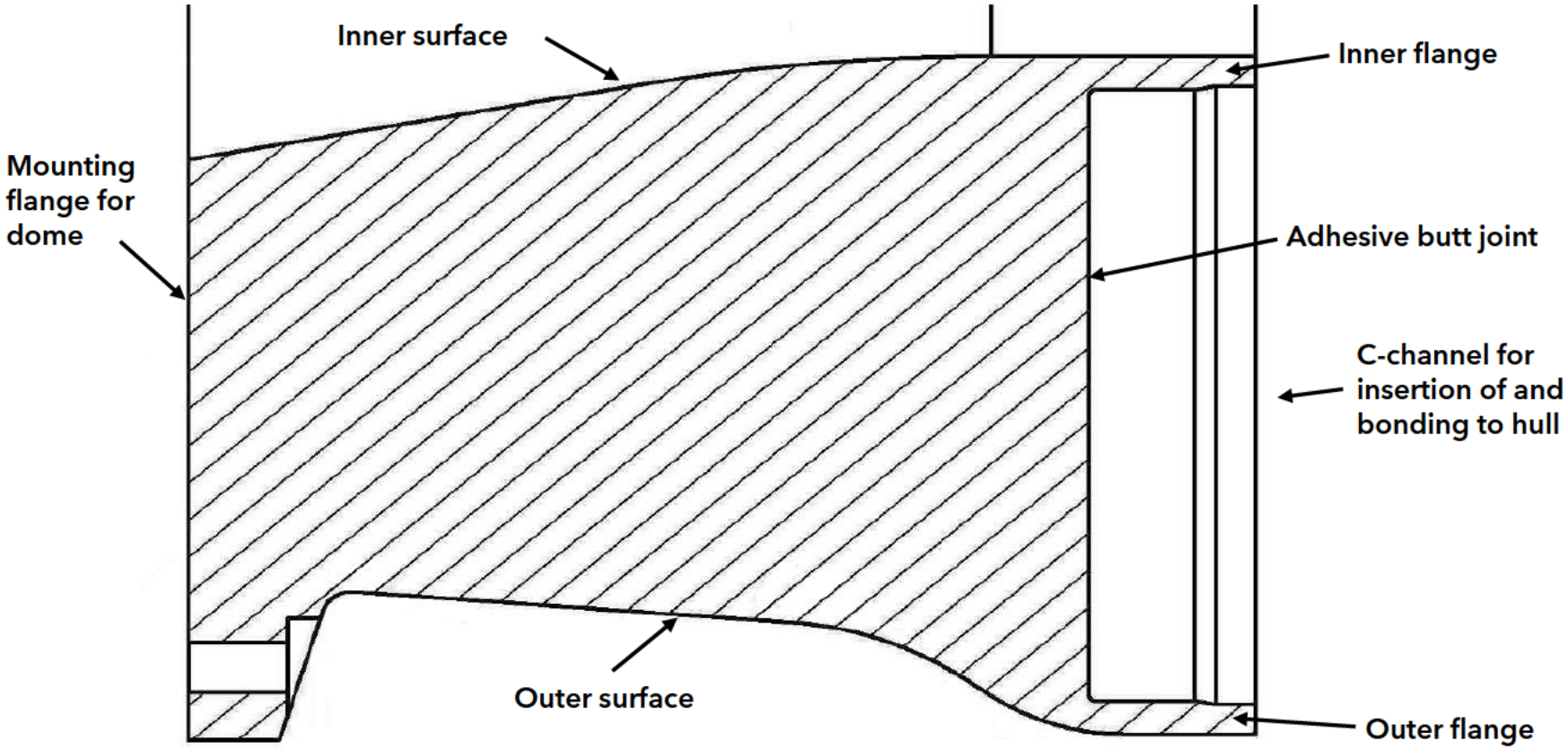

Figure 5. Illustration showing the cross-section profile of the annular segment including the C-channel for adhesive bonding to the composite hull.

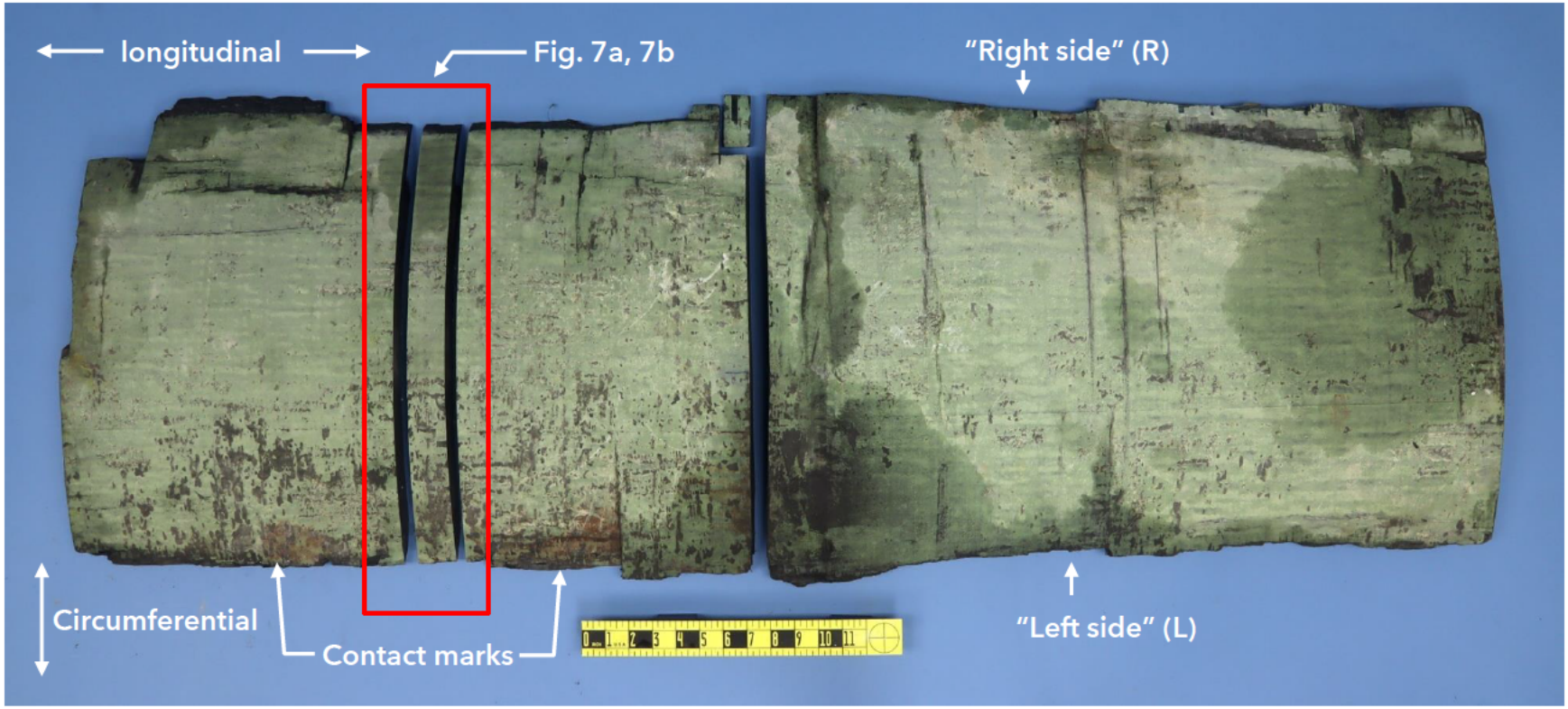

Figure 6. Strip of hull piece cut for closer examination.

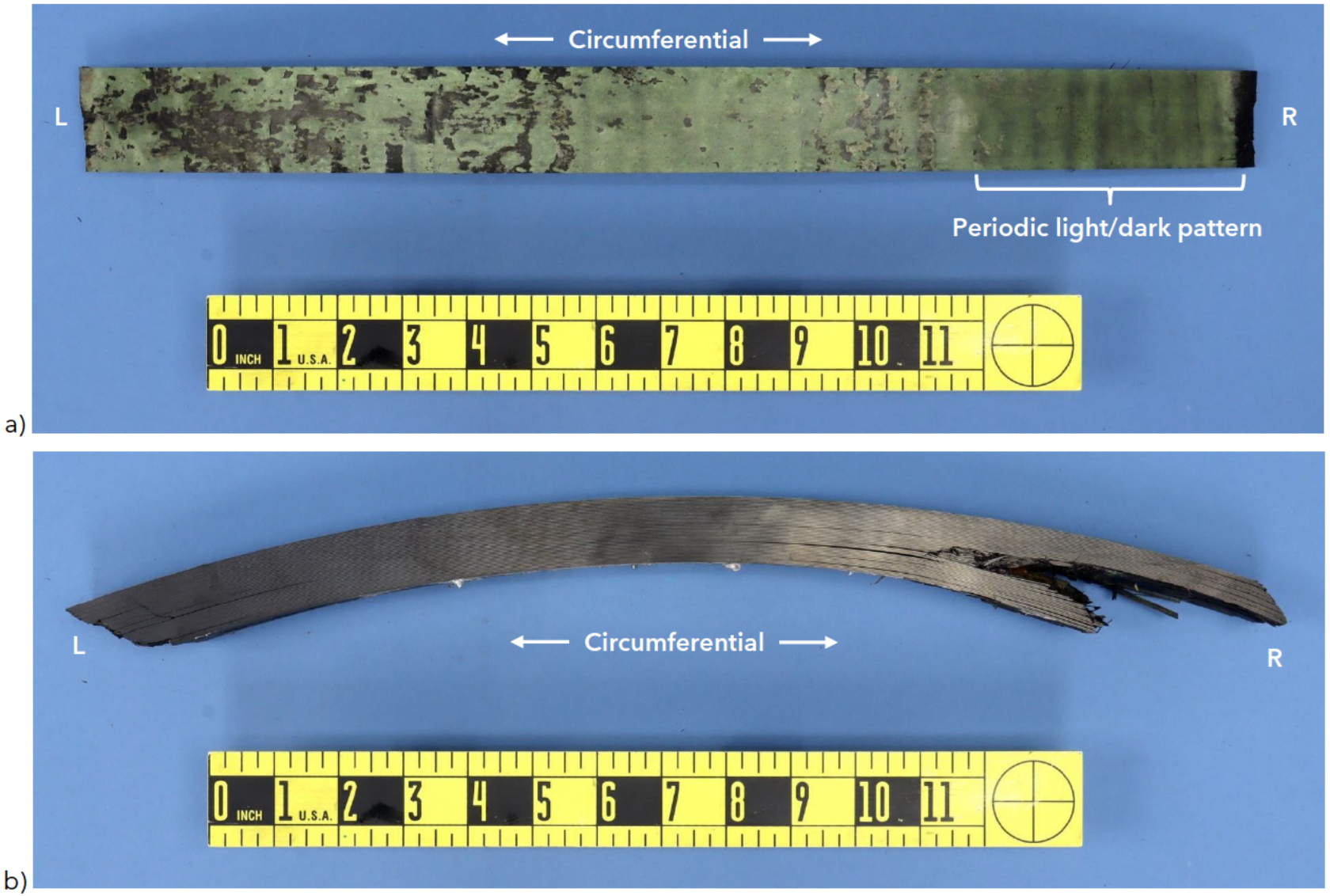

Figure 7. Images of hull piece cut for closer examination: a) plan view and b) cross section view.

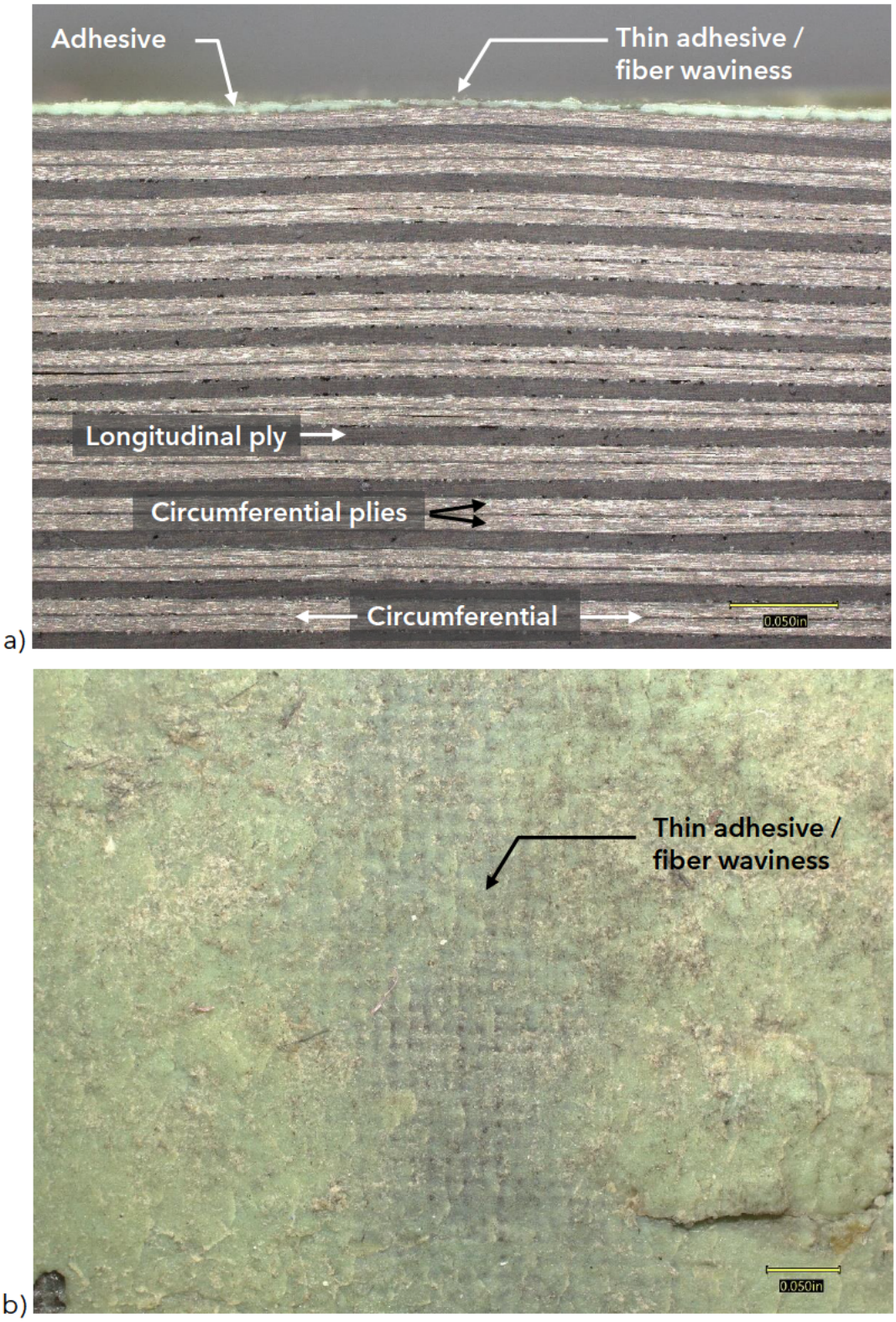

Figure 8. a) Cross section image showing waviness of composite plies and variation in adhesive thickness and b) plan view image showing variation in adhesive color.

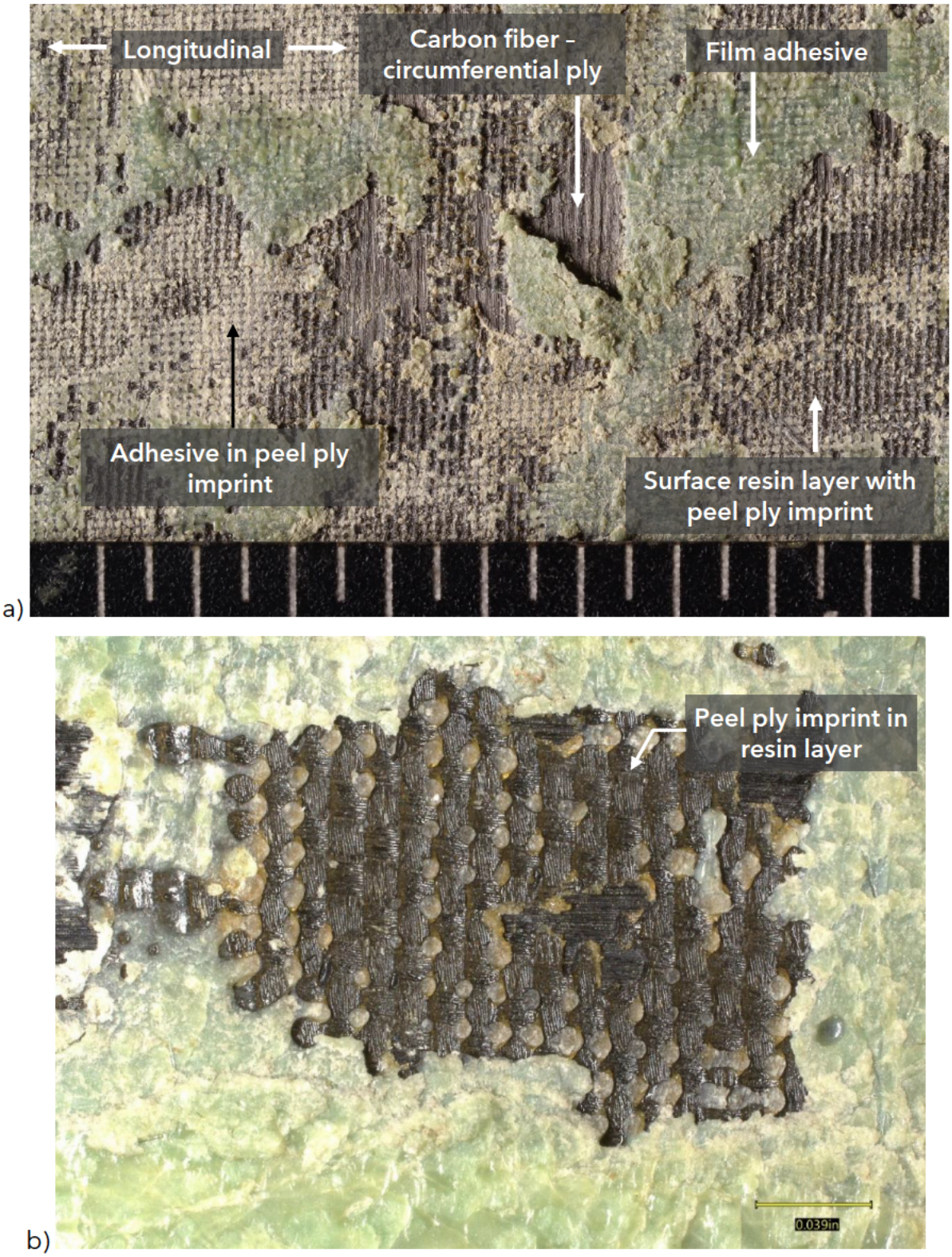

Figure 9. Images of layer 1 surface: a) region with all the components of the layer interface with labels; b) void in adhesive. Underlying resin with a peel ply imprint is exposed.

c)

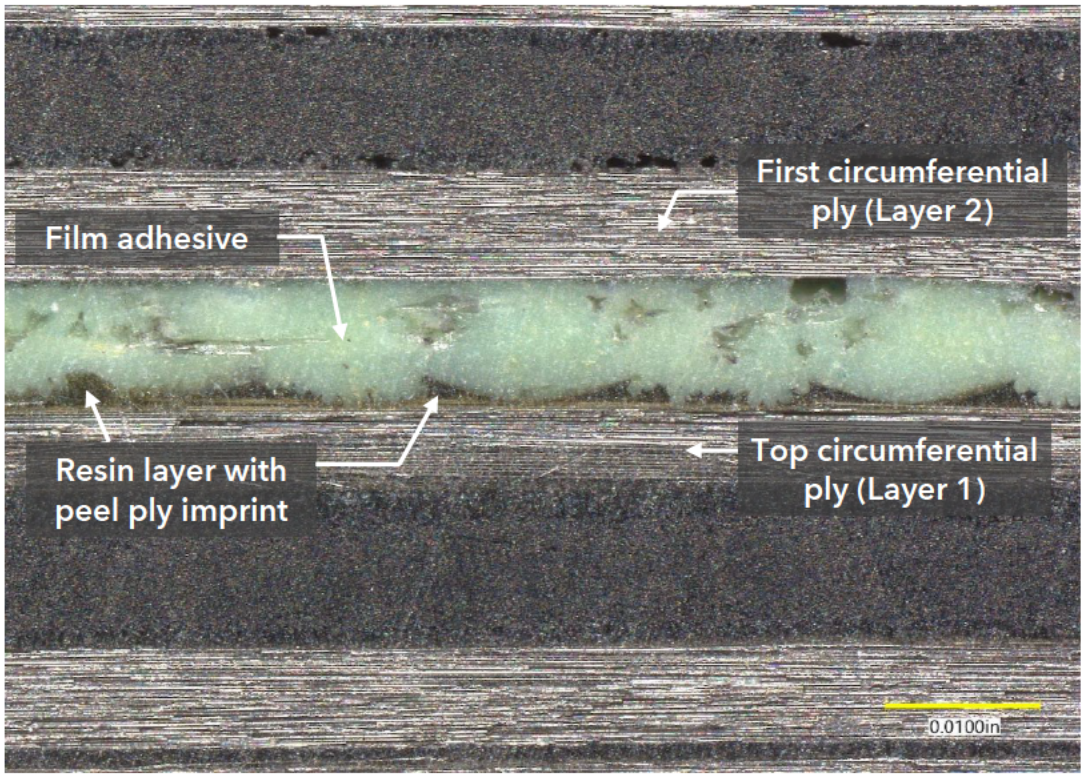

d)

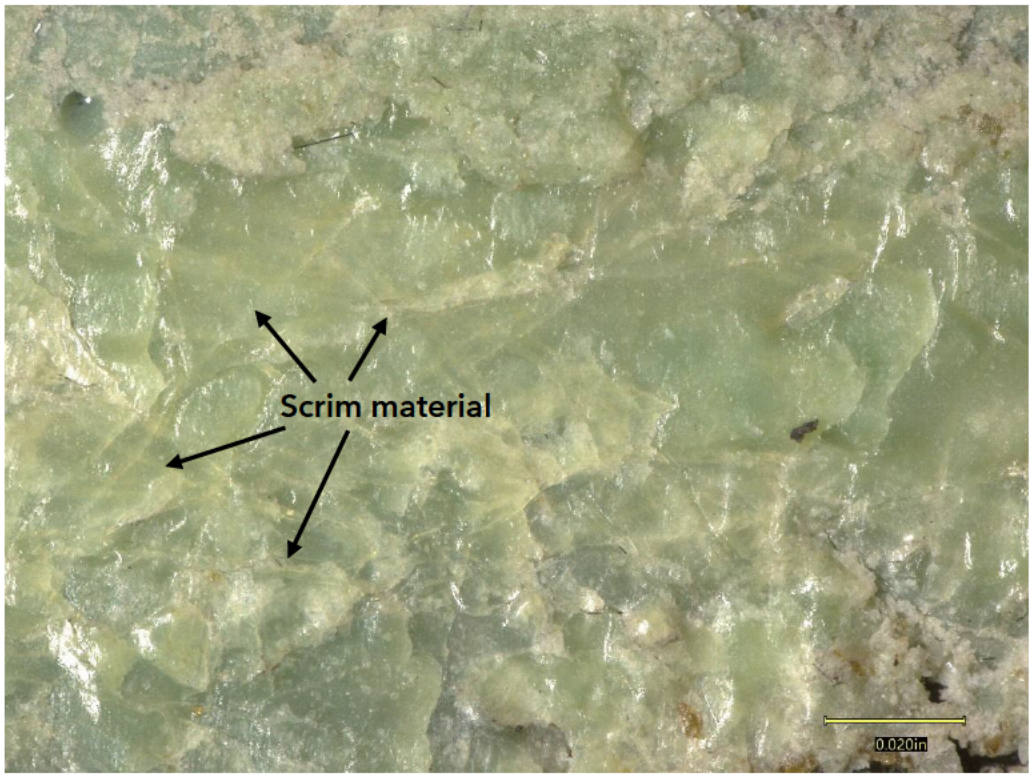

Figure 9 (cont.). c) cross section from a trimmed end piece of the Titan hull showing the location of the amber resin layer, overlying adhesive, and interface between the adhesive and the second co-bonded layer; and d) image showing non-woven scrim material.

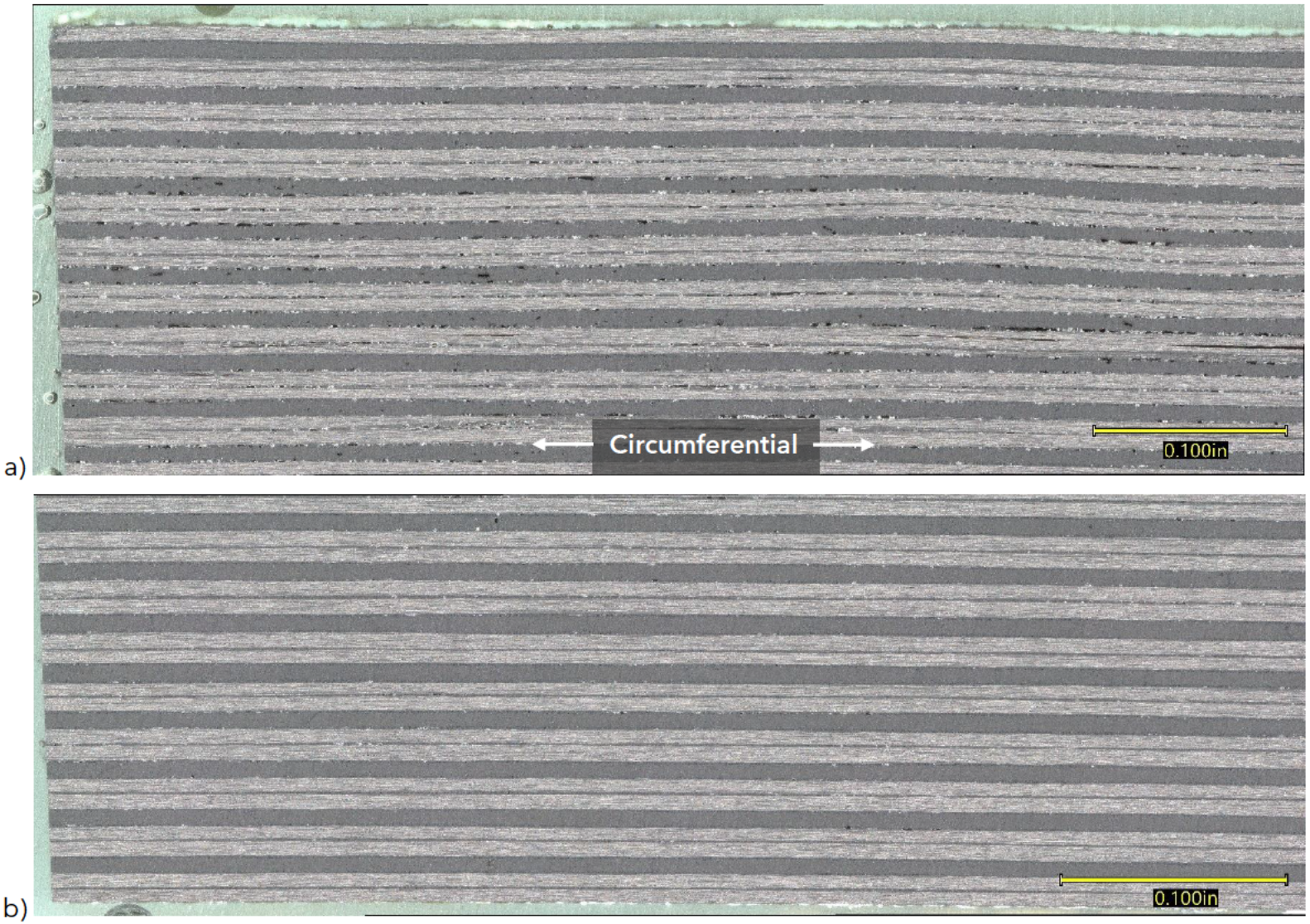

Figure 10. Images showing the composite ply stack: a) near the top of layer 1 and b) near the base of layer 1.

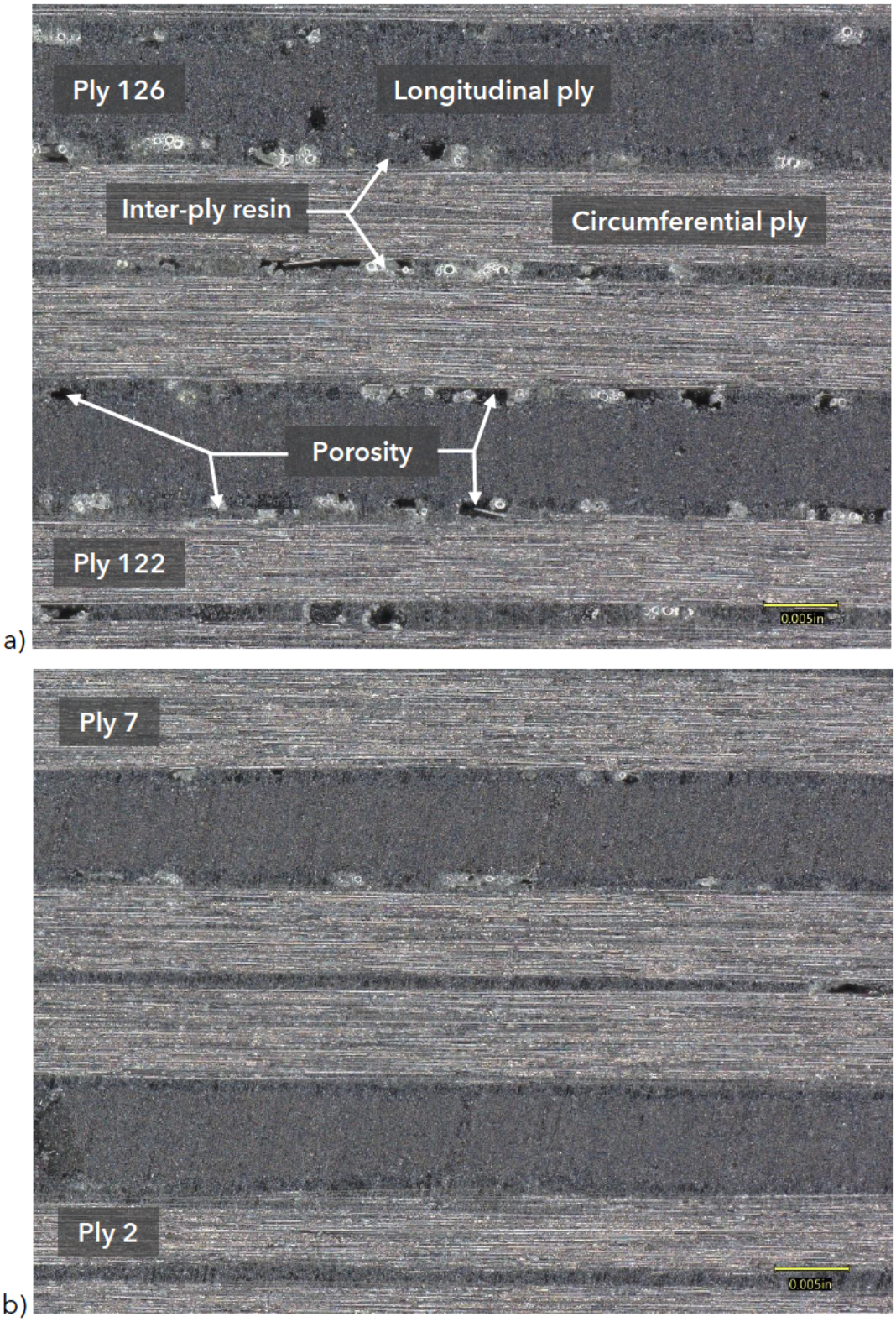

Figure 11. Higher magnification cross section images showing the variation in porosity in the inter-ply resin layers: a) plies 122 – 126 and b) plies 2 – 7.

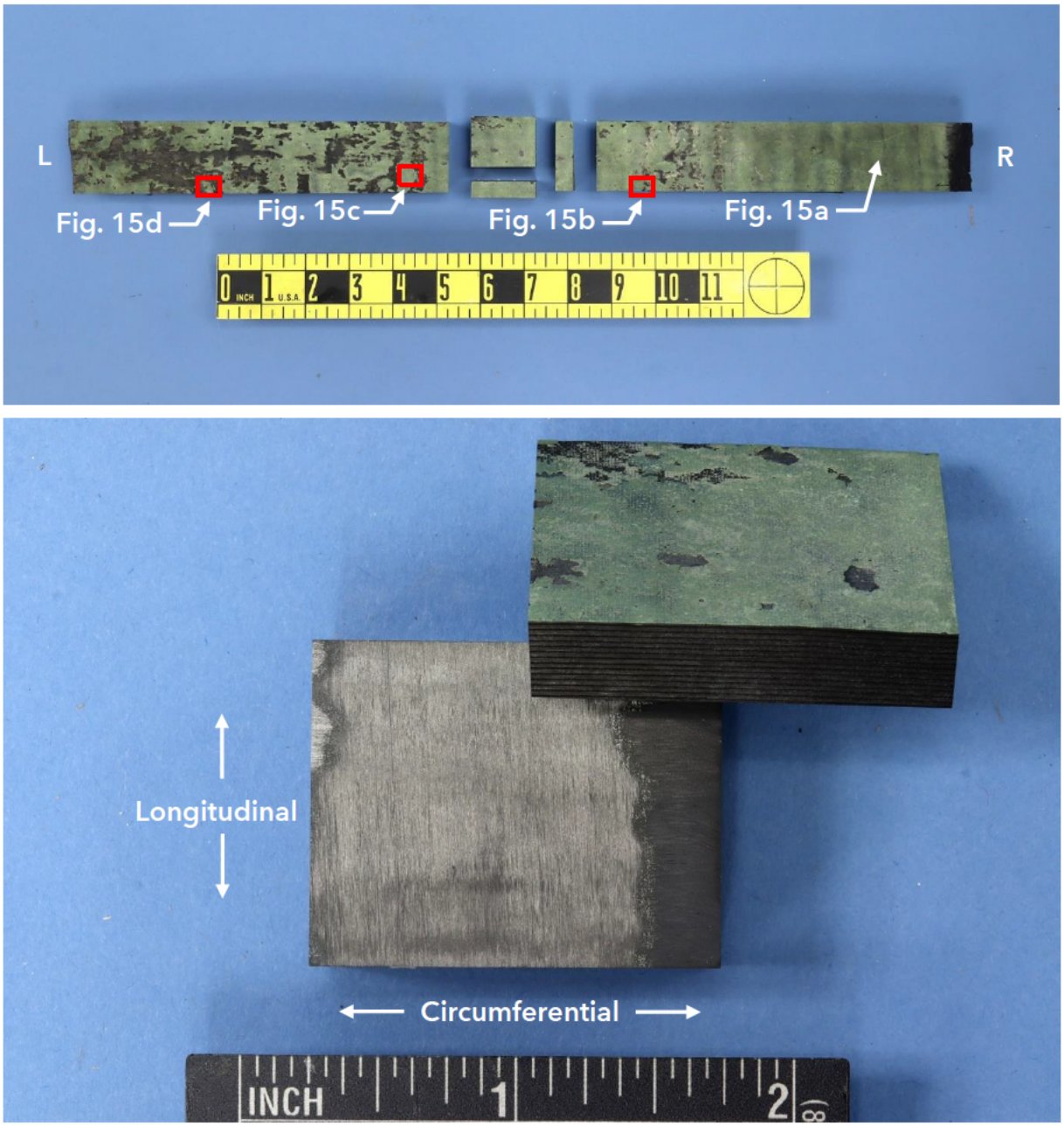

Figure 12. Upper image: overview image showing the location of cut pieces and the locations of images in figure 15. Lower image: Cross section cut roughly parallel to the hull outer and inner surfaces and near the middle of the layer.

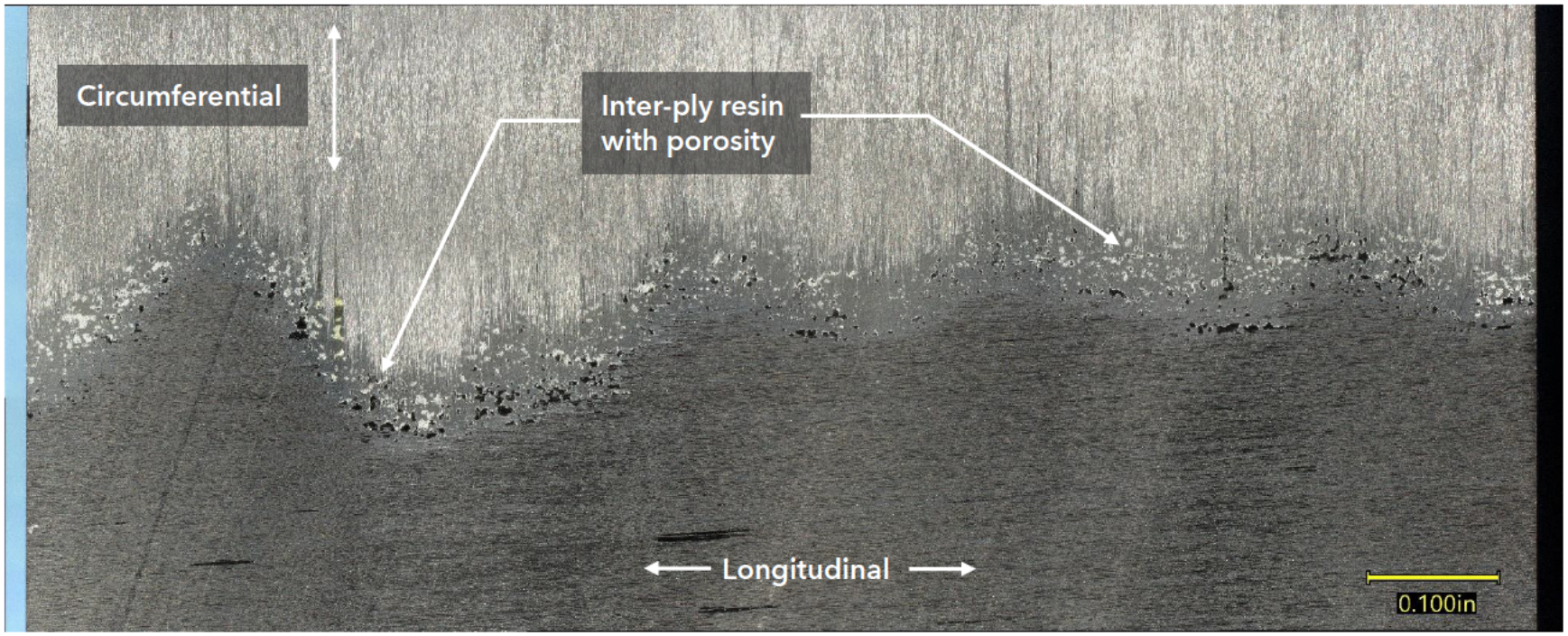

Figure 13. Oblique cut through inter-ply resin layer showing porosity within the layer.

a)

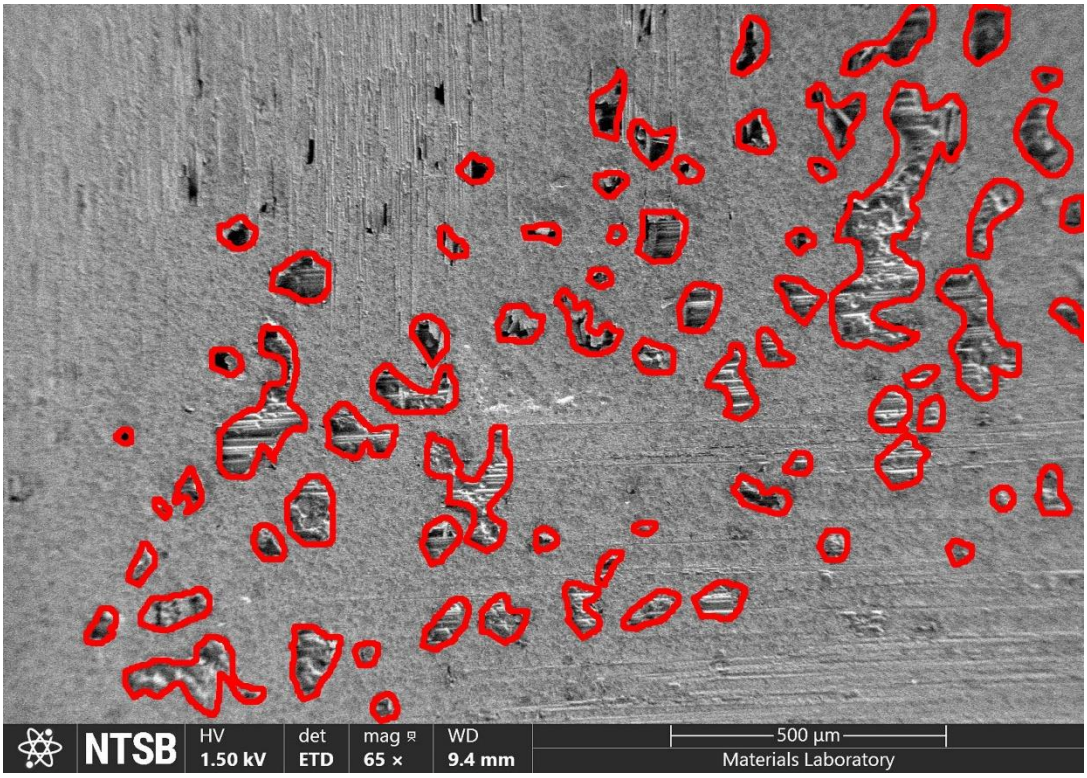

b)

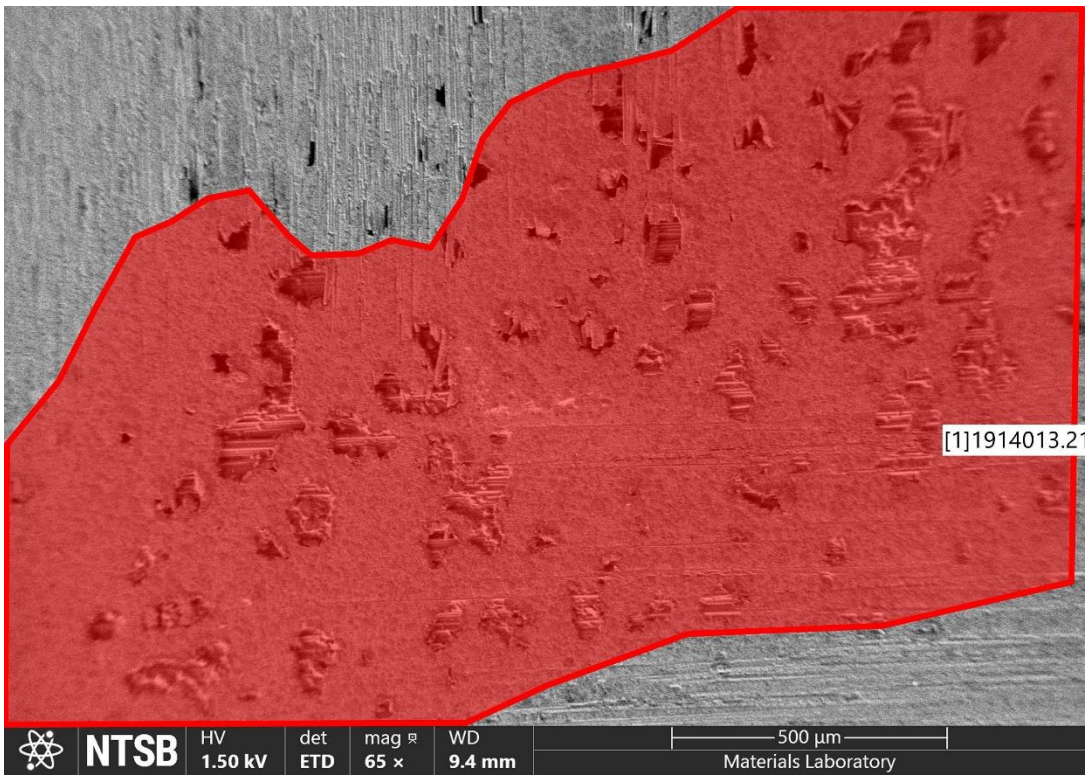

Figure 14. a) and b) images used for porosity fraction based on area measurement.

a)

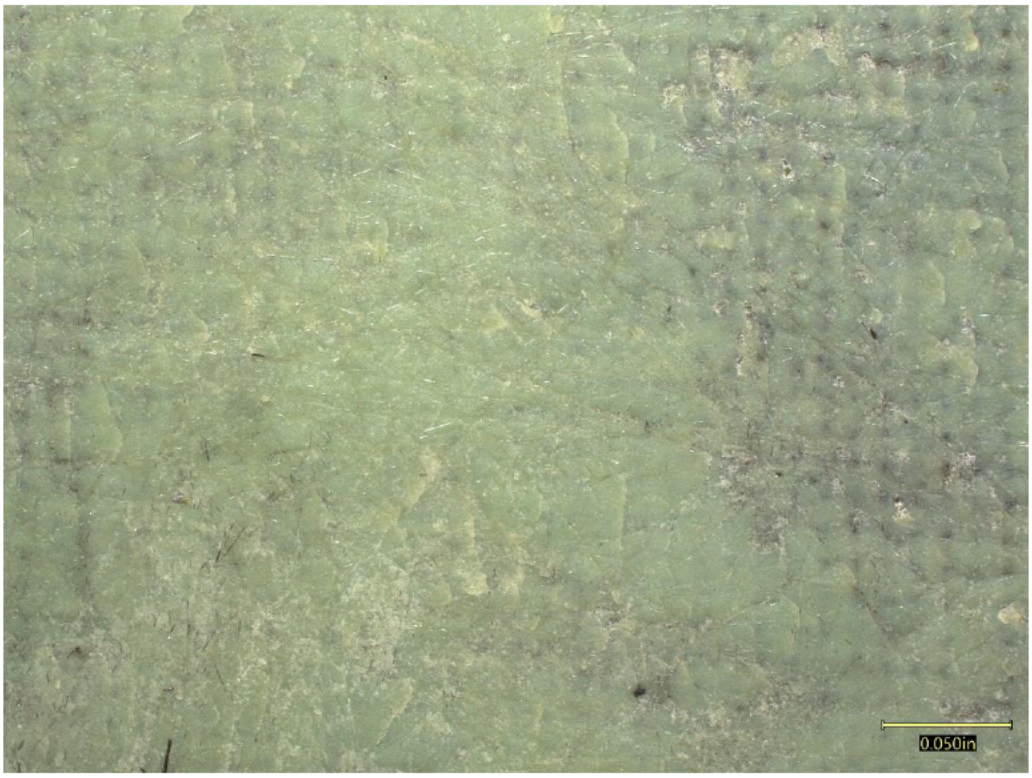

b)

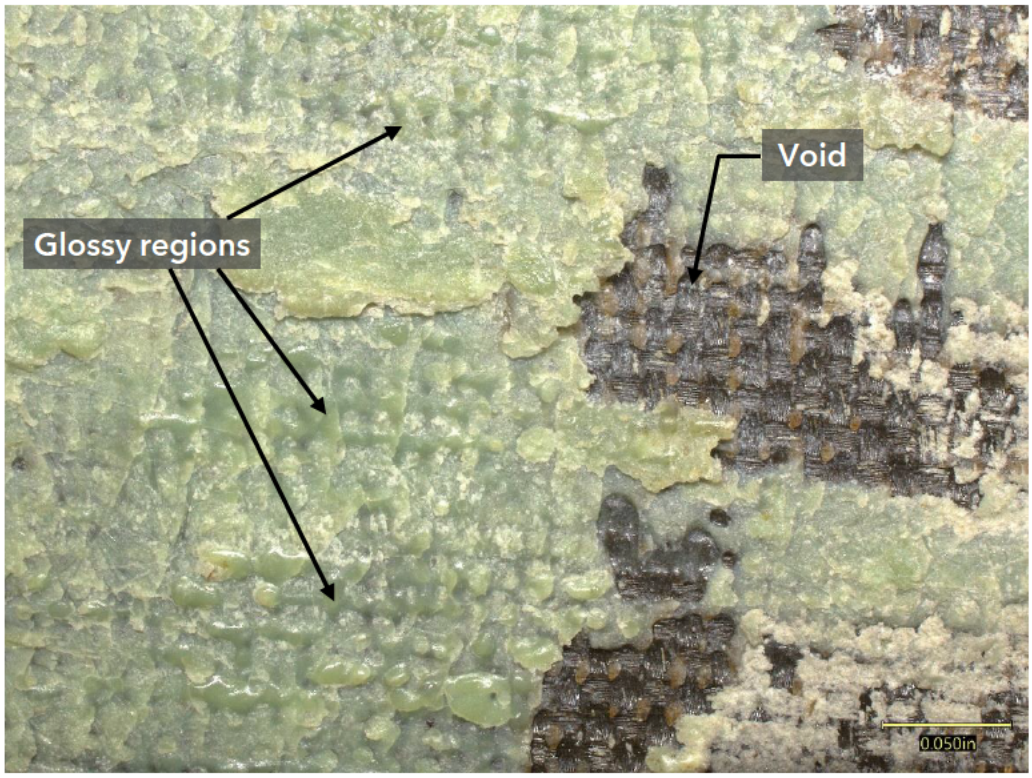

Figure 15. Image of adhesive surface as indicated in figure 12: a) rubbed appearance near "right side"; glossy regions and voids.

c)

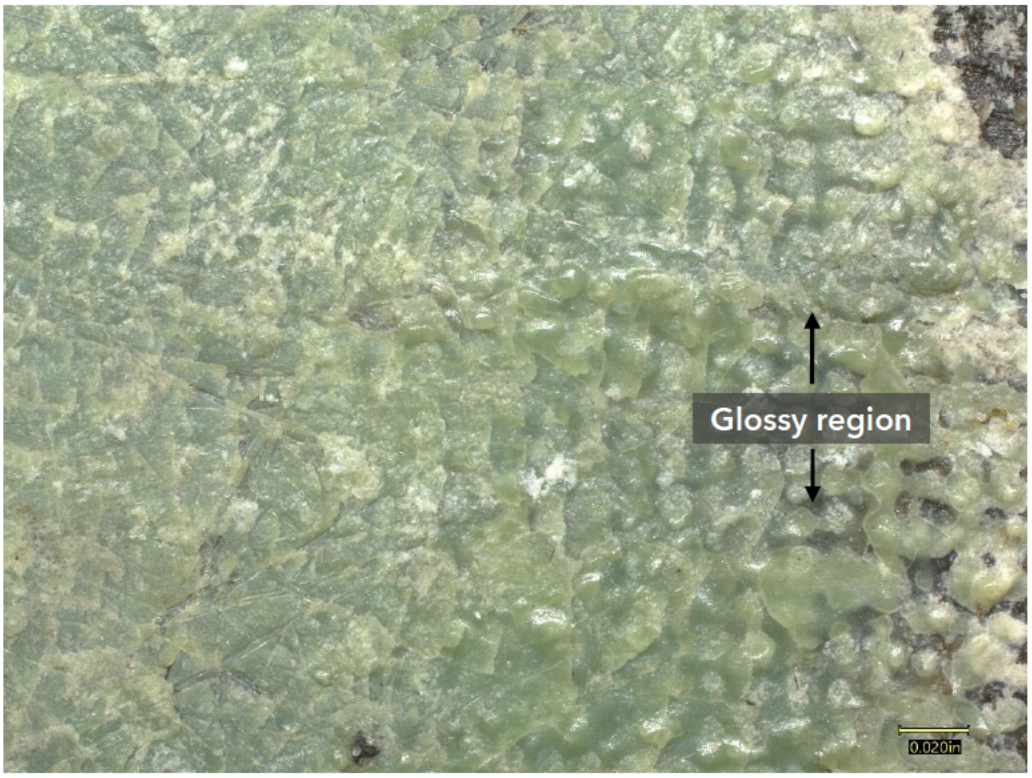

d)

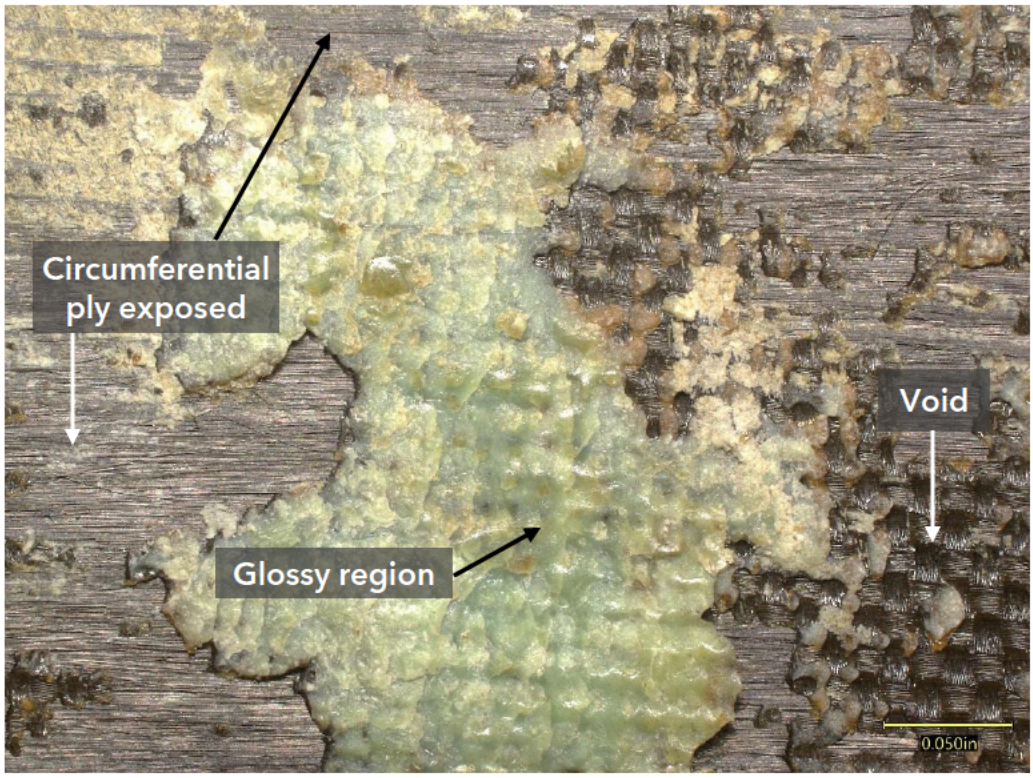

Figure 15 (cont.). c) more glossy regions; and d) similar features but with additional regions where the adhesive and resin have separated exposing the underlying composite ply.

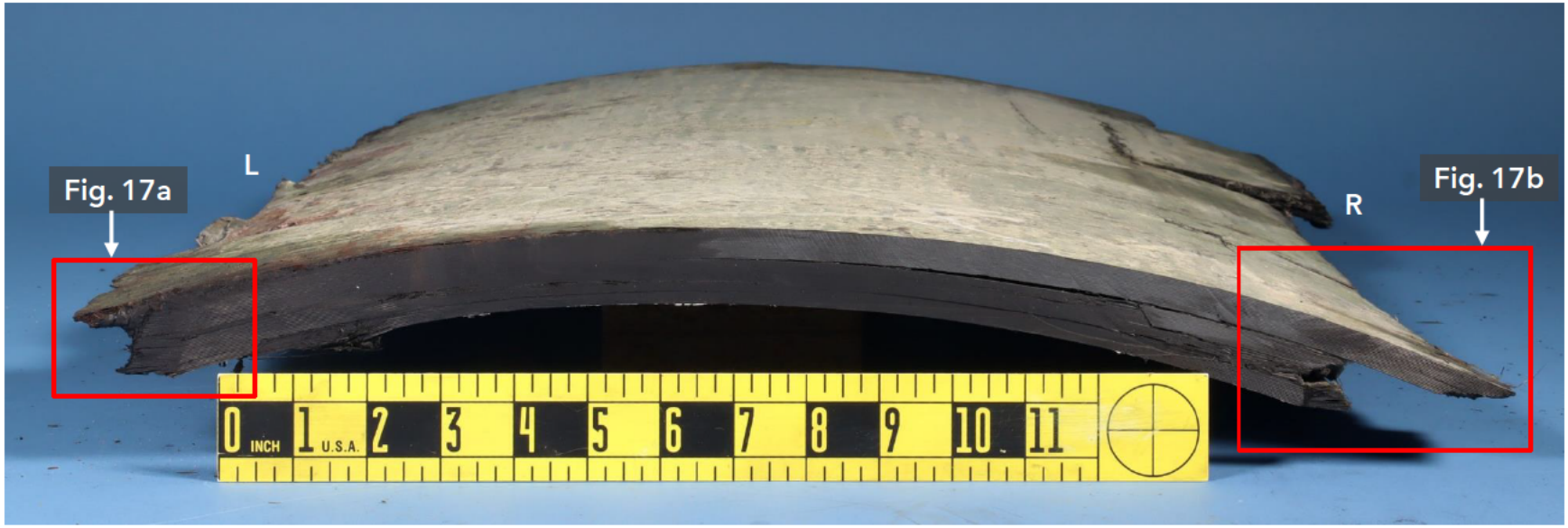

Figure 16. Image of hull with the locations of additional images indicated.

a)

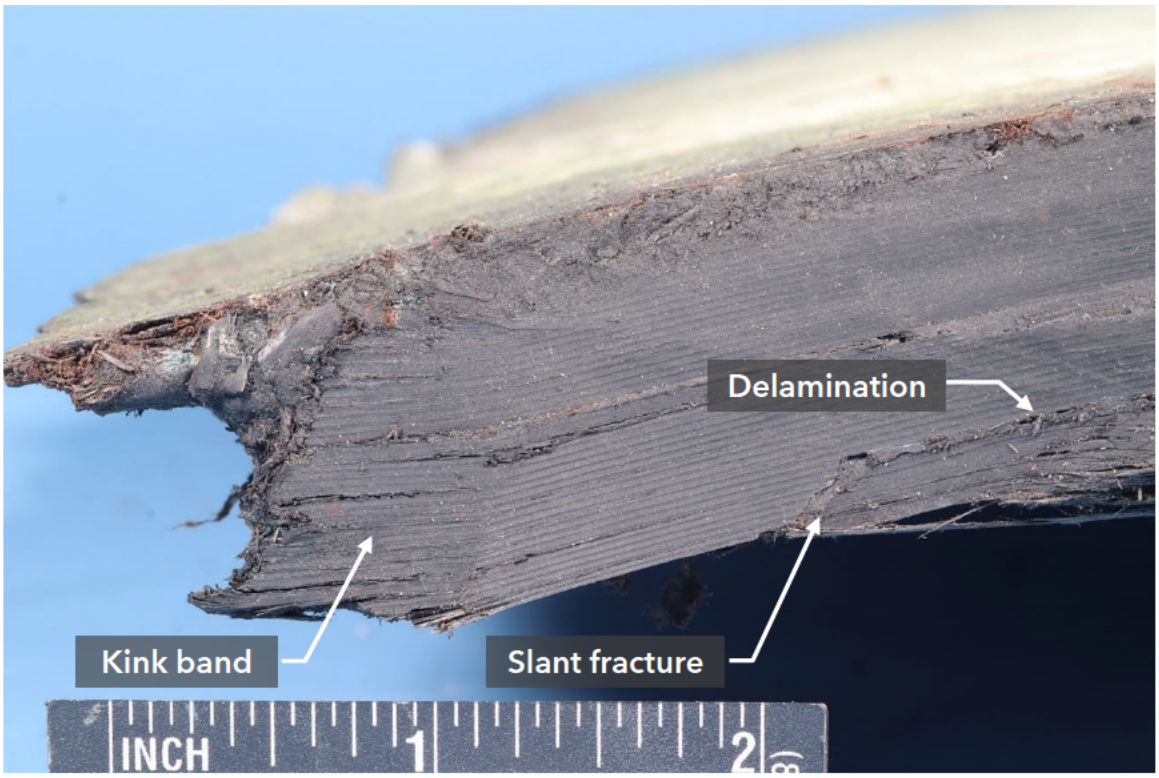

b)

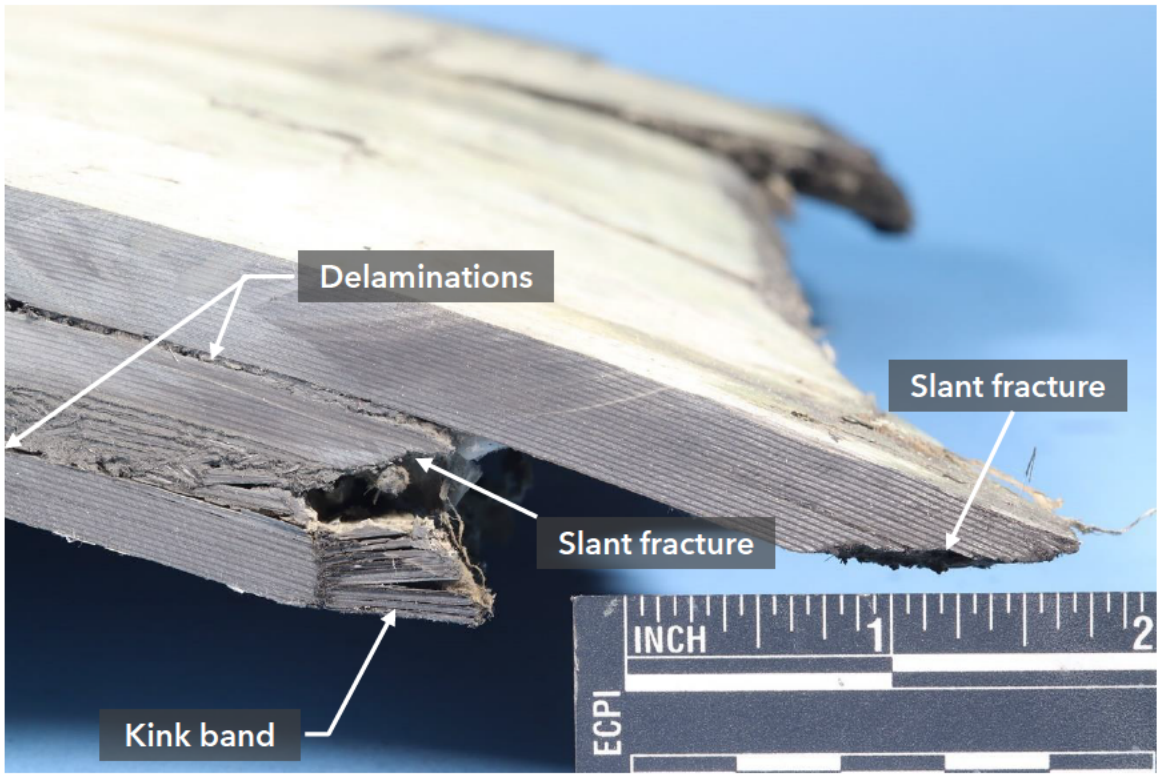

Figure 17. a) Fracture along left side and b) fracture along right side.

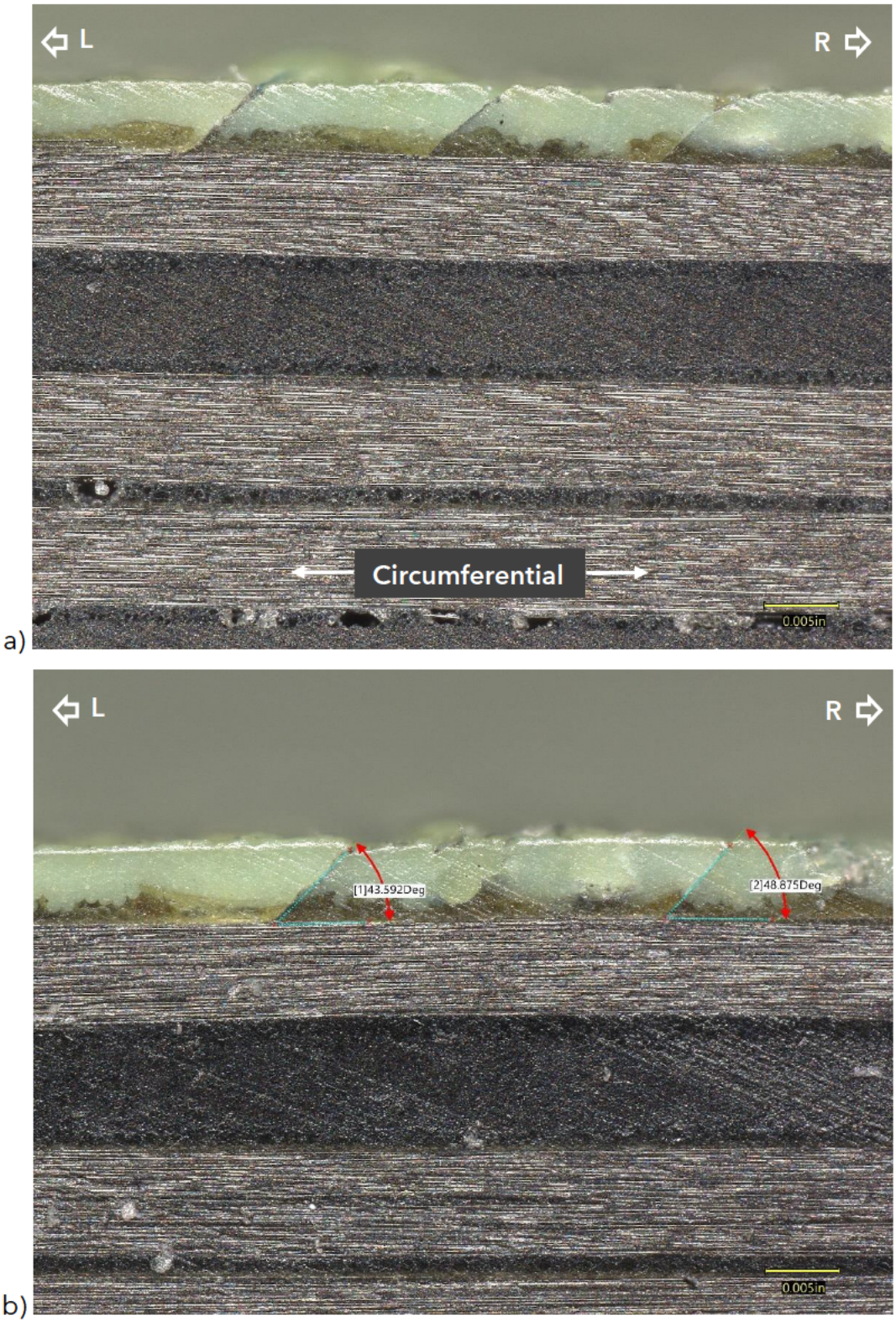

Figure 18. a) and b) 45° slant cracks in the adhesive atop layer 1.

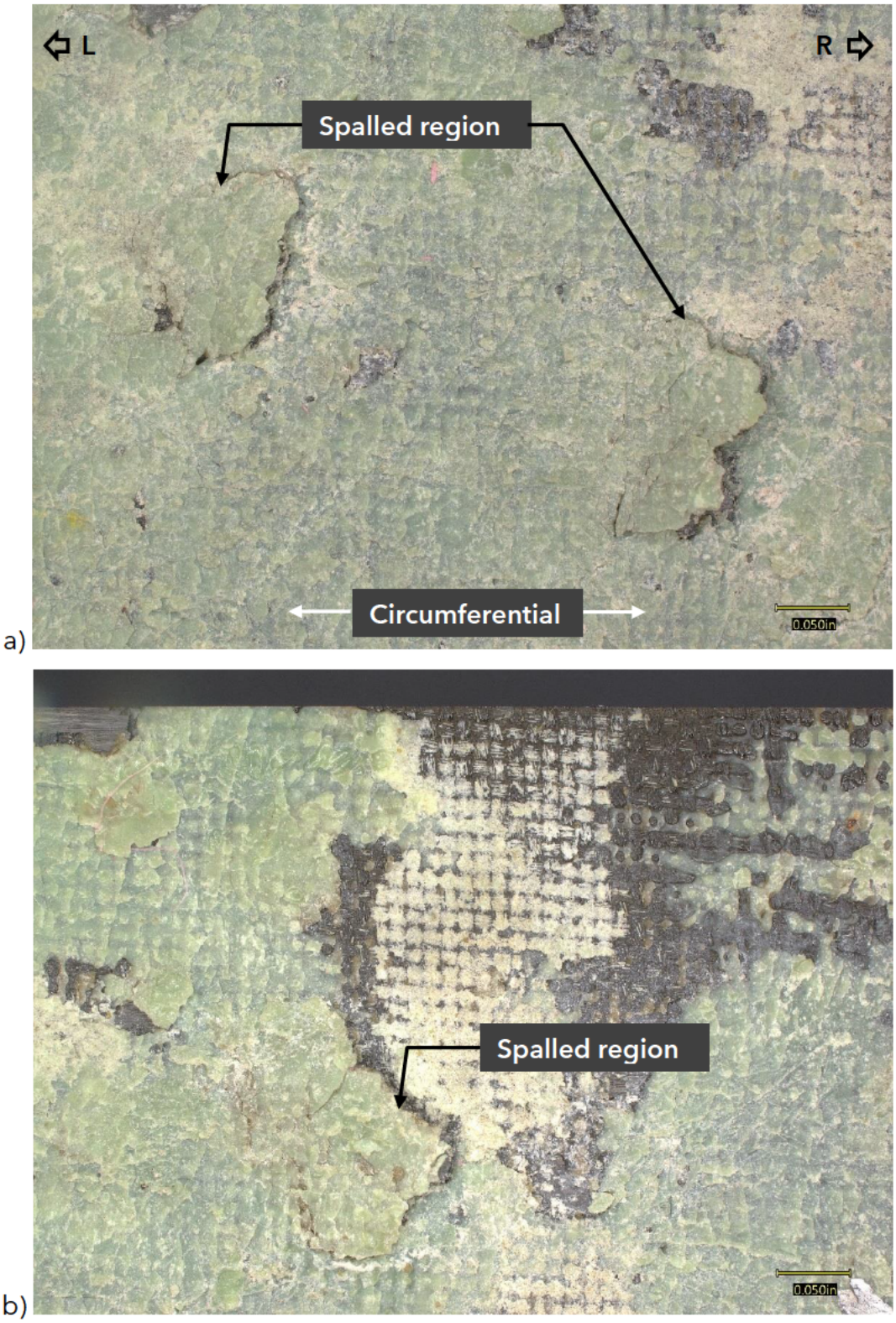

Figure 19. a) and b) regions with spalled adhesive layer.

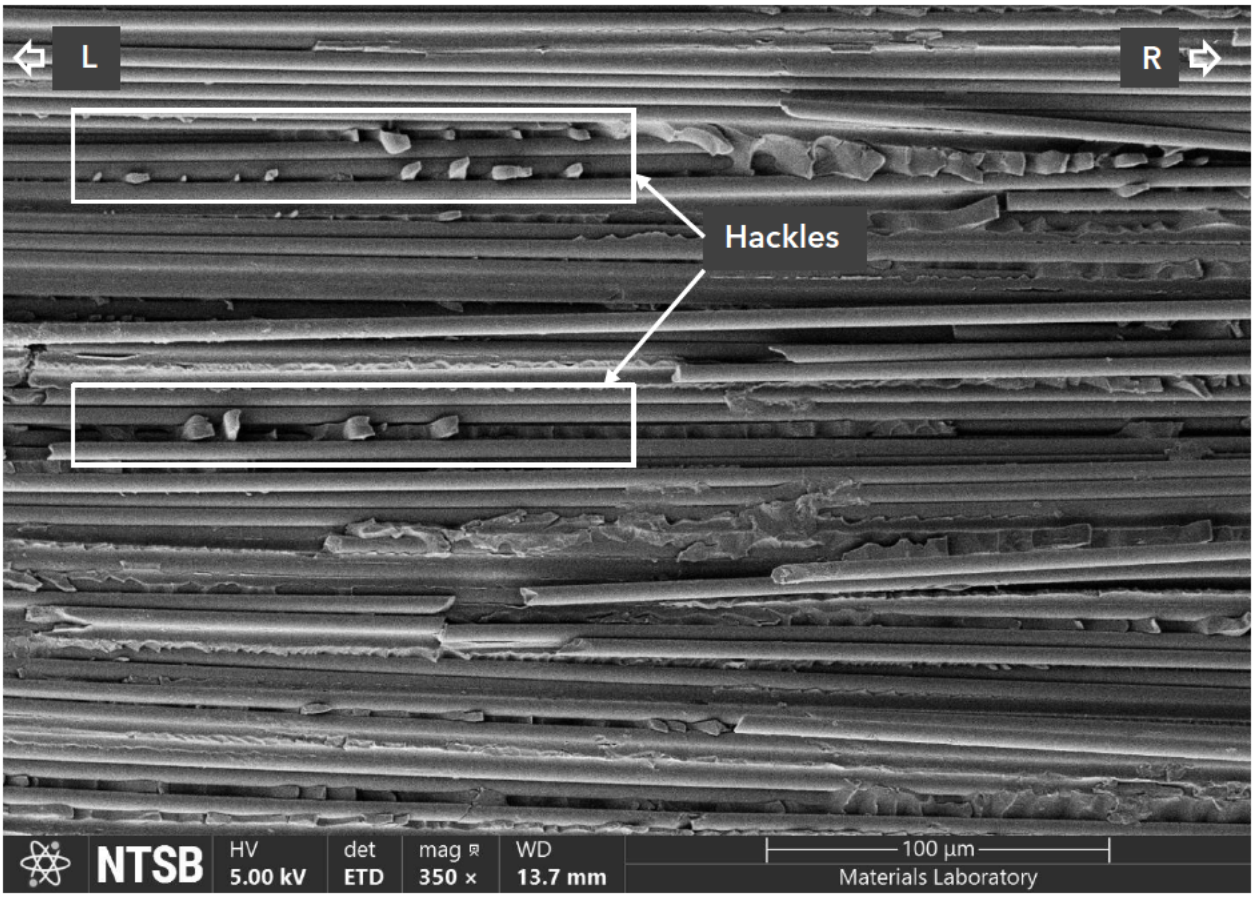

Figure 20. Hackle marks in the epoxy matrix consistent with shear separation.

a)

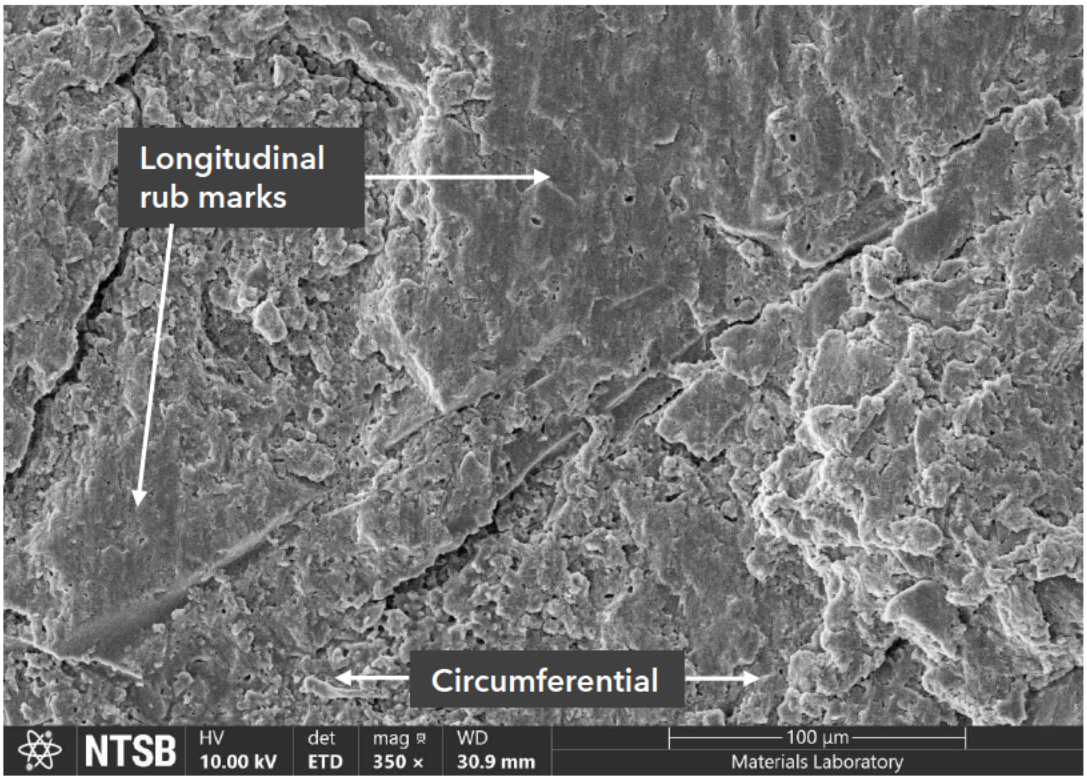

b)

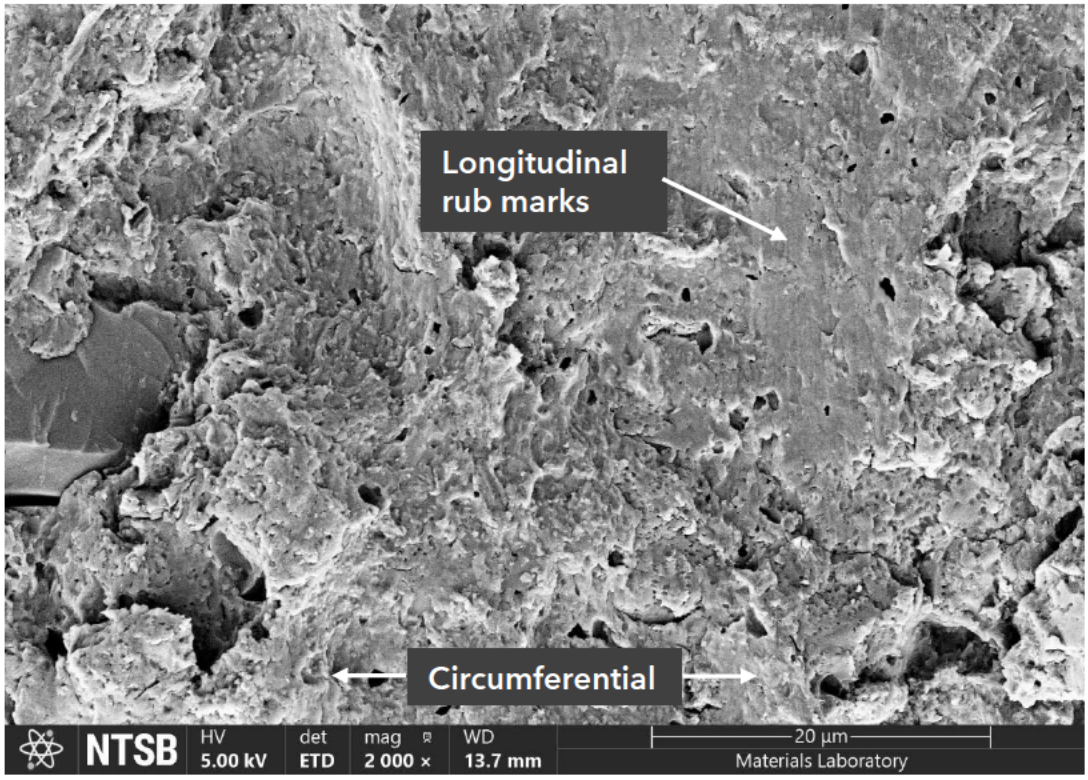

Figure 21. a) and b) longitudinal rub marks on the adhesive surface.

c)

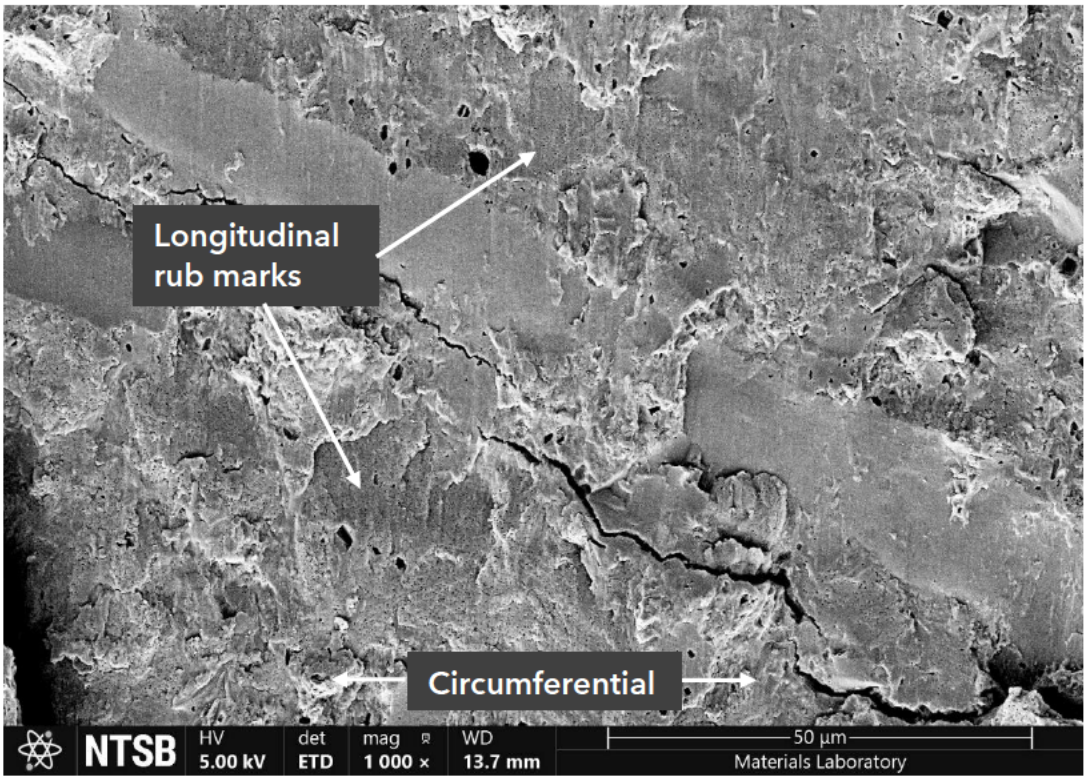

Figure 21 (cont.). c) additional longitudinal rub marks.

a)

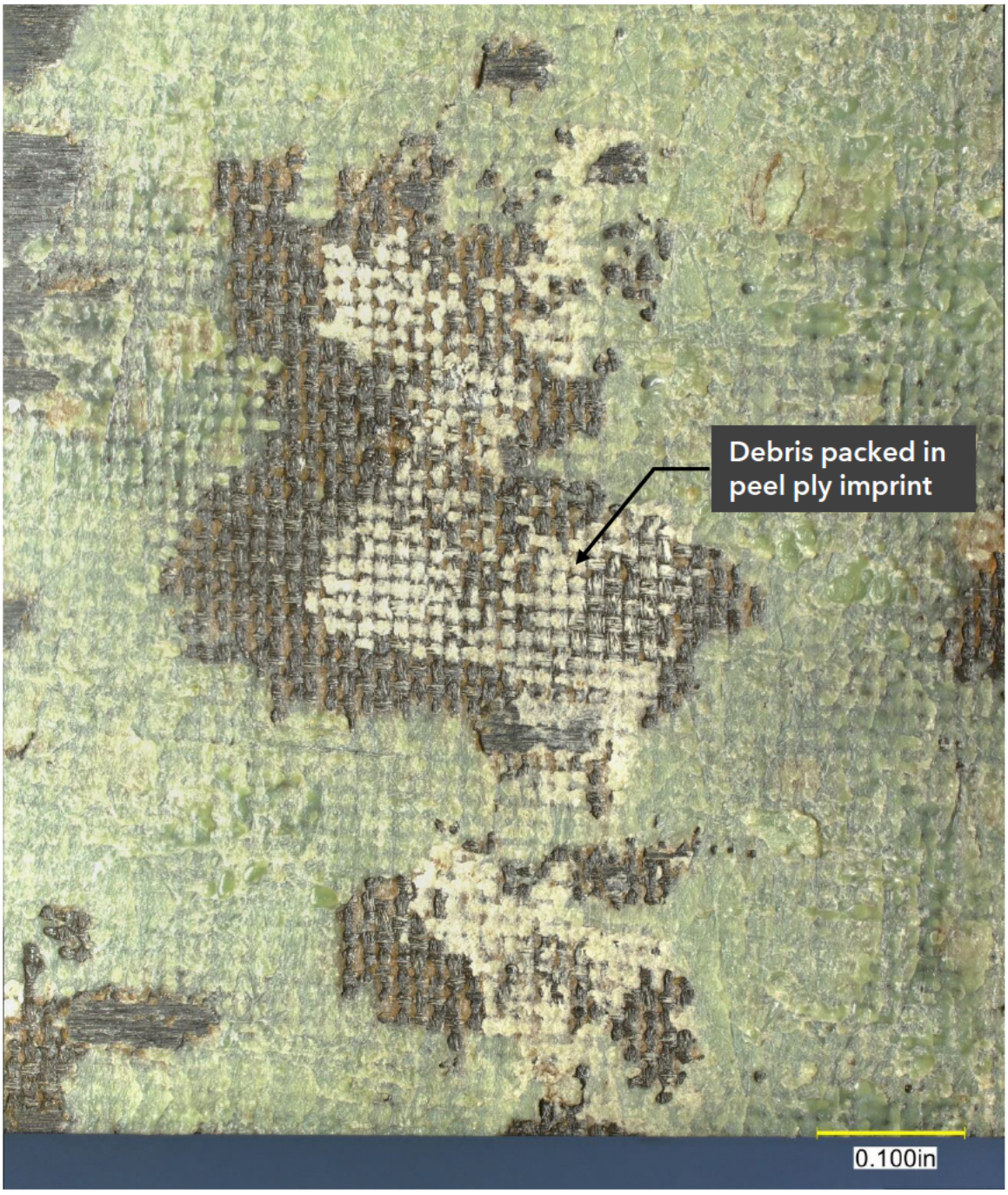

Figure 22. a) Void in adhesive layer prior to cleaning with debris packed into the peel ply imprint and

b)

Figure 22 (cont.). b) same void after cleaning and removal of the debris.

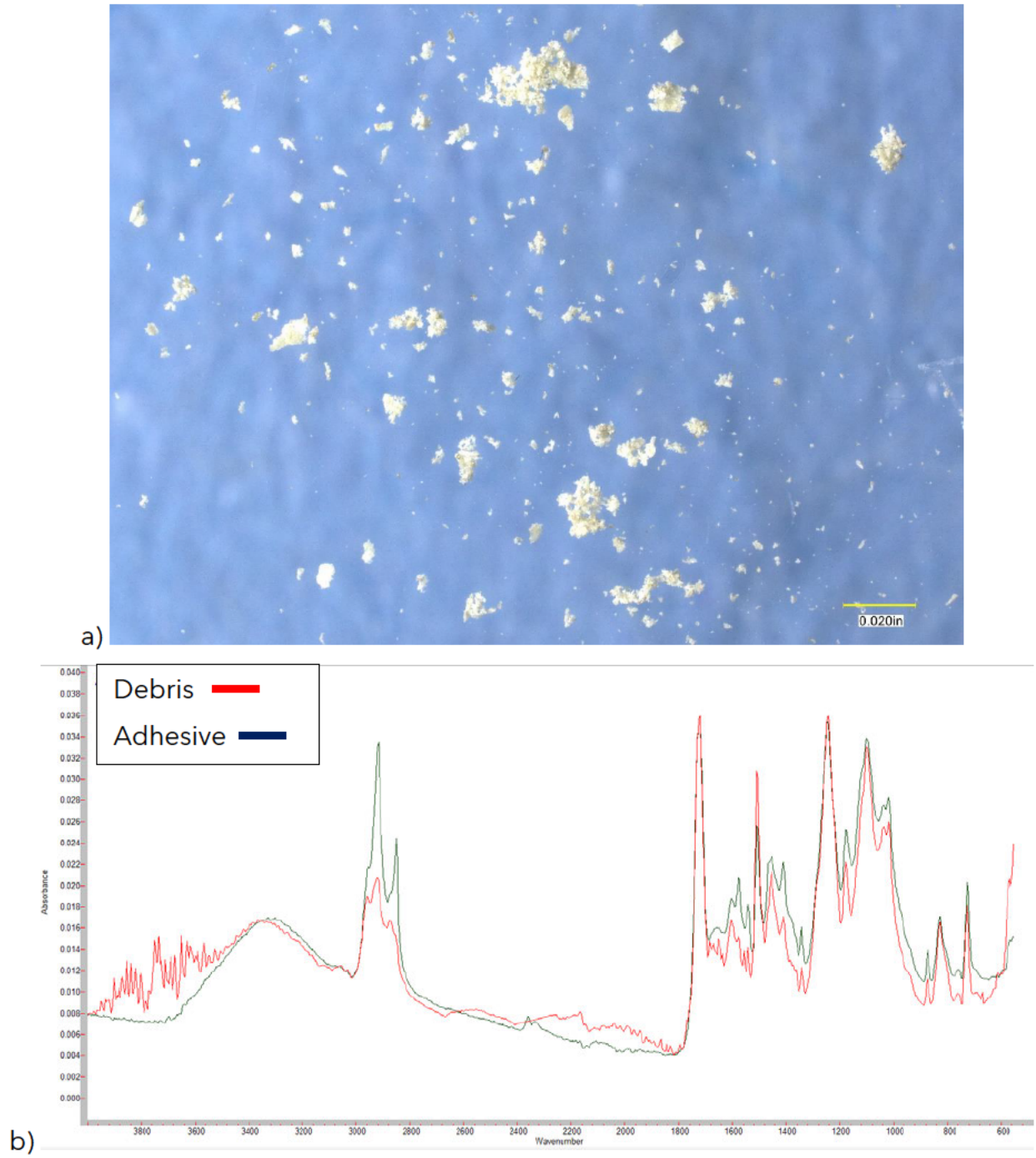

Figure 23. a) Image of debris removed from peel ply impressions in figure 22 and b) comparative FTIR-ATR spectra of the debris and of a sample of adhesive.

a)

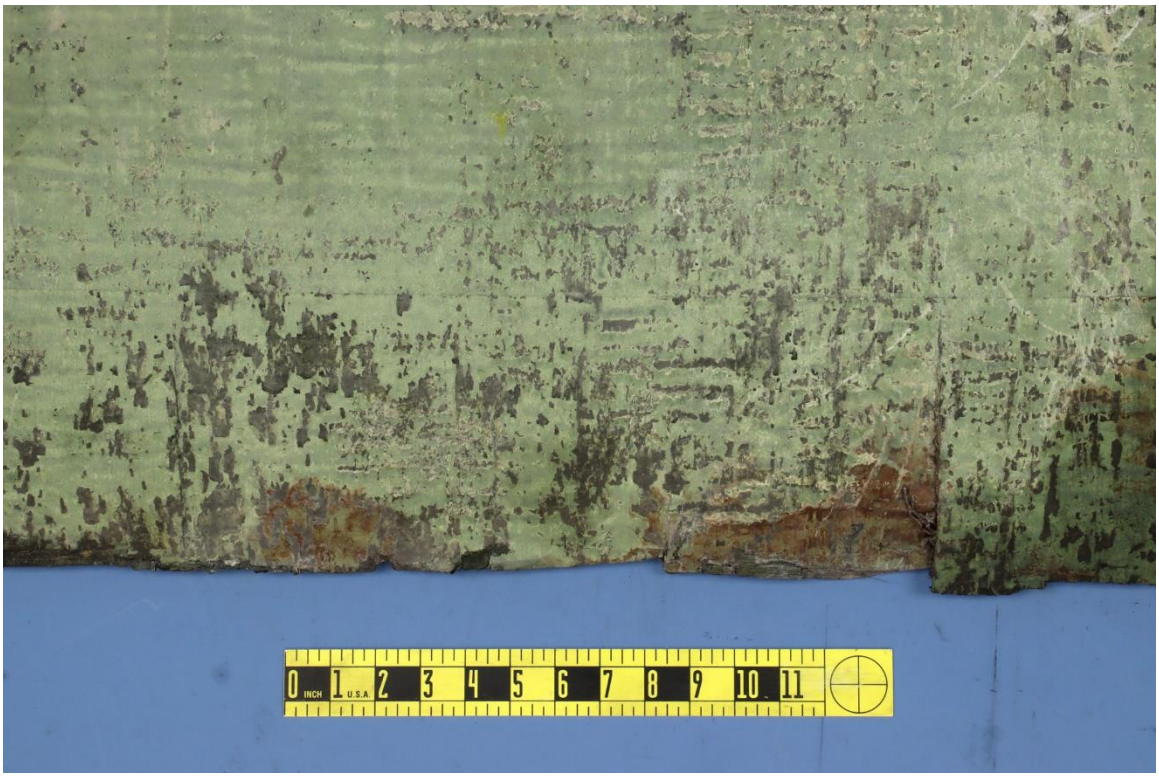

b)

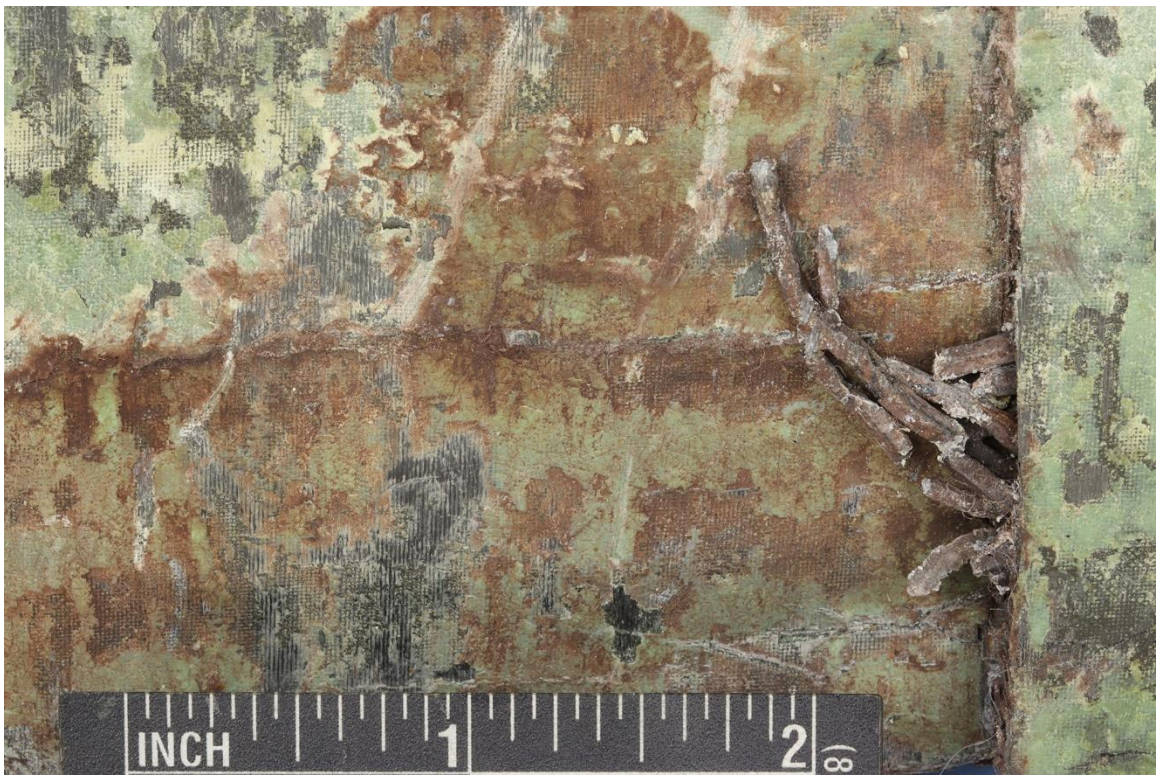

Figure 24. Contact marks on the left side: a) image showing both contact marks and b) higher magnification image of the forward mark showing the embedded object, identified as lead.

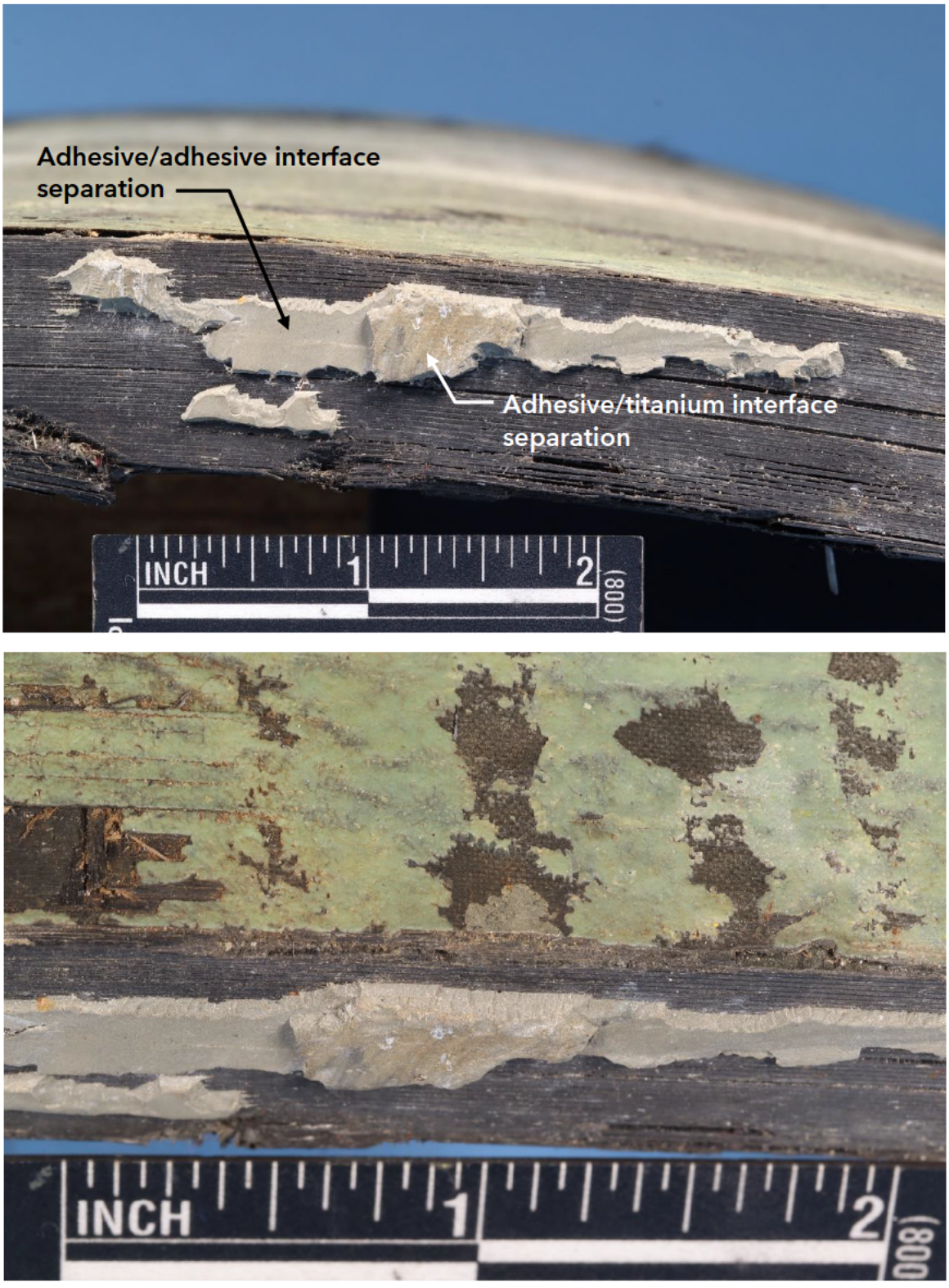

Figure 25. a) and b) Images of the machined end of the hull piece showing the size and thickness of the remaining adhesive bits.

Figure 26. Images of trimmed end 'A' from the Titan hull; a) view of cut end face and b) side view.

a)

b)

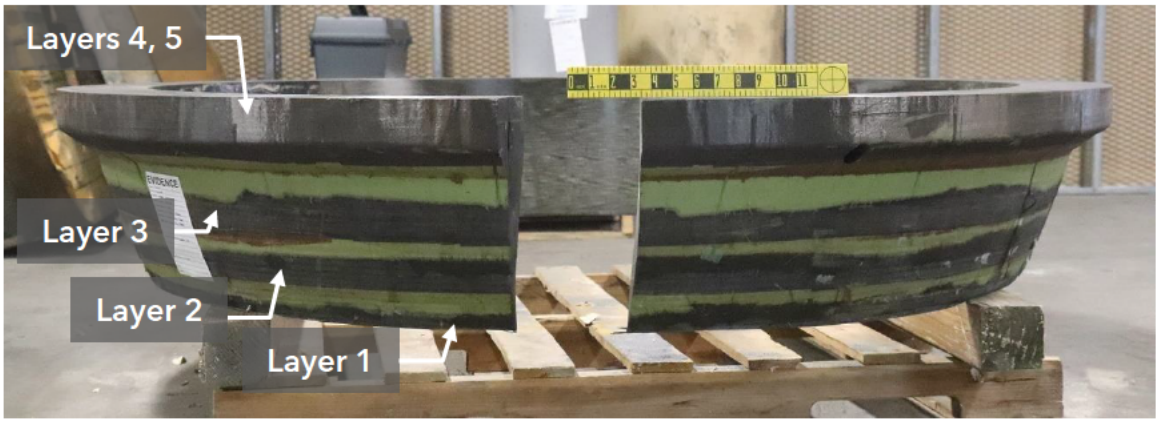

Figure 27. Images of trimmed end 'B' from the Titan hull; a) view of cut end face and b) side view.

a)

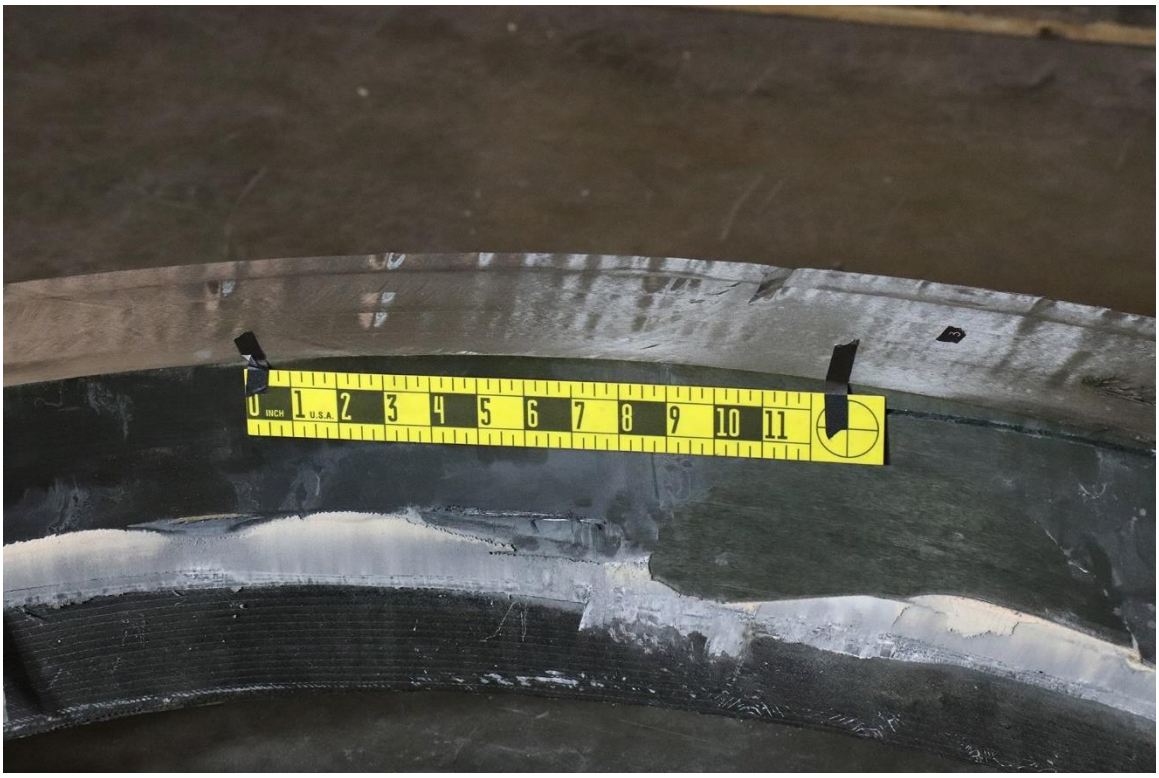

b)

Figure 28. Images of the trimmed end faces under oblique lighting showing wrinkles and waviness in the carbon fiber orientation. Local variations in fiber orientation result in the observed light/dark brightness variations; a) trimmed end 'A' and b) trimmed end 'B'.

a)

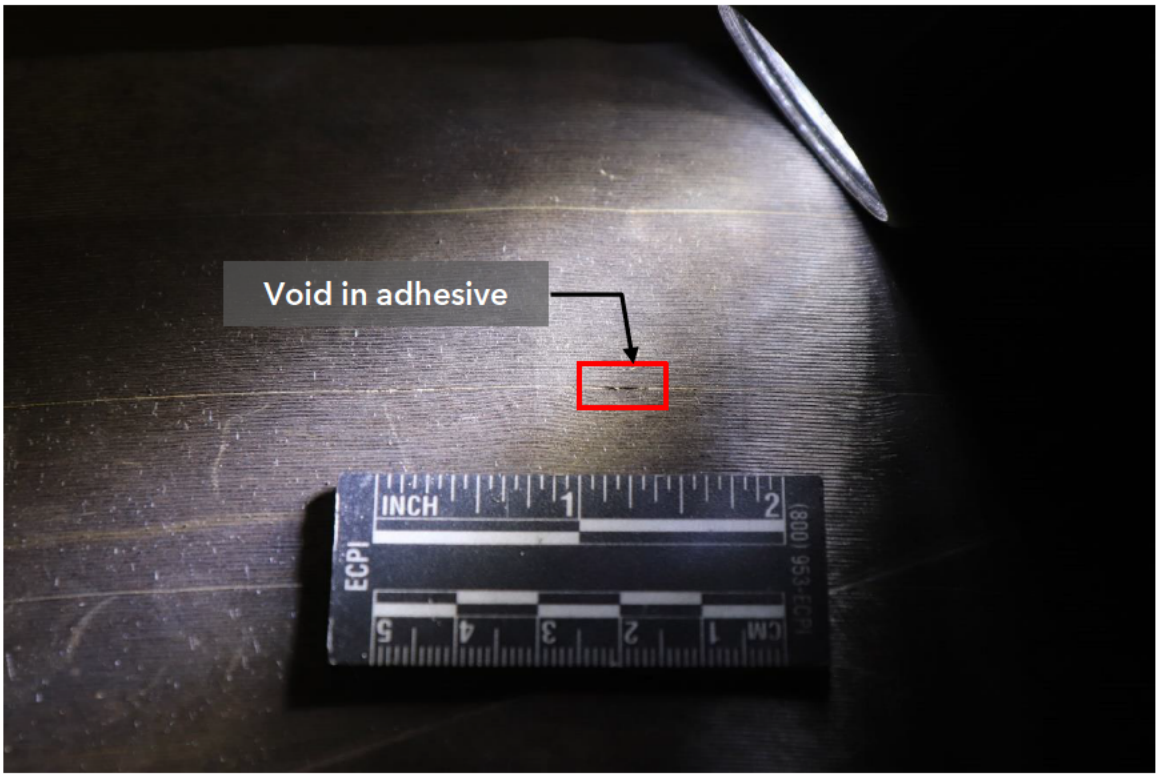

b)

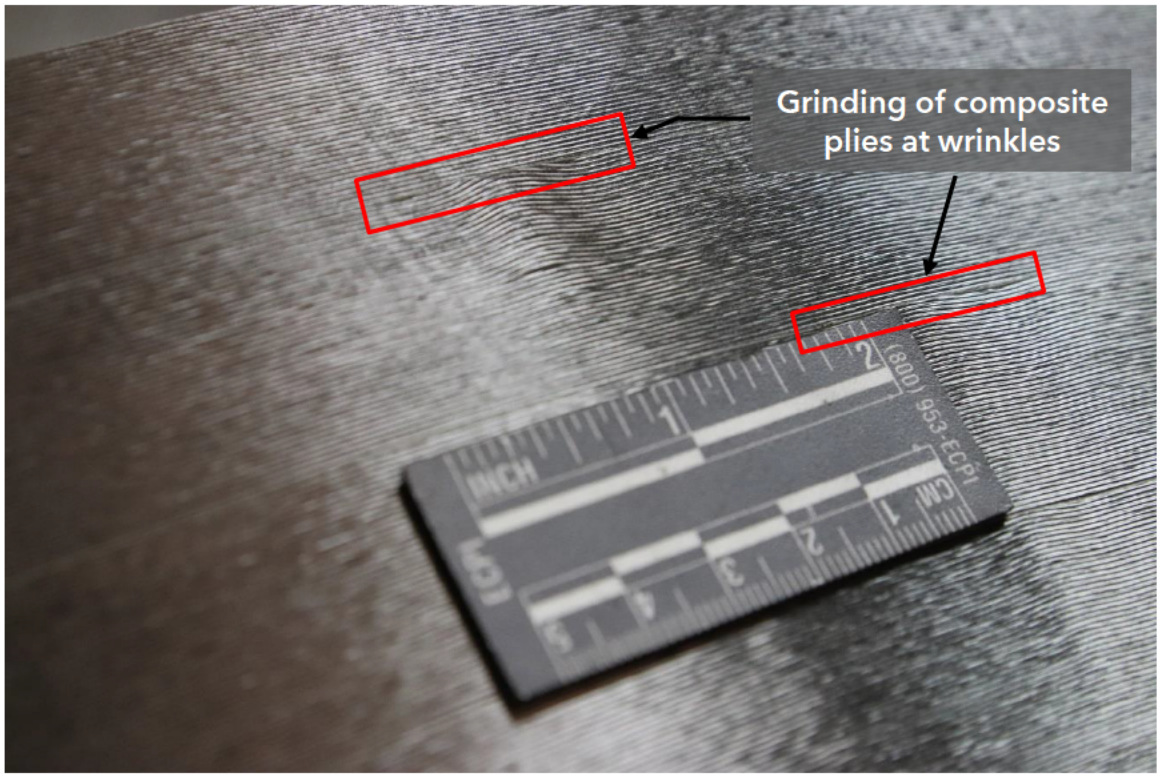

Figure 29. a) Image showing a void in the adhesive layer associated with fiber bridging / tenting around a wrinkle and b) image showing grinding of outer carbon fiber plies at a wrinkle.

a)

b)

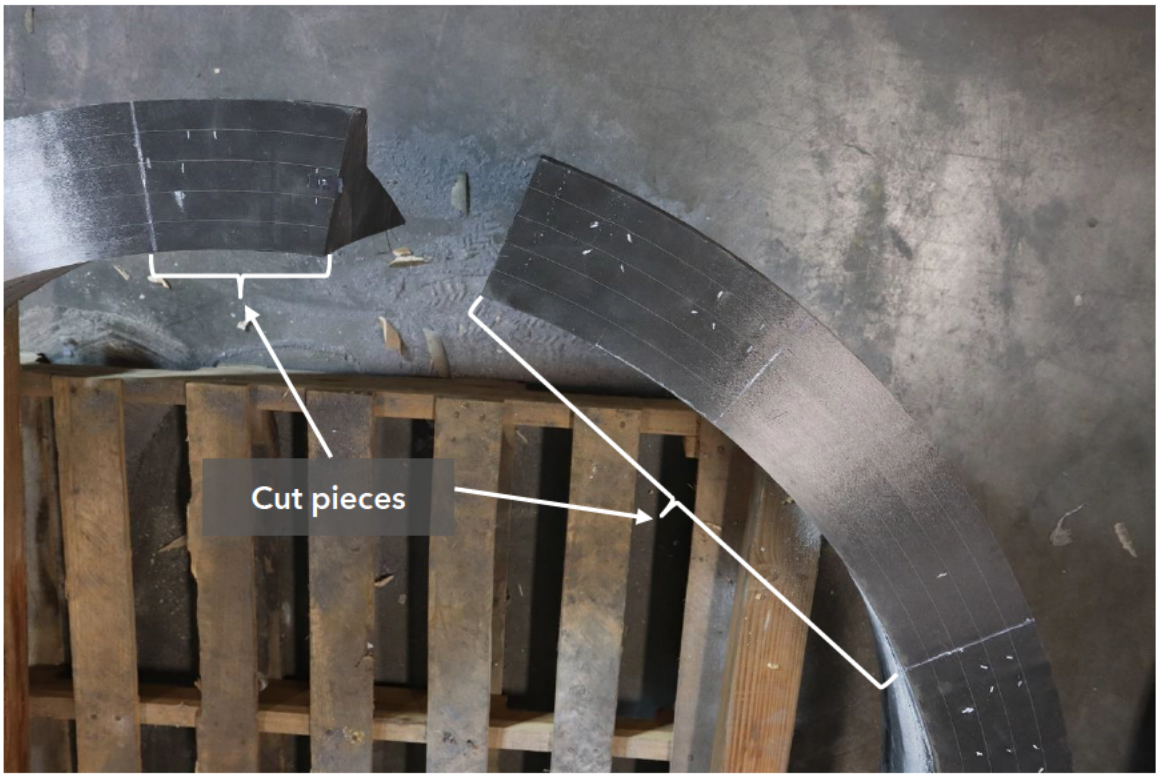

Figure 30. Image of end 'B' after grease pen markup: a) overview image showing distribution of fiber bridges with voids (marked with '/ \') and ground wrinkles (marked with '|') and b) closer image showing the location of samples cut for laboratory examination and testing.

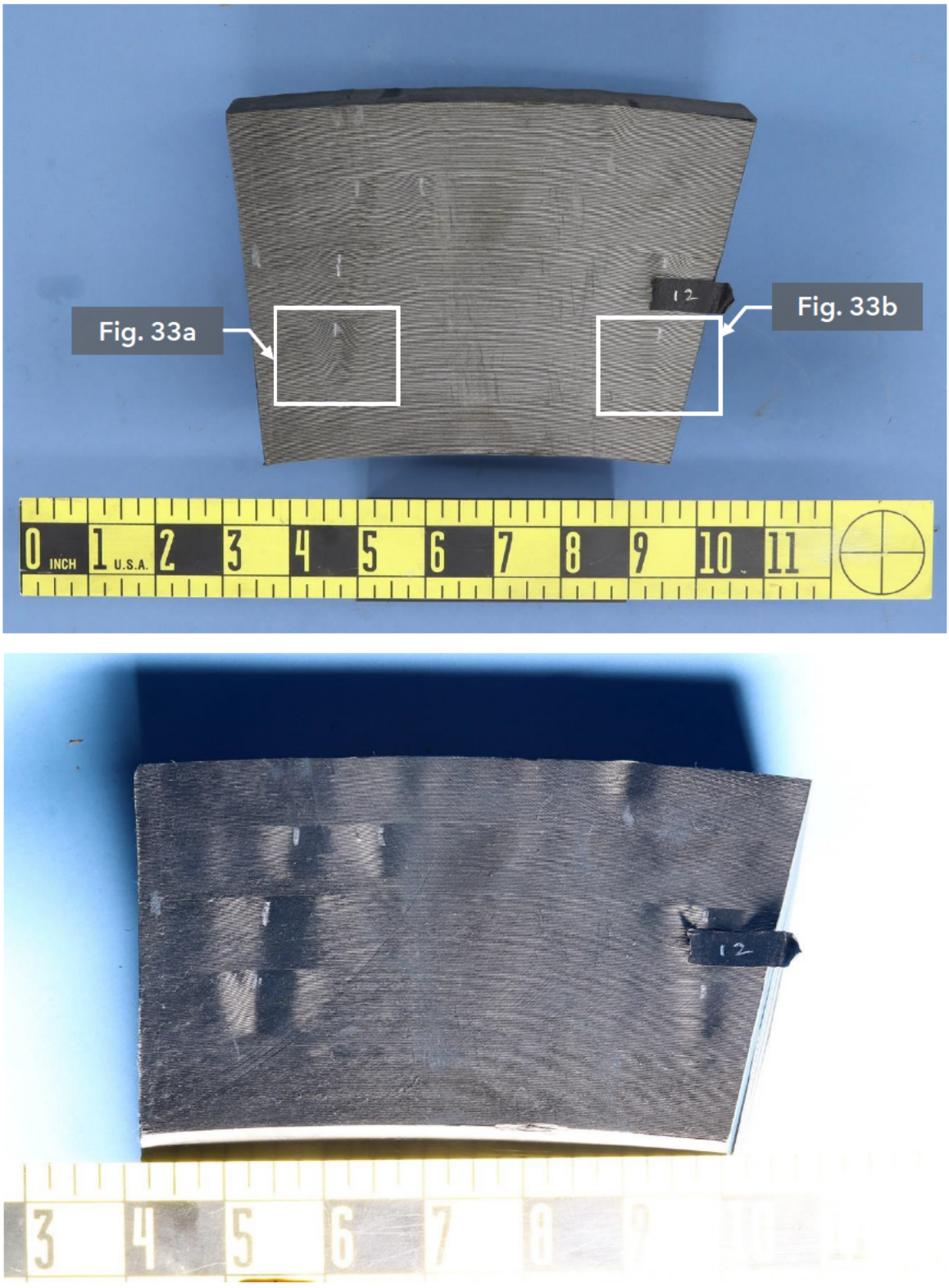

Figure 31. Images of the smaller piece cut from trimmed end 'B': a) cut face under general lighting; b) cut face under oblique angle lighting, which highlights wrinkle features;

c)

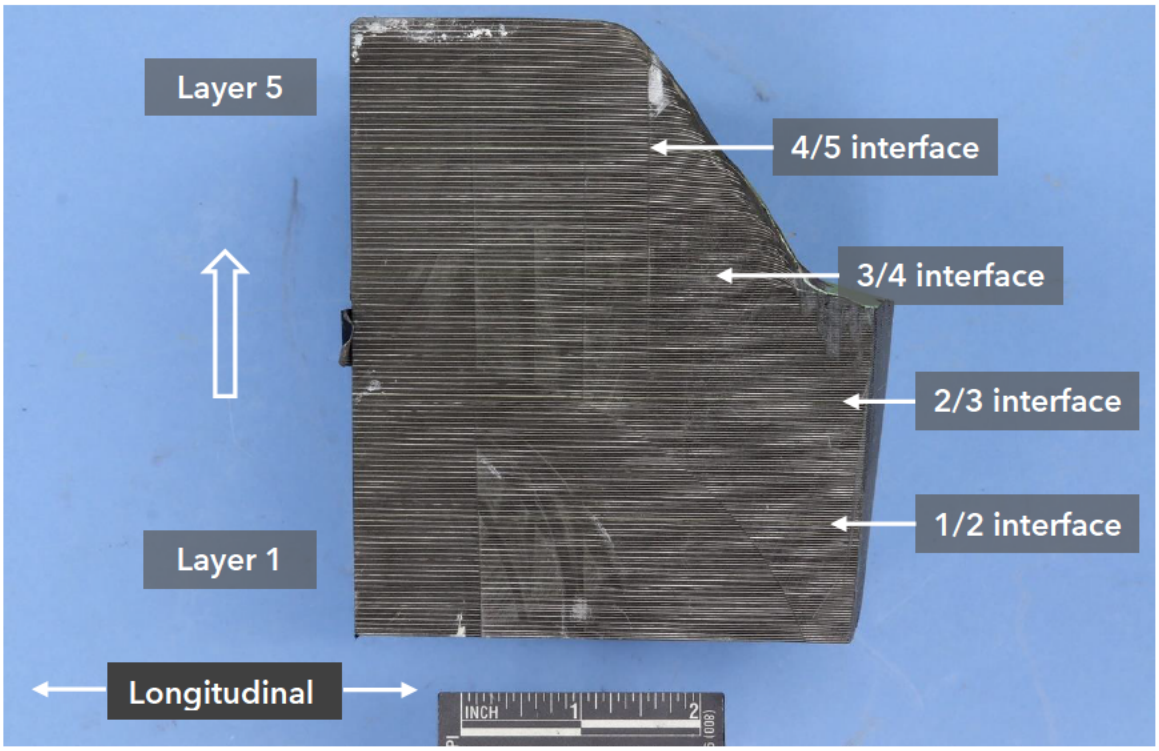

d)

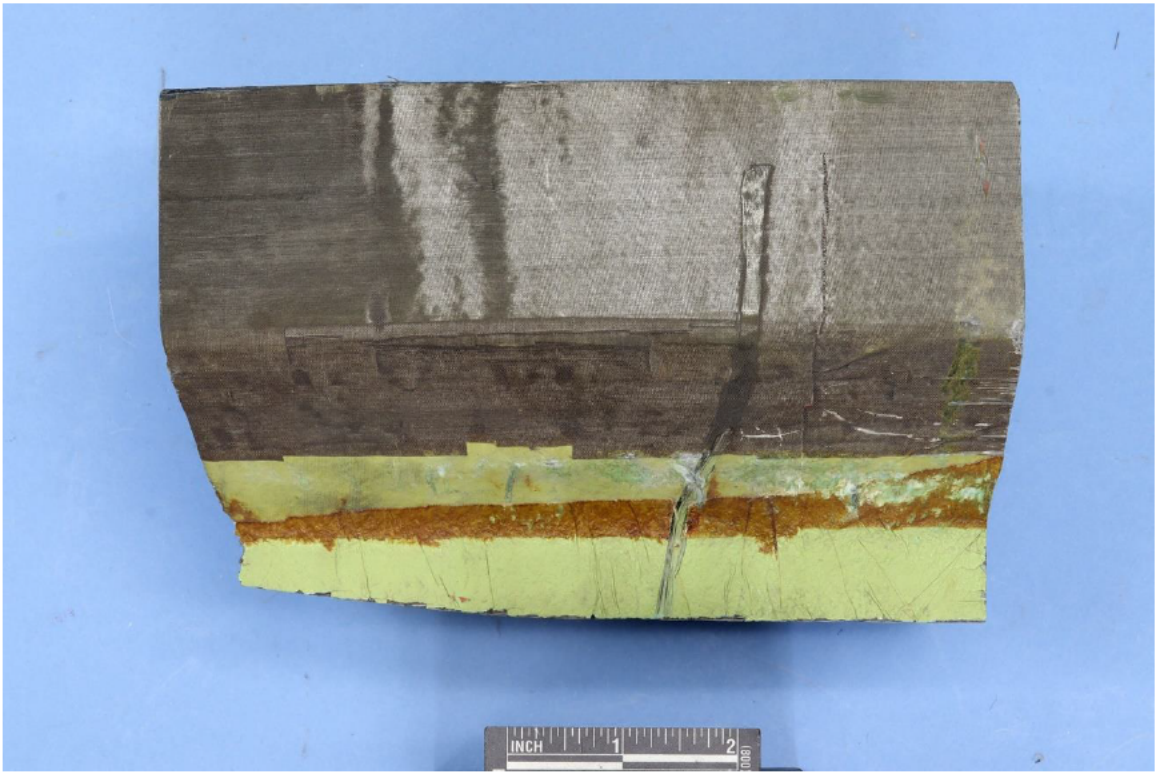

Figure 31 (cont.). c) longitudinal cross section with the layers and interfaces labelled; and d) outer surface of the piece viewed radially inward.

a)

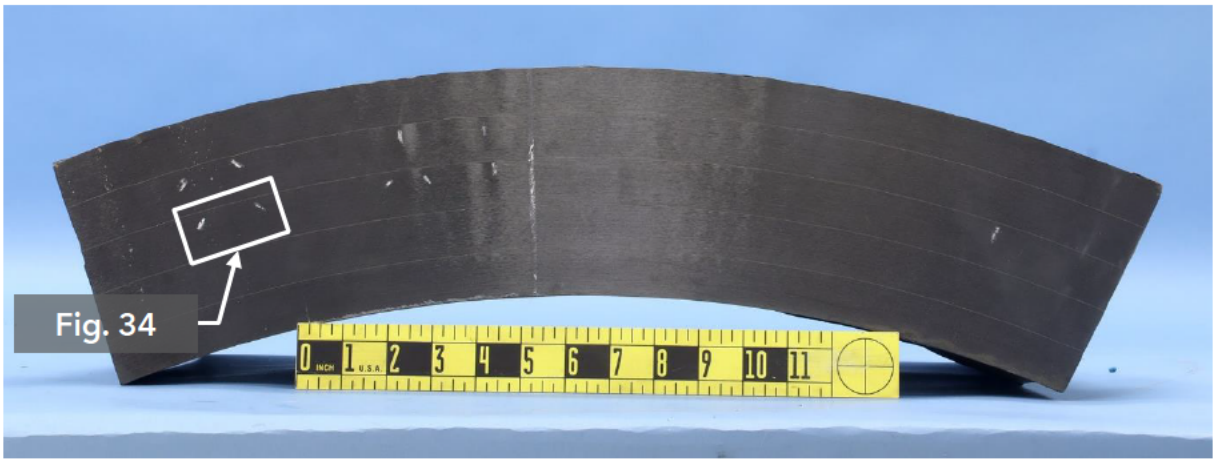

b)

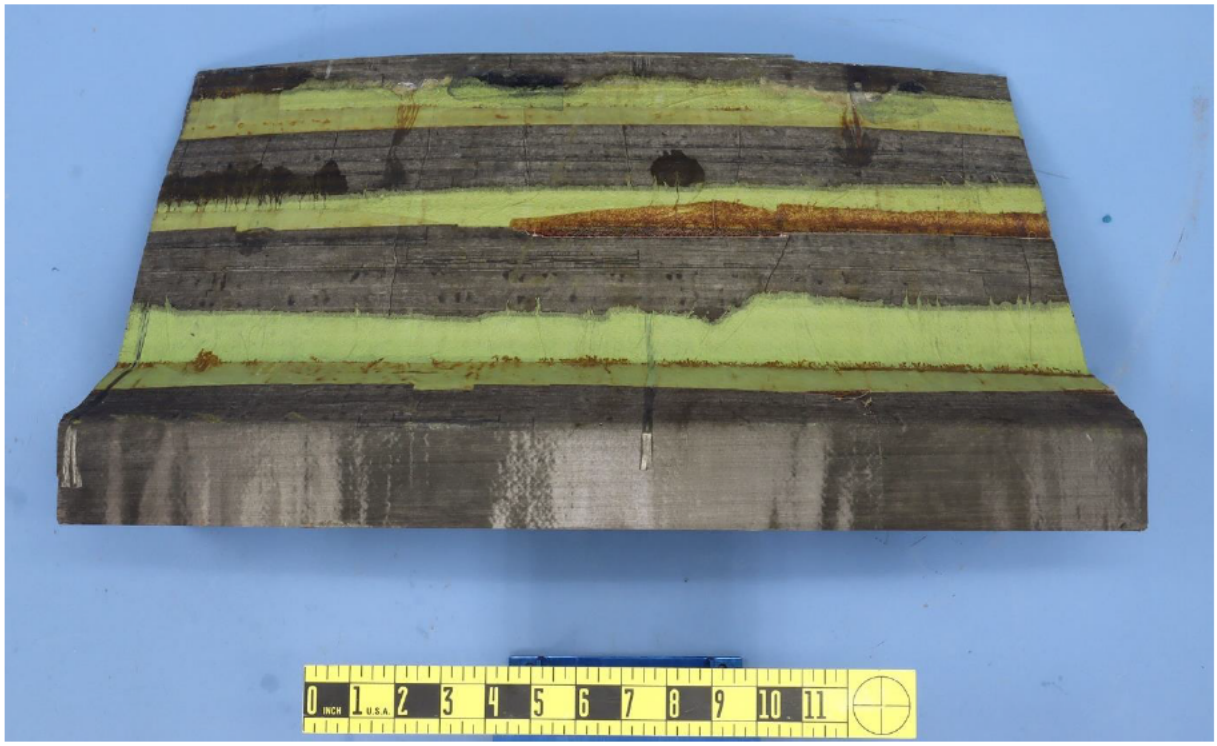

Figure 32. Image of the larger piece cut from end 'B'; a) viewed in the longitudinal direction and b) outer surface viewed radially inward.

a)

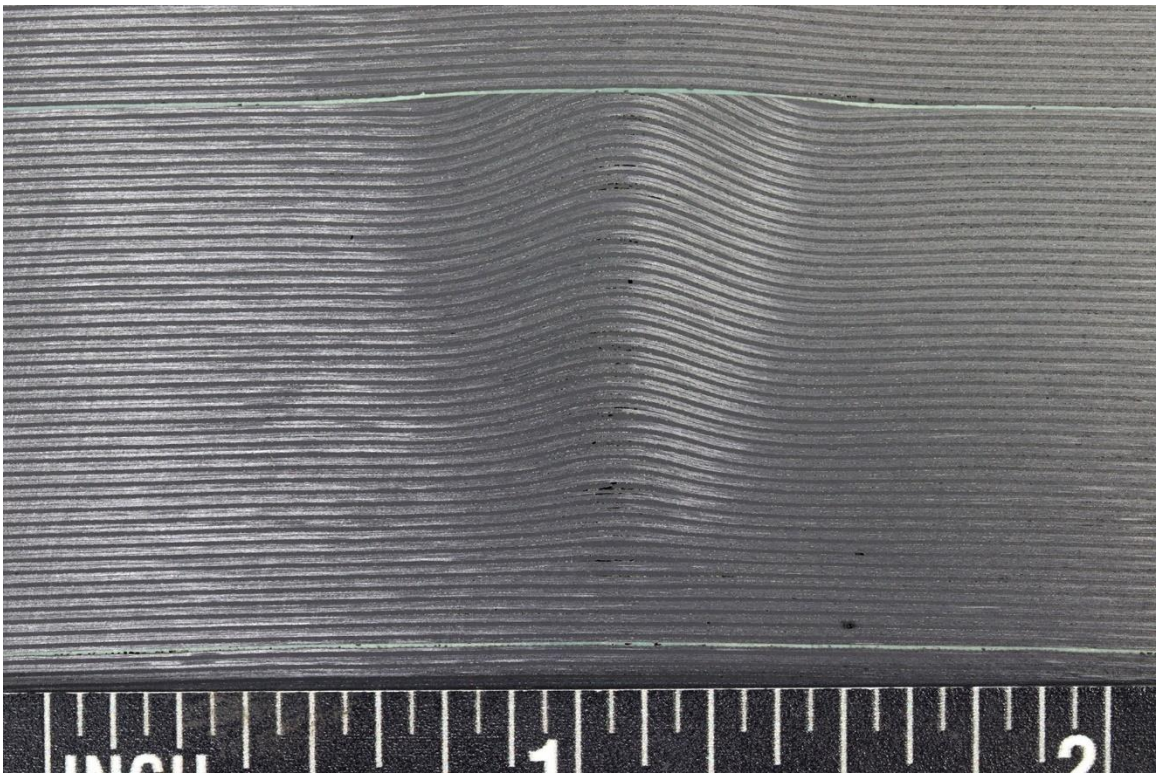

b)

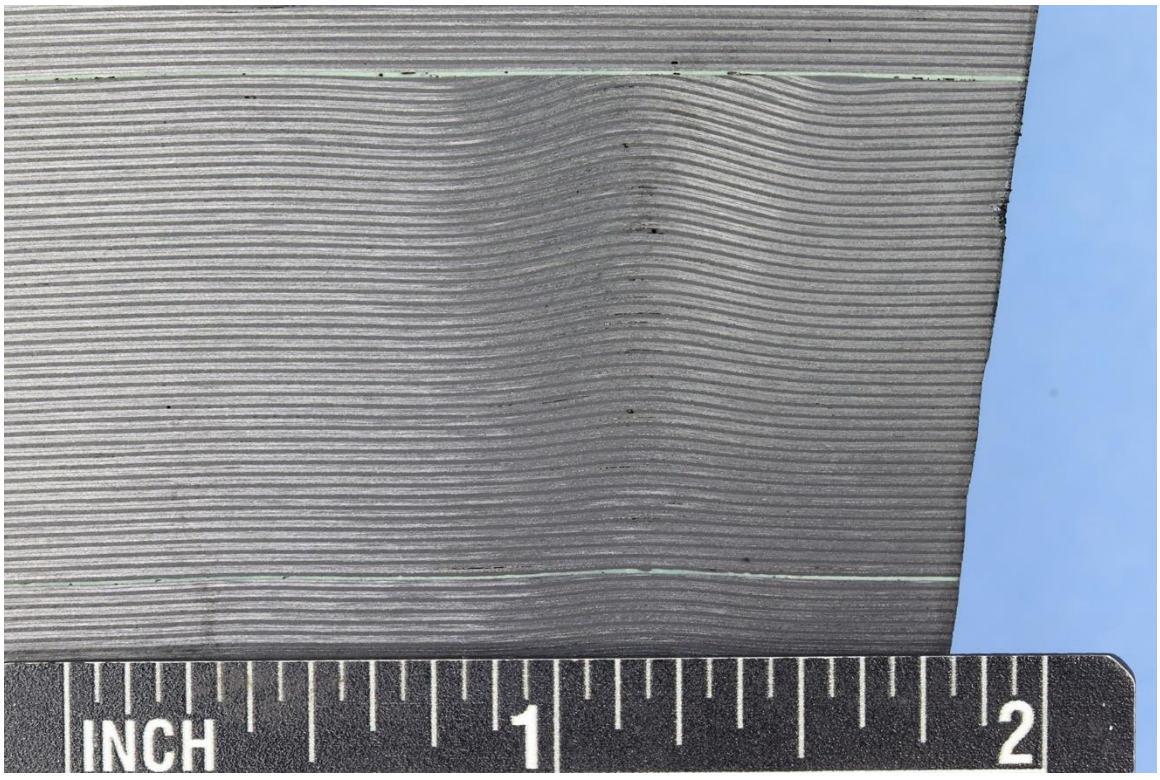

Figure 33. Two images of ground wrinkles on the smaller piece from trimmed end 'B'.

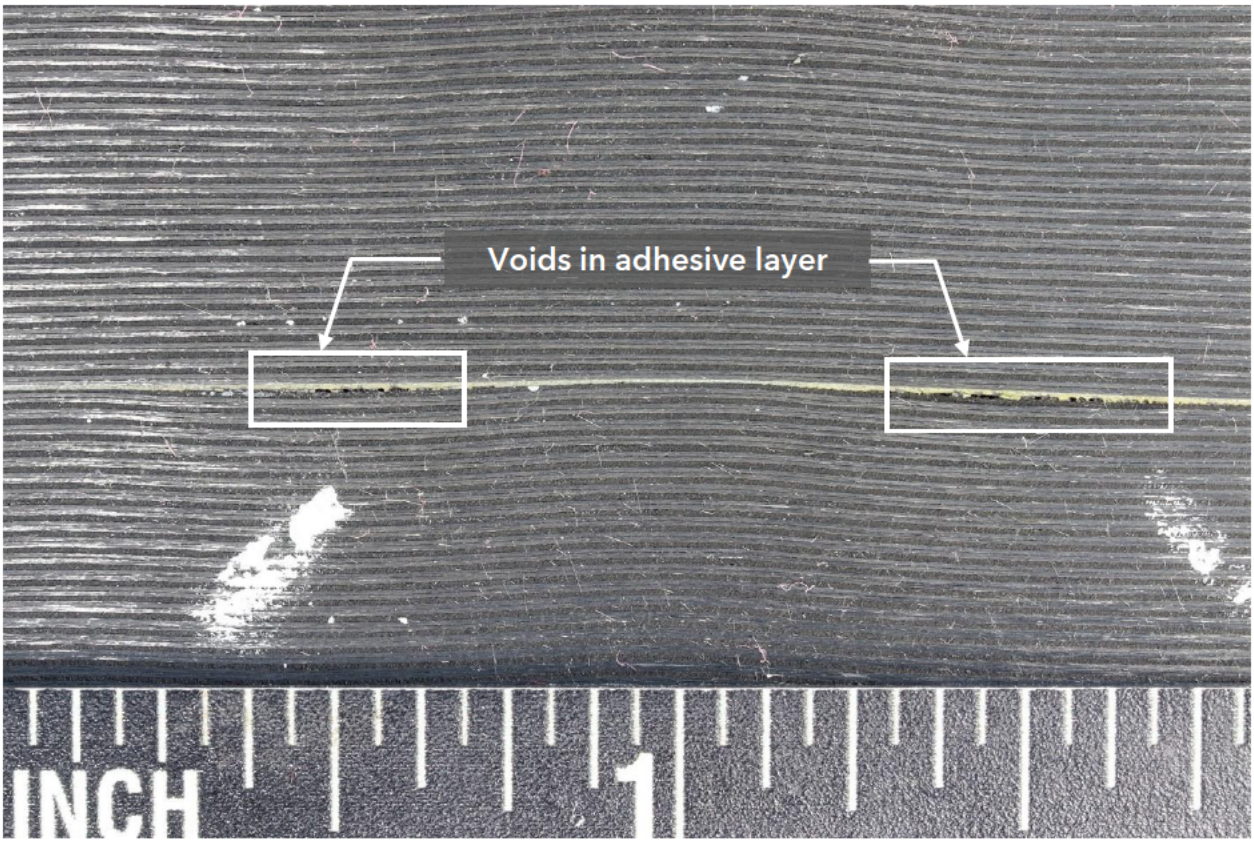

Figure 34. Image of the layer 3/4 interface showing voids / porosity on either side of a waviness-induced fiber bridging feature.

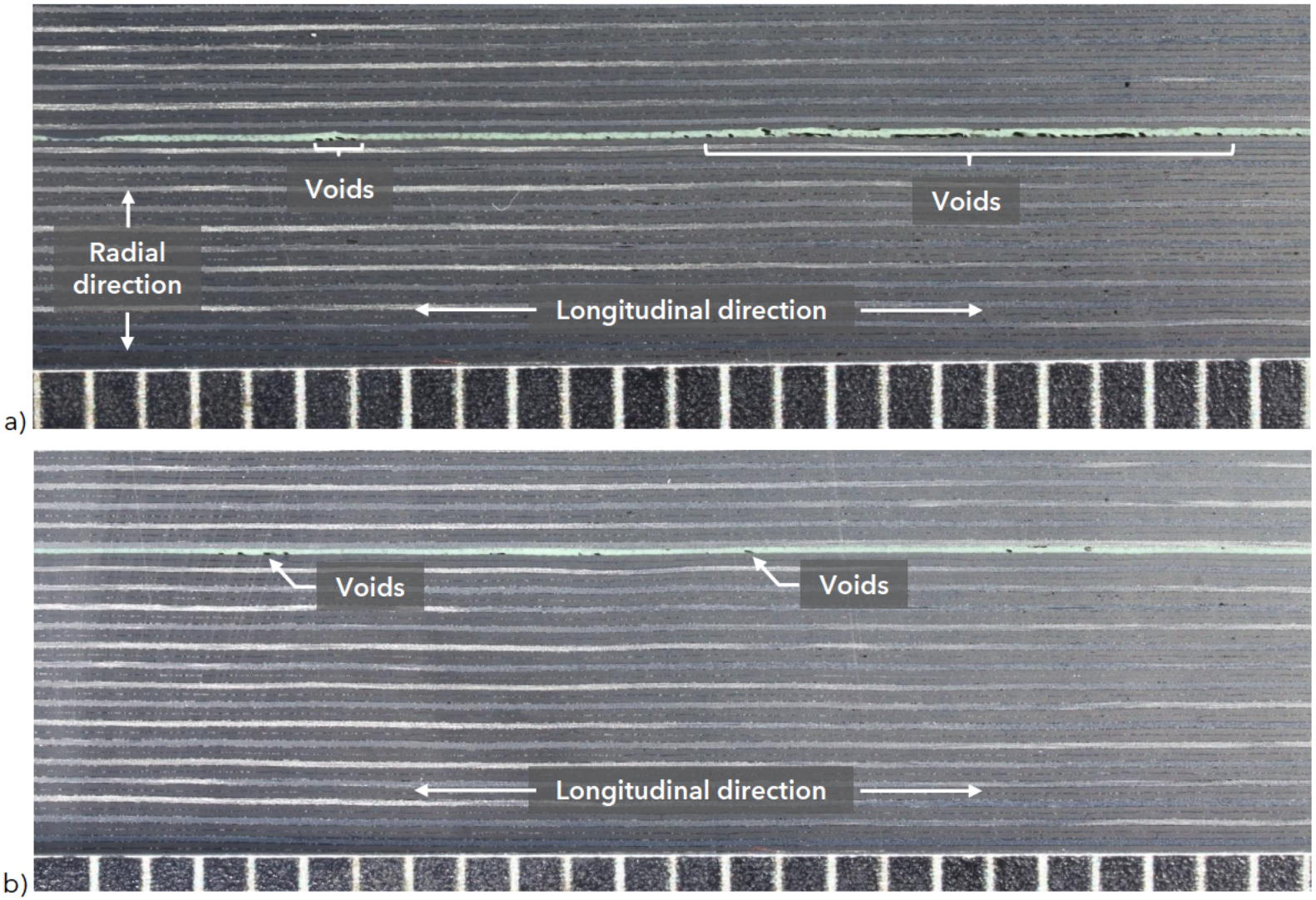

Figure 35. Adhesive layers between co-bonded carbon fiber composite layers, viewed on longitudinal cross sections: a) joint between layers 1 and 2; b) joint between layers 2 and 3;

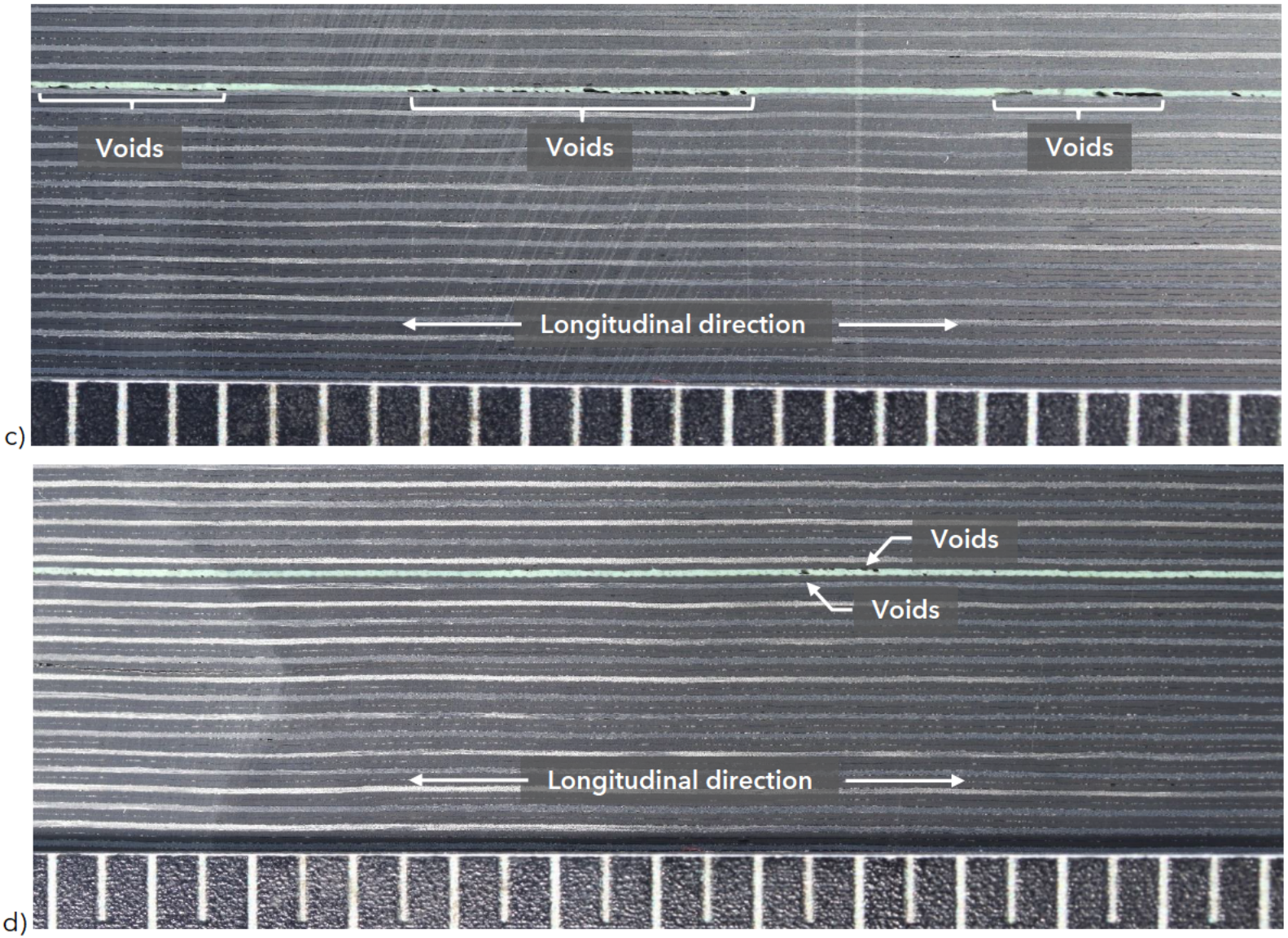

Figure 35 (cont.). c) joint between layers 3 and 4; and d) joint between layers 4 and 5.

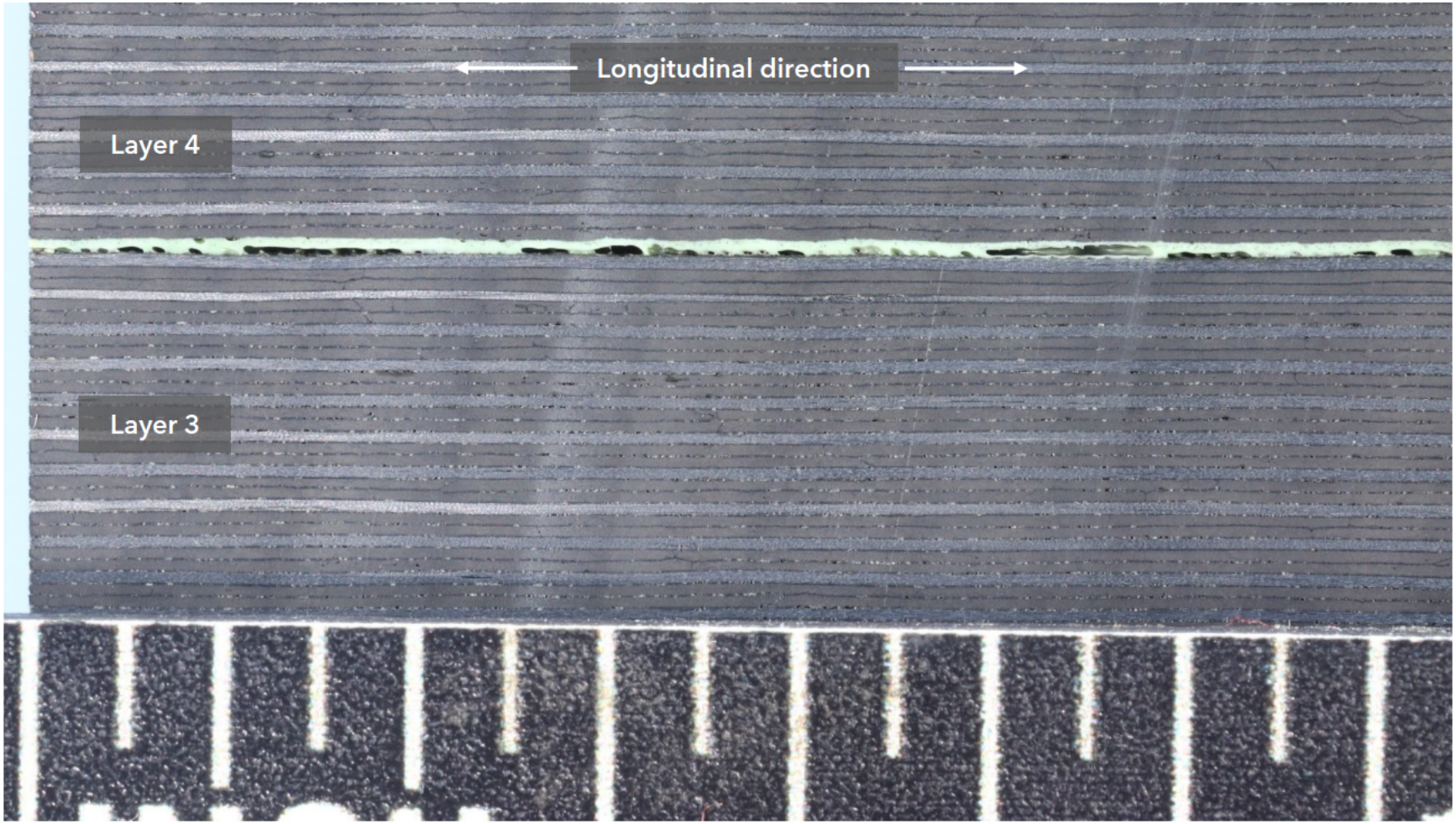

Figure 36. Closer image of the adhesive between layers 3 and 4 showing voids at the layer 3/4 adhesive interface.

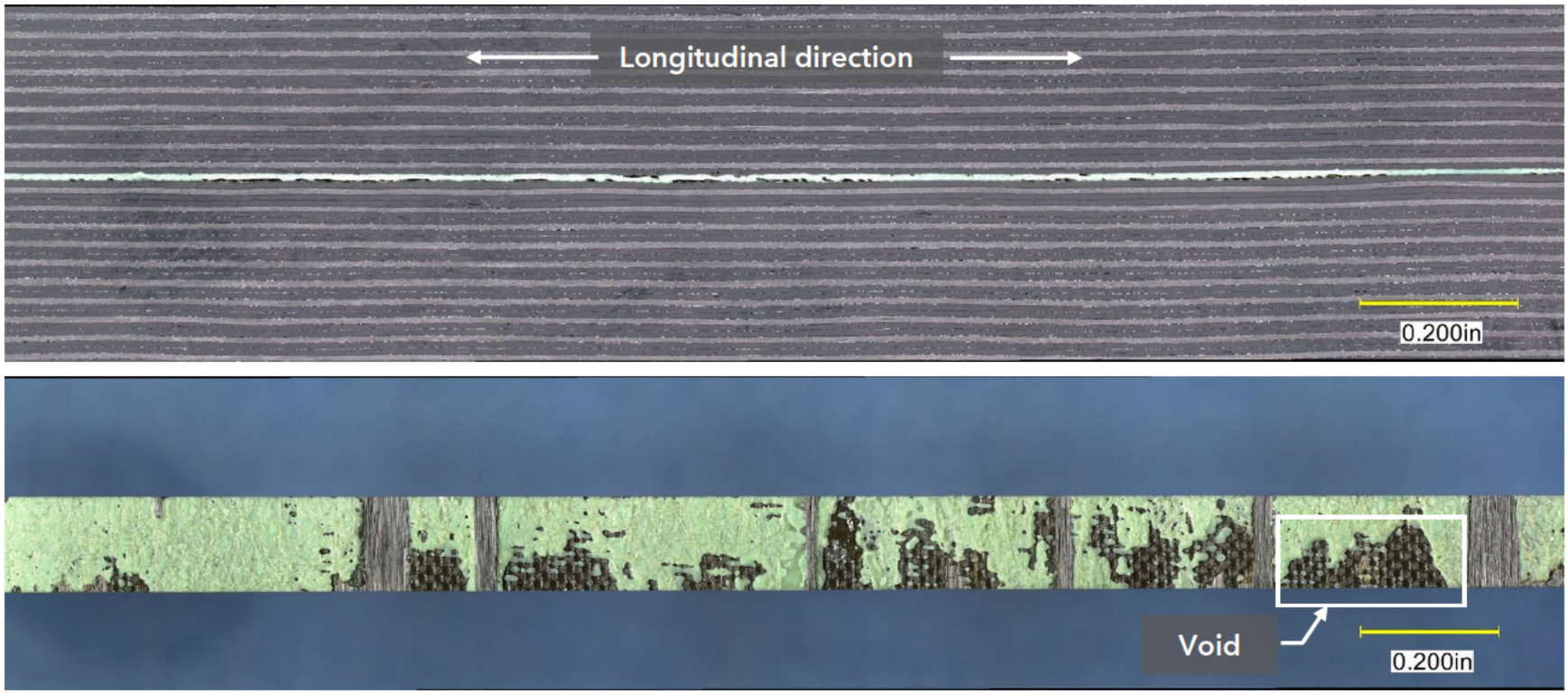

Figure 37. Top image: Cross section image of the adhesive between layers 1 and 2. Similar to previous images, areas of voids are present at the layer 1/2 interface. Lower image: plan view of the adhesive layer after lab fracture.

a)

Figure 38. a) Circumferential cross section of the trimmed end piece from the first full scale Titan hull and

b)

Figure 38 (cont.). b) longitudinal cross section of the trimmed end piece from the first full scale Titan hull.

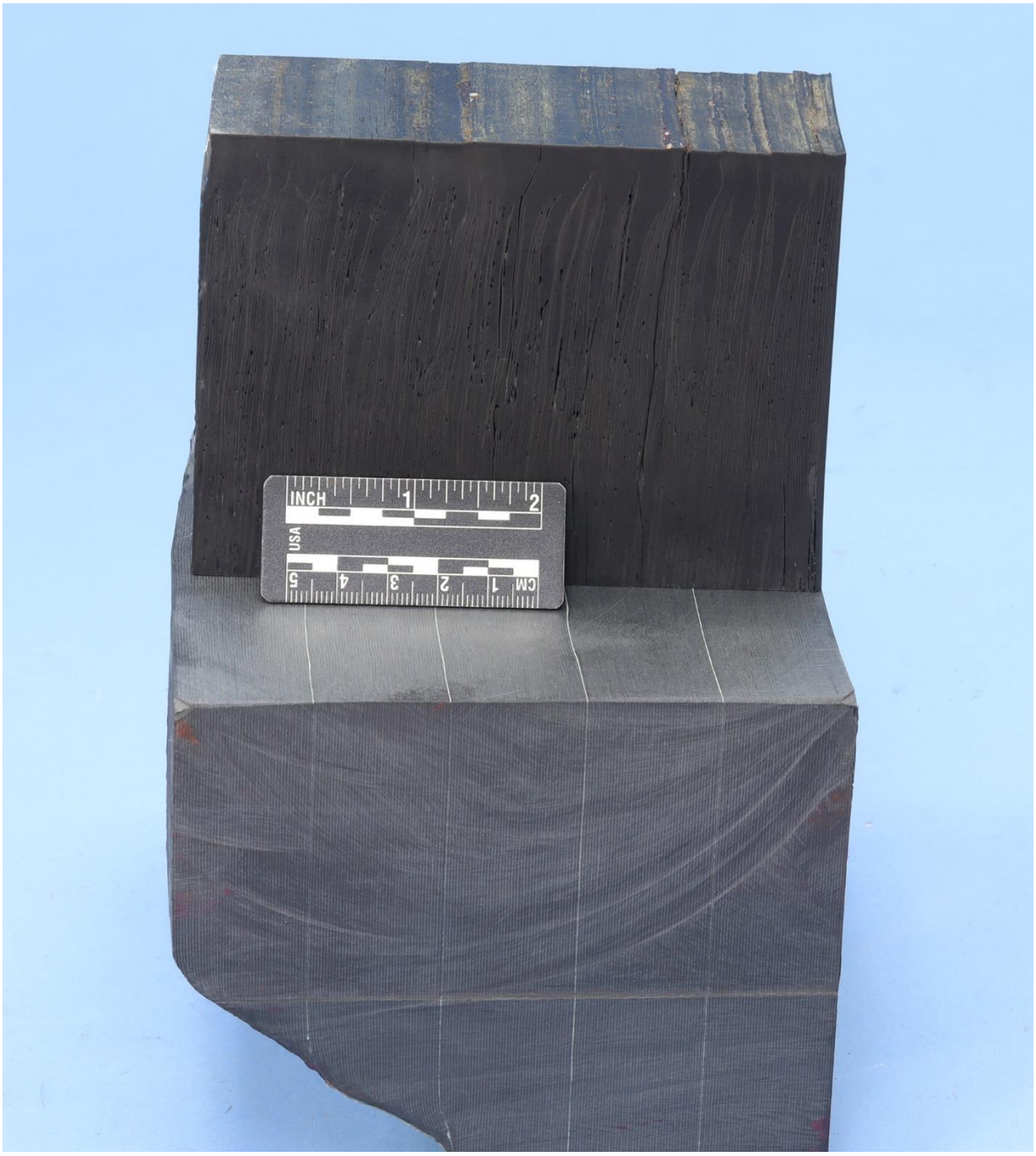

Figure 39. Visual comparison of the thickness of scrap end pieces from the first and second full-scale Titan hulls.

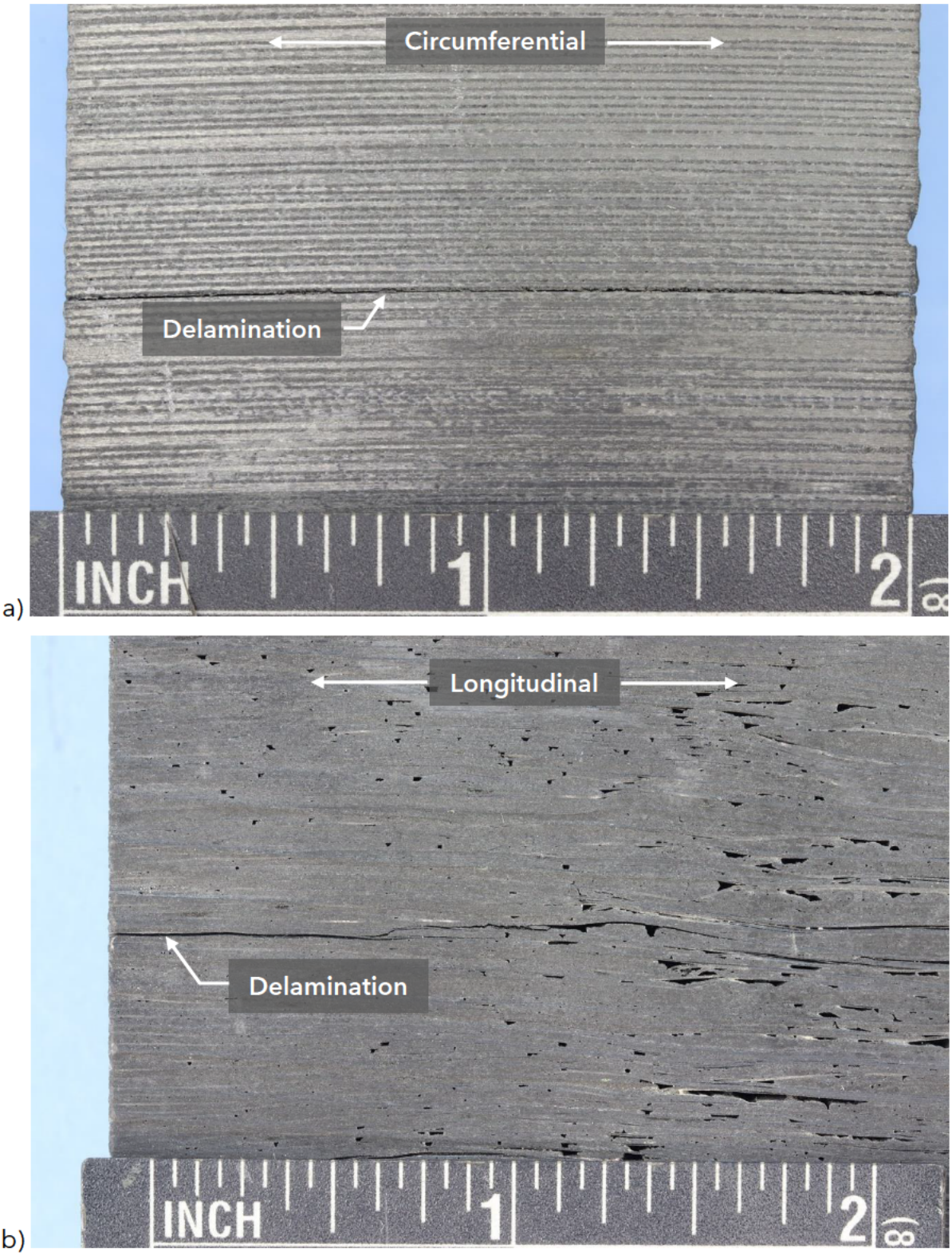

Figure 40. Images of the centerline delamination in the first full-scale Titan hull trimmed end piece: a) circumferential cross section and b) longitudinal cross section.

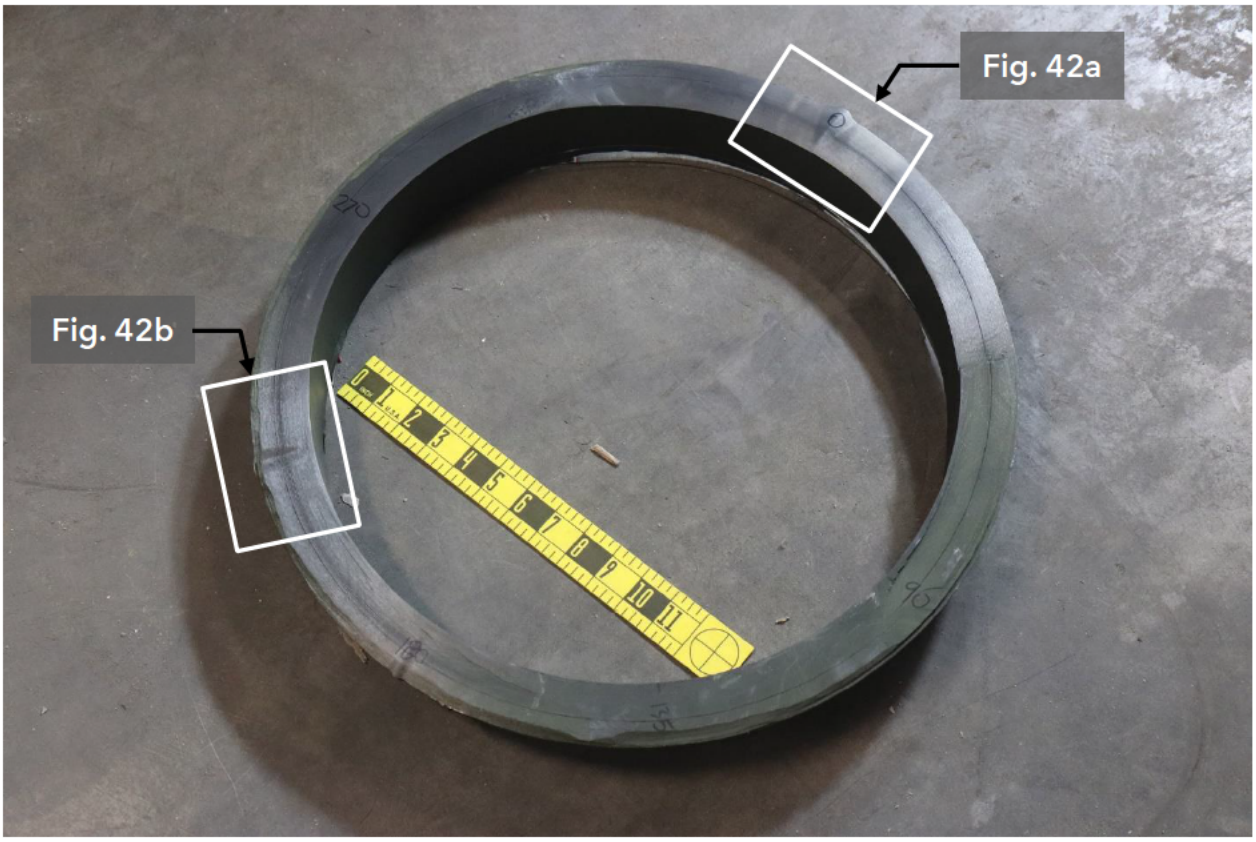

Figure 41. Trimmed end from the first of two one-third-scale test articles manufactured from prepreg carbon fiber after the retirement of the first Titan hull. The locations of two wrinkles are indicated and are shown below in figures 42a and b.

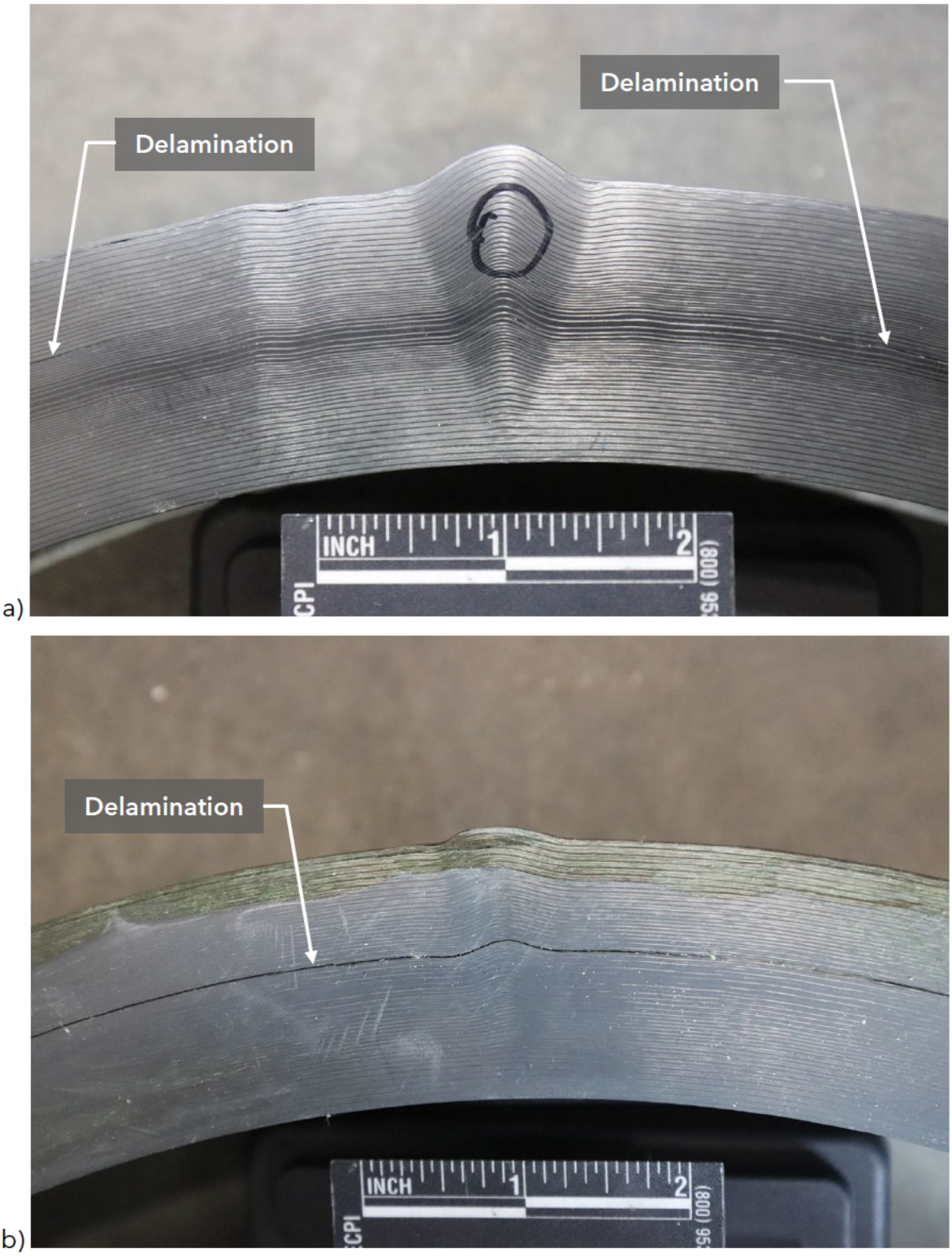

Figure 42. Images of wrinkles in the third-scale test article trimmed end piece: a) primary wrinkle and b) secondary wrinkle with a near-centerline delamination also present.

a)

b)

Figure 43. a) Overview image of forward segment and b) overview image of aft segment.

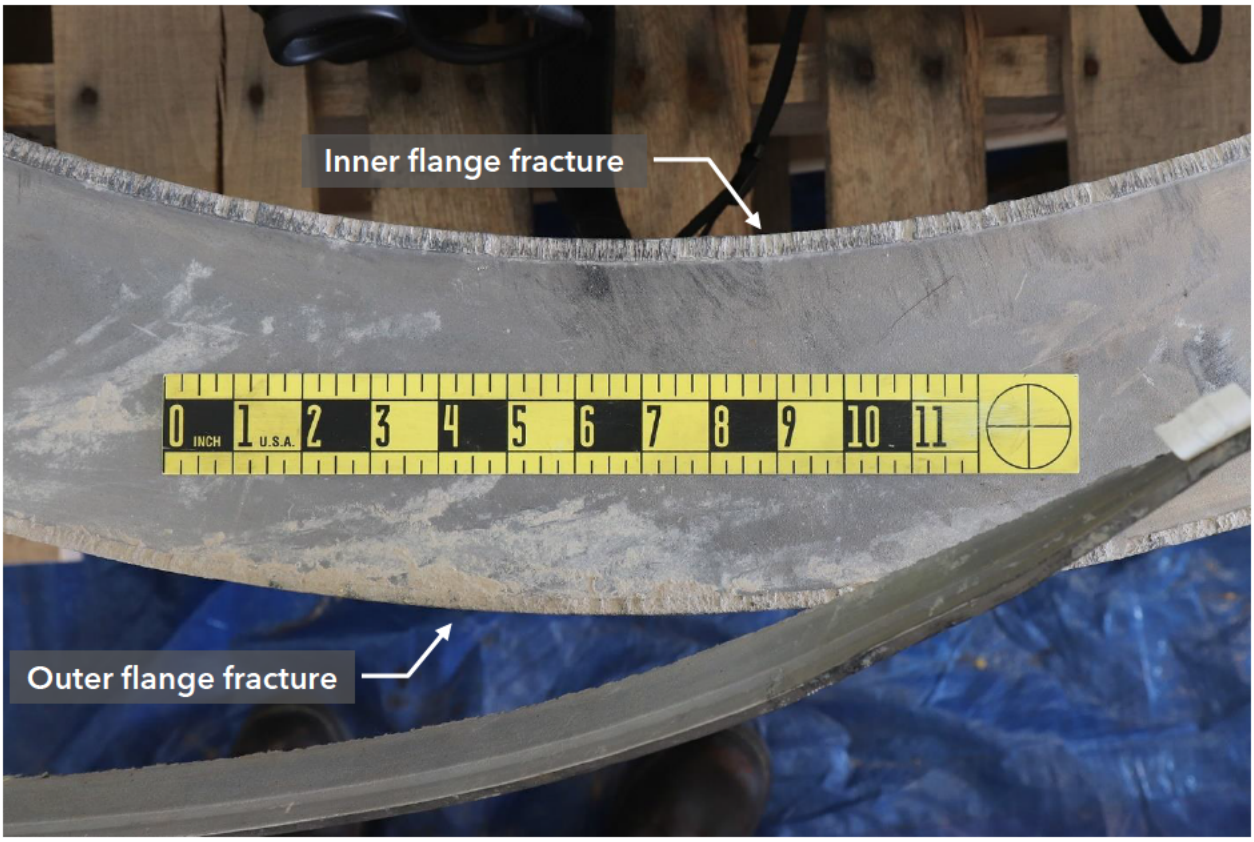

Figure 44. Image from the forward segment bonding C-channel showing the shear fracture of the inner rim, bending/tensile fracture of the outer rim, and disbondment of the adhesive.

a)

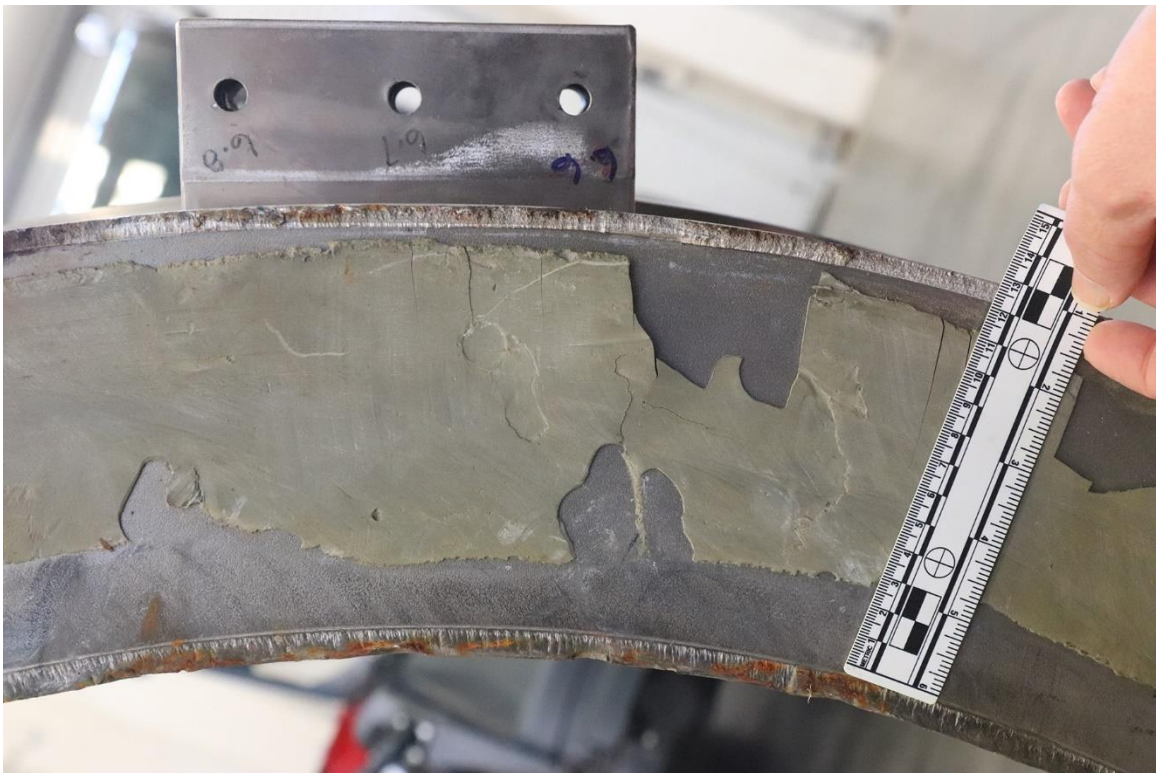

b)

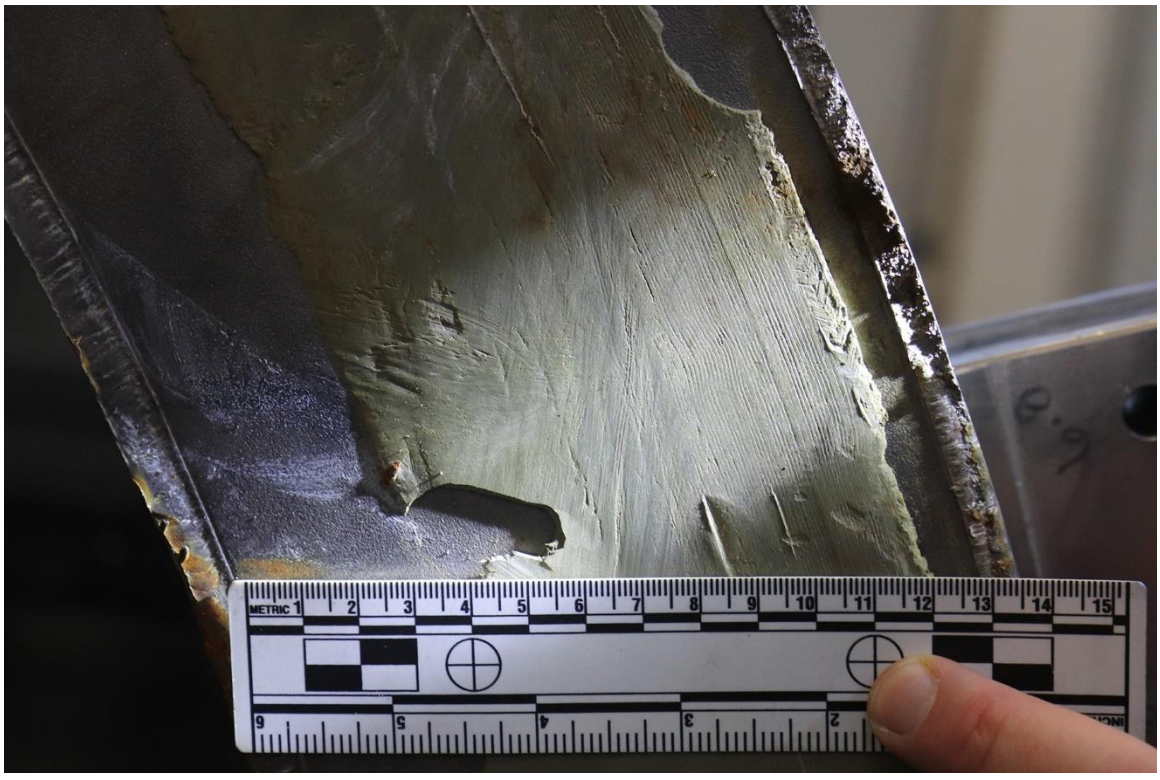

Figure 45. Images from the aft segment bonding C-channel near the top (12:00 position) where an approximately 90° arc of adhesive remained bonded to the segment: a) general lighting conditions and b) oblique lighting conditions showing the disappearance of the hull end machining marks towards the inner surface.

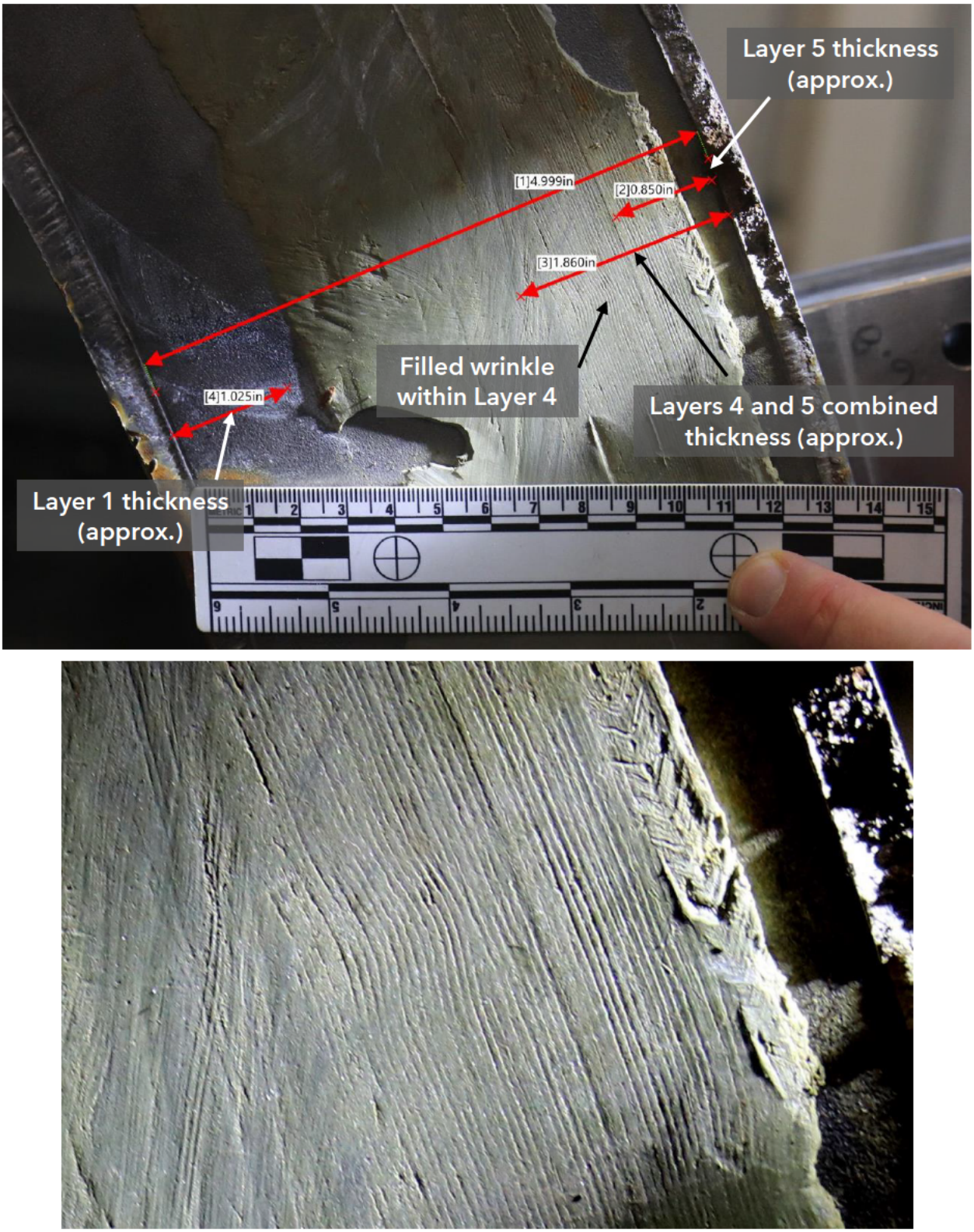

Figure 46. Top image: Annotated image showing the approximate location of co-cured layer interfaces and the location of a filled wrinkle. Bottom image: closer image of the filled wrinkle.

a)

b)

Figure 47. a) Image of aft dome and b) image of viewport seat on forward dome.

a)

b)

Figure 48. Images of large layer 4 and 5 hull piece: a) outer surface and b) inner surface.

Figure 49. Images showing waviness on the outer surface of the hull: Upper image: retrieved hull piece. Lower image: Rough hull post-curing with mandrel removed.

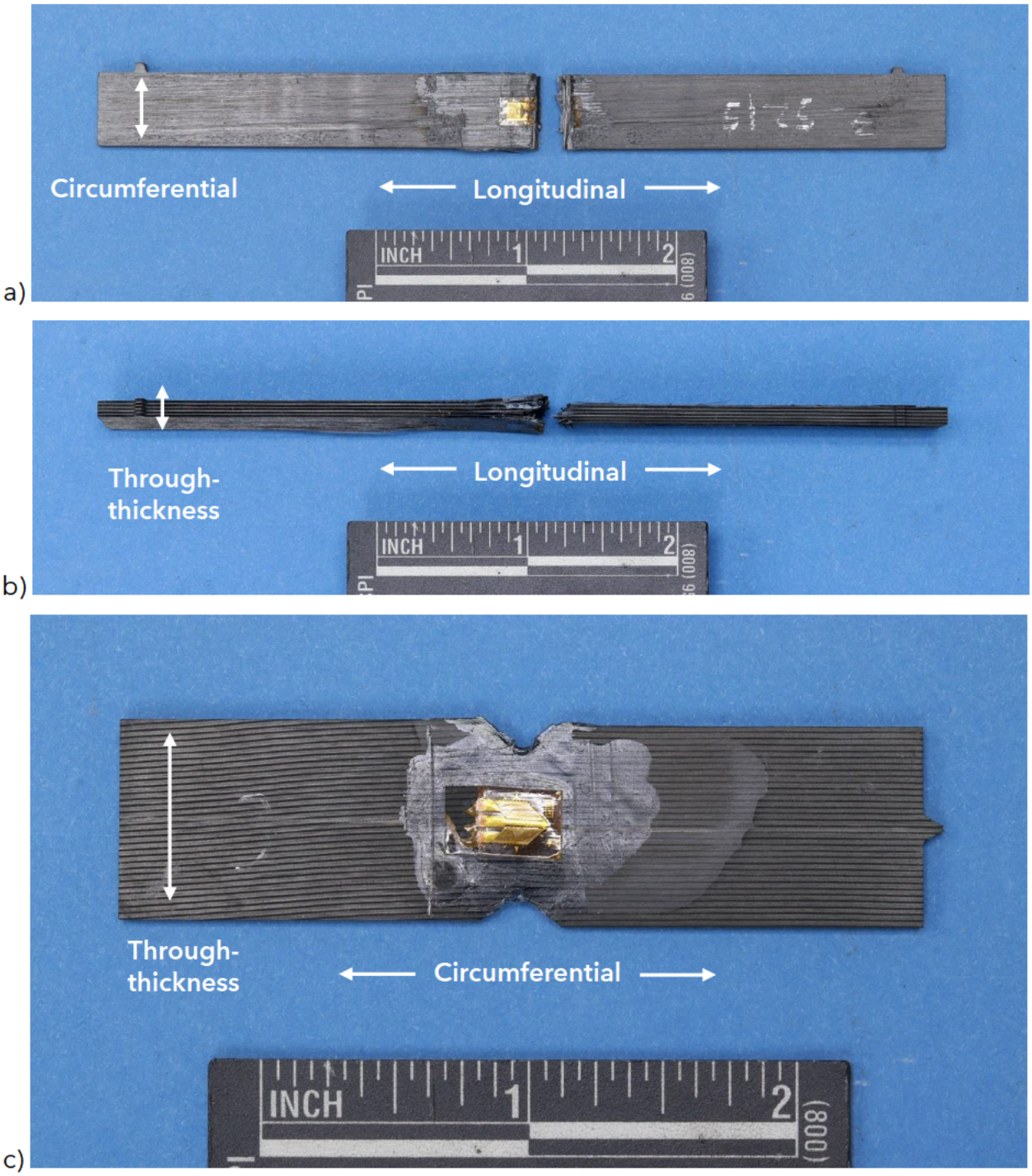

Figure 50. Images of mechanical test coupons: a) long side of compression test specimen; b) short side of compression test specimen; and c) V-notch shear test specimen.

a)

b)

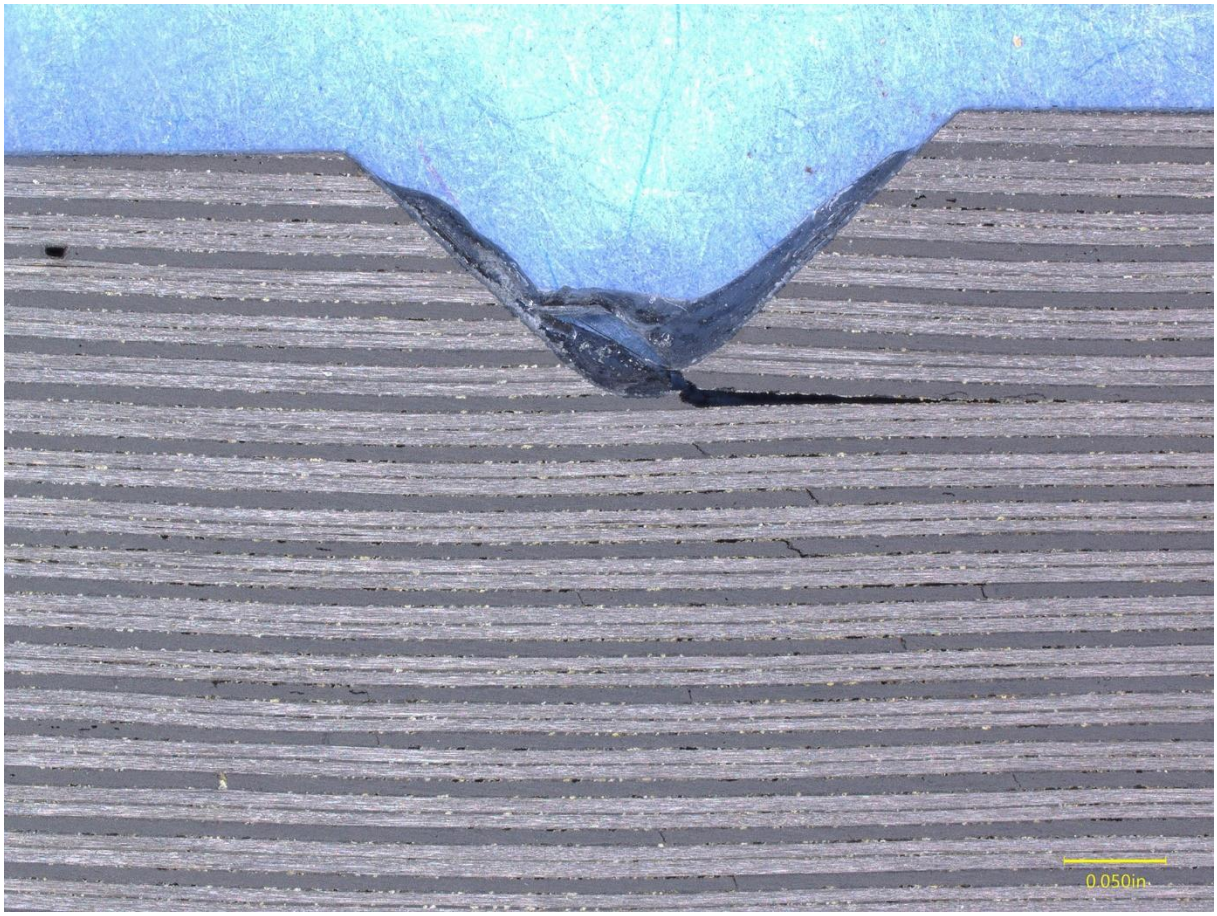

Figure 51. Images of fractured test specimens: a) compression specimen and b) shear specimen.